In presenting the dissertation as a partial fulfillment of the requirements for an advanced degree from the Georgia Institute of Technology, I agree that the Library of the Institution shall make it available for inspection and circulation in accordance with its regulations governing materials of this type. I agree that permission to copy from, or to publish from, this dissertation may be granted by the professor under whose direction it was written, or, in his absence, by the dean of the Graduate Division when such copying or publication is solely for scholarly purposes and does not involve potential financial gain. It is understood that any copying from, or publication of, this dissertation which involves potential financial gain will not be allowed without written permission.

MOBILITY MEASUREMENTS OF IONS IN NITROGEN AND HYDROGEN WITH SIMULTANEOUS MASS IDENTIFICATION OF THE IONIC SPECIES

A THESIS

Presented to

The Faculty of the Graduate Division

by

William Spencer Barnes

In Partial Fulfillment

of the Requirements for the Degree

Doctor of Philosophy in the

School of Physics

Georgia Institute of Technology

May, 1963

MOBILITY MEASUREMENTS OF IONS IN NITROGEN AND HYDROGEN WITH SIMULTANEOUS MASS IDENTIFICATION OF THE IONIC SPECIES

Approved:

Date approved by Chairman: May 20, 1963

PREFACE

The investigation described in this thesis took place at Georgia Institute of Technology over a period of approximately three years ending in October of 1962. During that period the investigation progressed through successive stages. In general each stage was preliminary and necessary to the succeeding one; however some of these stages produced their own independent results. The purpose of this thesis is to present and summarize the several results achieved by this investigation and to show their relationship to investigations in the field of gaseous electronics carried out elsewhere.

Partial financial assistance by the Air Force Office of Scientific Research received during the entire course of this investigation is gratefully acknowledged.

The author also wishes to acknowledge the assistance of many individuals in the carrying out of this research and in the preparation of this thesis. First and foremost he wishes to thank Dr. David Martin for his supervision and assistance during the entire course of the research and in the preparation of the thesis. The author wishes to acknowledge his debt to Drs. David Martin and Earl McDaniel, whose several years of prior developmental work on the drift tube and associated apparatus laid much of the experimental foundation for the present research. Much valuable assistance was received on the mathematical and statistical portions of the investigation from Drs. Don Harmer, E. I. Perlin, and Joseph Moder of the Georgia Tech Faculty. A part of the tedious gathering and

reduction of data was carried out with the assistance of several individuals: Messrs. George Keller, Ralph Milford, Larry Franks, and Larry Puckett. The preparation of this thesis was carried out with the assistance of Drs. Martin, and McDaniel and of Dr. Peter B. Sherry of the Georgia Tech faculty. The author also wishes to thank Comdr. Albert Smith of the staff of Lawrence Radiation Laboratory at Livermore, California, for proof reading this thesis and pointing out many faults in its composition.

Last but not least, the author wishes to acknowledge the assistance of his wife Elinor, whose encouragement and whose many hours of typing and proof reading made possible the completion of the thesis.

TABLE OF CONTENTS

Page

PREFACE. ii

LIST OF ILLUSTRATIONS. vi

SUMMARY. viii

Chapter

I. INTRODUCTION. 1

Basic Concepts
Summary of Mobility Theories
Previous Mobility Measurements
The Problem
The Present Experiment

II. APPARATUS AND TECHNIQUES. 23

Apparatus
Experimental Techniques

III. MATHEMATICAL FORM AND EVALUATION OF THE DATA. 44

Basic Equations of the System
Solution of the Equation of the System for the Pulse Mode of Operation
Normalization of the Distribution in Time
Statistical Estimators for K, D, and A
A Least Squares Fit of the Theoretical Curve to the Data

IV. RESULTS 61

Ion-Molecule Reactions of the System
Factors Affecting Mobility Measurements
Results for the Primary Ions
Results for Product Ions
Diffusion Coefficients and Rate Constants

V. CONCLUSIONS 90

VI. RECOMMENDATIONS 92

Provision for the Continuous Variation of z
Improvement of the Source Geometry
Use of a Diluent Gas in the Investigation of Reaction Rates

TABLE OF CONTENTS (Continued)

Page

Appendix

A. VALUES OF HASSE'S FUNCTION A FOR VARIOUS VALUES OF THE PARAMETER ν 96

B. CALCULATION OF THE MOBILITY K. 97

Fortran Program Listings
Calculated Values of K

C. OTHER POSSIBLE INITIAL DISTRIBUTIONS 110

Bell-Shaped Distribution
Square-Shaped Distribution

D. ION BURST FROM A POINT SOURCE IN A UNIFORM ELECTRIC FIELD 115

E. FORM OF THE SECONDARY ION BURSTS 120

Basic Equations for Secondary ions
Solutions of the Partial Differential Equation for Secondary Ions for the Pulse Mode of Operation

F. STEADY STATE MODE OF OPERATION 125

Primary Ions
Secondary Ions
More Complicated Situations

BIBLIOGRAPHY. 132

VITA. 135

LIST OF ILLUSTRATIONS

Figure		Page
1.	Previous Measurements of the Drift Velocity of Nitrogen Ions in Nitrogen at 0° C.	14
2.	Previous Measurements of the Normalized Mobility K_o of Hydrogen Ions in Hydrogen at 300° K	14
3.	Vertical Section of the Drift Tube and Differential Pumping Chambers.	25
4.	An Ion Source in Position Between Two Drift Field Electrodes.	26
5.	Emission Regulator Circuit for the Ion Source	28
6.	Mass Spectrometer Tube Circuitry.	36
7.	Drift Tube Pressure vs Time for a Filling of Nitrogen Leaking Through the Pin-Hole.	40
8.	Contour of Integration.	52
9.	Representative Mass Spectra of Ions in Nitrogen at 35 and 175 Microns	63
10.	Variations with Pressure of the Fractions of N_2^+, N_2H^+ and H_3^+ Ions in Nitrogen	65
11.	Variations with Pressure of the Fractions of H_2^+, H_3^+, and N_2H^+ Ions in Hydrogen	67
12.	Histogram of an Experimental Time Distribution of N_2^+ Ions in Nitrogen and the Fitted Theoretical Distribution Function.	70
13.	Two Time Distributions of N_2^+ Ions in Nitrogen Showing Variations in the Shape	71
14.	Time Distributions of N_2^+ Ions in Nitrogen for Three Different Drift Distances	75
15.	Time Distributions of N_2^+ Ions in Nitrogen for Three Different Values of the Drift Field	76
16.	Time Distributions of N_2^+ Ions in Nitrogen for Several Values of the Pressure.	77

LIST OF ILLUSTRATIONS (Continued)

Figure		Page
17.	Experimental Results for the Normalized Drift Velocity of N_2^+ Ions in Nitrogen.	79
18.	Experimental Results for the Normalized Drift Velocity of N^+ Ions in Nitrogen.	82
19.	Comparison of the Time Distributions of N_2^+, N_2H^+, and H_3O^+ Ions in Nitrogen under Identical Conditions.	87
20.	Comparison of the Time Distributions of N_2^+, N_3^+, and N_4^+ Ions in Nitrogen under Identical Conditions	89

SUMMARY

Introduction

Since the first measurement of the average velocity of drift of ions in gases under the influence of an electric field, investigators have been troubled by uncertainties as to the exact identity of the ions whose drift velocity was being measured. These uncertainties were caused by ion-molecule reactions between the ions and molecules of both the parent gas and impurities. These reactions produced changes in the identity of the ions during the course of the experiments.

Langevin, Chapman, Enskog, and others have developed theories of mobility based on the kinetic theory of gases. These theories were applicable to a range of E/p low enough that the energy acquired by the ions from the electric field E between collisions was small compared to the random thermal energy of the ions. Here p is the pressure. According to these theories the drift velocity varies directly as E/p and, when comparing the mobilities of different ions, varies as $\sqrt{1+M/m}$, where M is the mass of the gas molecule and m is the mass of the ion. Wannier extended the theory of mobility into a higher range of E/p where the energy acquired by the ions from the electric field is not negligible compared to the random thermal energies. At these higher values of E/p it was shown that the drift velocity should vary as $\sqrt{E/p}$.

Tyndall and Powell verified the dependence of the mobility on $\sqrt{1+M/m}$ for highly polarizable gases in a series of measurements of the mobilities of alkali ions in noble gases. In these experiments great

care was taken to eliminate impurities. Mitchell and Ridler made a similar series of measurements for various ions in nitrogen. The mobilities of all ions examined agreed with the proportionality very well except for the ions of nitrogen itself, for which a much lower mobility was obtained. This lower mobility was tentatively explained as the result of resonance charge exchange. In recent years Varney and others have found that the drift velocity of nitrogen ions in nitrogen varied as $\sqrt{E/p}$ above a value of E/p of about 100-volts/cm-torr. Below this value they found that the drift velocity curve formed a minimum, then a maximum, and then started back down along a curve that would suggest an ion with a mobility larger than that suggested by the upper portion of the curve. Varney proposed that in the high E/p region the observed ion was N_2^+ and in the low E/p region it was N_4^+. In the middle region he proposed that there was a mixture of N_2^+ and N_4^+ in equilibrium with one another. Appearance potential measurements of the various ions in nitrogen have tended to support Varney's point of view.

Almost all of the ionic species observed in early mobility measurements of the ions in hydrogen were actually species formed in ion-molecule reactions between the original hydrogen ions and traces of impurities. Once this problem was overcome, uncertainty still remained as to the identity of the ion whose mobility was being measured. Hirschfelder and others showed theoretically that the triatomic molecular ion H_3^+ was stable and could be formed by an exothermic reaction from H_2^+. Mason and Vanderslice computed the theoretical values of the mobility of H^+, H_2^+, and H_3^+. From comparison of their theoretical values they concluded that H_2^+ was the positive ion whose mobility was being measured in hydrogen

mobility experiments. In 1960 Varney published his opinion that the ion whose mobility was being measured was H_3^+. As evidence he pointed to the large rate constant for the reaction forming H_3^+ from H_2^+ as given by Stevenson and Schissler. He also pointed out that Mason and Vanderslice had not considered the possibility of proton exchange in making their calculation of the mobility of H_3^+.

The Present Experiment

In the present experiment a method has been developed in which the drift velocity of ions can be measured with the simultaneous positive identification of the ions as to mass. This method has been used to measure the drift velocity and, hence, the mobility of the several ionic species in nitrogen and hydrogen.

The apparatus used in this experiment consists essentially of a drift tube containing several ion sources, two differential pumping chambers, a mass spectrometer and various electronic components to count or otherwise analyze the ion current. The ion sources generate ions inside the drift tube. These ions drift under the influence of an electric field through whatever gas is in the drift tube until they arrive at one end of the tube. Here they stream out through a pin-hole into a series of two differential pumping chambers and finally into a mass spectrometer where ions of a selected mass may be counted. The electronic components amplify, count, and analyze the pulses taken from the mass spectrometer detector in several different ways depending upon the mode of operation.

Two modes of operation are used. In one mode of operation the sources are operated continuously and the variation of the different ion currents with pressure is measured. This mode of operation was used to

attempt to determine the chemical relationship between the various ionic species in the drift tube. The density of primary ions in the neighborhood of the pin-hole is given to a first approximation by the expression

$$n(z) = C \exp\left\{\left[\frac{KE}{2D} - \sqrt{\frac{K^2E^2}{4D^2} - \frac{A}{D} + s^2}\right]z\right\}$$

Here D is the diffusion coefficient, A is the probability per unit time that a given primary ion will react, and s^2 is determined by cylindrical boundary conditions.

In the other mode of operation the sources are operated in such a way that they produce bursts of ions. If the generation of these bursts of ions were of relatively short duration compared to the time of drift and if these bursts were of small spatial extent compared to the distance of drift, then the time spectrum of these ion bursts, as detected by the mass spectrometer and the twenty channel time analyzer, could be described by the relation:

$$f(z,t) = \frac{KE}{\sqrt{4\pi Dt}} \exp\left[\frac{(A + s^2D)(z - KEt)}{KE} - \frac{(z - KEt)^2}{4Dt}\right]$$

In this expression z is the distance from the source to the pin-hole and t is the time of travel. Despite the fact that the given conditions are not ideally realized in this experiment, it was still possible to use this relationship to obtain a first approximation to K, even though the values obtained for D would be too large. The exact configuration of the initial ion burst was not known, with the simple type of ion source used, but any initially bounded ion distribution would lead to a time spectrum

which would approach that described by the above relation asymptotically if the time of drift were increased. The configuration of the ion distribution in space at a given time was determined as follows for (1) an initial Dirac-delta function distribution, (2) an initial bell-shaped distribution, and (3) an initial square-shaped distribution:

$$(1)\quad n(r,z,t) = \frac{N_o}{\sqrt{4\pi Dt}} \sum_i C_i J_o(s_i r) \exp\left[-(A+s_i^2 D)t - \frac{(z-KEt)^2}{4Dt}\right]$$

$$(2)\quad n(r,z,t) = \frac{N_o}{\sqrt{4\pi(Dt+\sigma^2/2)}} \sum_i C_i J_o(s_i r) \exp\ -(A+s_i^2 D)t - \frac{(z-KEt)^2}{4(Dt+\sigma^2/2)}$$

$$(3)\quad n(r,z,t) = n\left\{\operatorname{erf}\left[\frac{z+a-KEt}{2Dt}\right] - \operatorname{erf}\left[\frac{z-a-KEt}{2Dt}\right]\right\}\sum_i C_i J_o(s_i r)\exp\left[-(A+s_i^2 D)t\right]$$

In these equations N_o is the number of ions in the original burst, r and z are cylindrical coordinates with respect to the ion source and the z axis coincides with the axis of the drift tube, 2a is the spatial width of the square ion burst, and $n = N_o/2a$.

For a point ion source generating ion bursts which remain uneffected by the cylindrical boundary condition the configuration of the ion distribution is given by

$$n(x,y,z,t) = \frac{N_o}{(4\pi Dt)^{3/2}} \exp\ - At - \frac{x^2+y^2+(z-KEt)^2}{4Dt} \quad .$$

Here x and y are rectangular cartesian coordinates perpendicular to z.

Results

a. The data obtained on the mobility of N_2^+ joined smoothly onto that portion of the existing data of Varney for the ions in nitrogen at values of E/p greater than about 90 volt/cm-torr, and extended it into the range of lower E/p. The behavior of the mobility is in general agreement with that expected from the mobility theory of Wannier for a single ionic species not appreciably perturbed by reactions. From this fact it is concluded that Varyney's assertion that the ion observed in the higher E/p portion of his data could be presumed to be N_2^+ is correct.

b. It is further concluded that the system of reactions hypothesized by Varney which convert N_2^+ and N_4^+ into each other at higher pressures does not significantly affect the mobility of N_2^+ ions in nitrogen for pressures of 0.7 torr and for values of E/p of more than 4 volts/cm-torr.

c. The range of E/p in which the drift velocity of N_2^+ ions in nitrogen is linear is E/p begins just below 100 volts/cm-torr, and the reduced mobility in this range is 1.4 ± 0.1 cm^2/volt-sec.

d. The range of E/p in which the drift velocity of N^+ ions in nitrogen is linear in E/p lies in a range somewhat below 100 cm^2/cm-torr. The reduced mobility of N^+ for this range is 2.4 ± 0.1 cm^2/volt-sec.

e. The time spectrum obtained for N_3^+ is not inconsistent with the mobility expected for these ions from a semi-empirical relationship determined by Mitchell and Ridler from their data.

f. The time spectrum obtained for N_4^+ is not inconsistent with the hypothesis that it is in equilibrium with N_2^+.

g. The predominating ion-molecule reactions of the N_2^+ ions in nitrogen at pressures below 0.7 torr are, with a minute trace of water

present, as follows:

$$N_2^+ + H_2O \rightarrow N_2H^+ + OH$$

$$N_2H^+ + H_2O \rightarrow H_3O^+ + N_2$$

h. The single ion observed in pure hydrogen under the conditions of most previous mobility experiments must certainly have been H_3^+.

i. The measurement of the mobility of H_3^+ ions attempted in this experiment was inexact due to source effects, but the results were of the same order of magnitude as previous measurements of the mobility of hydrogen ions in hydrogen.

j. The predominating ion-molecule reactions taking place in hydrogen containing a trace of nitrogen at pressures below 0.7 torr are:

$$H_2^+ + H_2 \rightarrow H_3^+ + H$$

$$H_2^+ + N_2 \rightarrow N_2H^+ + H$$

$$H_3^+ + N_2 \rightarrow N_2H^+ + H_2$$

CHAPTER I

INTRODUCTION

Since the first measurements of the average velocity of drift of ions in gases under the influence of an electric field, investigators have been troubled by uncertainties as to the exact identity of the ions whose drift velocity was being measured. These uncertainties were caused by ion-molecule reactions between the ions and molecules of both the parent gas and impurities which produced changes in the identity of the ions during the course of the experiments.

In the present experiment a method has been developed in which the drift velocity of ions can be measured with the simultaneous positive identification of the ions as to mass. This method has been used to measure the drift velocity of N_2^+ ions in nitrogen. A straight line fitted to these measurements by the method of least squares joins onto and extends measurements at higher E/p made by previous investigators of the drift velocities of ions which they supposed were N_2^+. A similar series of measurements of the drift velocity of N^+ was made and the reduced mobilities of both N^+ and N_2^+ were estimated. The experimental apparatus in its present form proved unsuitable for making accurate measurements of the drift velocity of the ions in hydrogen. Nevertheless it was definitely established that the ions whose drift velocity was measured in most previous experiments were H_3^+.

Basic Concepts

Mobility

For many years investigators have been aware that gases may act as electric conductors under various circumstances. In 1785 Coulomb showed conclusively that at least part of the charge lost by an insulated, charged body over a long period of time was attributable to conduction through the air. Two general types of conduction have been recognized:

(1) Discharges. In this type of conduction the gas is subject to strong electric fields. Ions are generated throughout certain parts of the region of conduction by the impact of electrons on neutral molecules. The resultant flow of electrons and ions through the gas constitutes a current.

(2) Conduction caused by the migration of existing electrons and ions under the influence of electric fields. In this type of conduction the electric field is too weak to produce ions in the manner described in (1) and therefore some agent must introduce ions continuously into the region of conduction for conduction to continue. In the case of Coulomb's experiment the agent was probably cosmic rays. This investigation was restricted to the second type of conduction.

After the discovery of X-rays, J. J. Thomson and Ernest Rutherford developed crude methods for measuring the average velocity of migration of ions and electrons through gases under the influence of an electric field, the so-called drift velocity. These and other investigators soon developed a wide variety of methods for measuring this drift velocity. In general, however, these methods fell into three general categories:

(1) Drift field reversal methods. The electric field is first established in such a direction that it draws ions across a fixed distance

through the gas for a definite interval of time; then it is reversed to oppose the ion flow. As this sequence occurs repeatedly the time interval during which the ions are drawn across the fixed distance is diminished while the magnitude of the ion current is monitored with some sensitive instrument. The minimum interval of time for which substantial ion flow can occur divided into the drift distance gives the drift velocity.

(2) Air blast methods. The electric drift field is established in a direction perpendicular to the flow of gas through a tube. Ions being generated at a point near one wall of the tube are carried to a point on the opposite wall determined by the ratio of the ion drift velocity to the velocity of the gas flow. This ratio is equal to the ratio of the perpendicular distance across the tube to the distance the ions are carried "downstream".

(3) Pulse methods. Bursts of ions are generated or released and allowed to drift across a fixed distance through a gas under the influence of a fixed drift field. The time of transit of an ion burst is measured by any one of several methods to determine the drift velocity. A more complete description of the various methods of measuring drift velocities may be found elsewhere.[1,2]

It was soon established that over a wide range of pressures and fields the drift velocity v_D might be given by

$$v_D = KE \tag{1}$$

where E is the electric field and K is a constant, independent of E, called the mobility. The mobility K was found to be characteristic of the

migrating ion and the gas through which it was migrating. It was also found to vary inversely with pressure.

Diffusion Coefficient

For many years prior to the investigation of the motions of ions through gases, the concept of diffusion had been useful in the explanation of the mixing of gases. Consider a situation in which molecules of one kind of a gas are initially concentrated within a bounded but not physically enclosed region in contact with an atmosphere of gas molecules of a different kind. Even though there might be no variation in pressure anywhere in this region, molecules of the first kind will flow out of this bounded region and will tend to distribute themselves uniformly throughout the surrounding atmosphere. Kinetic theory explains this effect as the result of the random thermal motion of the molecules of the gases. This randomness of motion causes the most probable direction of motion of a molecule of a given gas at the edge of a region of greater concentration of that gas to be away from the region of greater concentration. The molecules of gas of the first kind, therefore, spread themselves throughout a larger region as time passes until finally they are uniformly distributed throughout the atmosphere of the gas of the second kind.

From a macroscopic point of view diffusion may be described to a first degree of approximation by Fick's law

$$\underline{J} = -D\nabla n \tag{2}$$

where $\underline{J}$ is the rate of outward flow of molecules in number per unit area per unit time, n is the local density of molecules in number per unit

volume, and D is called the diffusion coefficient. Like the mobility, D has been found to vary inversely with pressure. Although the interaction between an ion and a molecule during a collision is somewhat different than the interaction between two molecules the mechanism of diffusion for ions in gases is basically the same as that for a molecular species in the absence of strong fields.

The diffusion coeffients of ionic species have been measured by techniques similar to the air blast method for measuring the drift velocity. The ratio of K to D of ionic species has also been measured by measuring the lateral spread of a stream of ions moving through a gas under the influence of an electric field.

Ratio of Mobility to Diffusion Coefficient

A relationship between K and D may be derived from macroscopic considerations. Consider a situation in which an ionic density gradient is maintained with no net ionic flow across a volume by means of a uniform electric field. Take the direction of the electric field as the z-direction in a rectangular, cartesian coordinate system. Since there is no net ionic flow, the current density, which is formed by the combined effect of diffusion and mobility, will be zero. Thus we will have

$$J = -D\frac{\partial n}{\partial z} + KEn = 0 \quad . \tag{3}$$

The partial pressure p exerted by the ions is proportional to their number density n so equation (3) becomes

$$\frac{K}{D} = \frac{1}{Ep}\frac{\partial p}{\partial z} \quad . \tag{4}$$

Now consider a right circular cylinder with unit cross section area and length dz parallel to the z-axis. If the ionic partial pressure at the lower end of this cylinder is p then the pressure at the upper end is p + dp. Thus the total "effective" force on the ions in this cylinder produced by the effects of diffusion is dp. For the gradient to be maintained with no net ionic flow this "effective" force must be balanced by the real force of the electric field which is neEdz. Thus

$$dp = neEdz \quad . \tag{5}$$

Use of the gas law,

$$p = nkT \quad , \tag{6}$$

where k is Boltzmann's constant and T is the absolute temperature, with the expression (5) and substitution of the result in (4) gives

$$\frac{K}{D} = \frac{e}{kT} \quad . \tag{7}$$

This relation is not exact. It depends directly upon the assumed proportionality between v_D and E which in general does not hold exactly. It also depends upon the validity of the ideal gas law for ions, a relationship which does not hold exactly for any molecular species. However, in the range of electric fields and pressures for which the mobility concept is acceptable it will give values for this ratio within 5 per cent of the exact value.

The expression (7) has proved so accurate compared with the results of experiments in this field that diffusion coefficients have not been measured for many ions but have simply been calculated from their mobilities.

Summary of Mobility Theories

This section shall consist of a summary of the results of some of the more successful theories of ionic mobility.

In 1903 Langevin published a theory of ionic mobility[3] based on the kinetic theory of gases in which he considered the interaction between ions and molecules as essentially that of hard elastic spheres. The expression for the mobility produced by this theory was

$$K = 0.815 \frac{e\lambda}{MC} \sqrt{1 + \frac{M}{m}} \tag{8}$$

where e is the electronic charge, M is the mass of the molecule, m is the mass of the ion, C is the root mean square (rms) thermal velocity of the molecules, and λ is the mean free path.

In 1905 Langevin published an improved theory of ionic mobility[4] in which account was taken of the attractive force between ions and both polar and non-polar molecules. A non-polar molecule becomes polarized by the electric field of a nearby ion. The force of attraction f between the ion and the dipole induced in the molecule in such a case is

$$f = \frac{(\varepsilon - 1)e^2}{2\pi N r^5} \tag{9}$$

where e is the electronic charge, ε is the dielectric constant of the gas, N is the Loschmidt number, and r is the distance between the centers of the ion and the molecule. Such an interaction between the ions and the molecules leads to the following expression for the mobility

$$K = \frac{A}{\rho\sqrt{\varepsilon - 1}}\sqrt{1 + \frac{M}{m}} \tag{10}$$

where ρ is the gas density. Here A is a function of the parameter ν whose value may be computed by

$$\nu = \frac{(\varepsilon - 1)e^2}{8\pi\, pS^4} \tag{11}$$

In this expression S is the sum of the ionic and molecular radii and p is the pressure. A table of values of A as determined by Hasśe corresponding to values of ν is given as Appendix A. As the polarization force between ions and molecules decreases the dielectric coefficient approaches one and ν approaches zero. This corresponds to the limit of hard elastic spheres interaction. In this case the mobility is given by

$$K = \frac{.75}{S^2\sqrt{8\pi\, p\rho}}\sqrt{1 + \frac{M}{m}} \quad . \tag{12}$$

As the polarization force between ions and molecules becomes dominant the expression for the mobility becomes

$$K = \frac{.5105}{\sqrt{\rho(\varepsilon - 1)}}\sqrt{1 + \frac{M}{m}} \quad . \tag{13}$$

According to Langevin's theory, the drift velocity of an ion in a gas should vary directly as E/p, the ratio of the electric field to the pressure. Langevin's papers on ionic mobility lay unnoticed for twenty years until their applicability was pointed out by Hasśe.

Following Langevin's work Chapman[5] and Enskog[6] developed a rigorous kinetic theory to calculate diffusion coefficients for molecules of one

gas diffusing through a different gas. Their theory was more general than Langevin's in that it applied to any gas in which the force between molecules was spherically symmetric. It could validly be applied to situations in which ions are diffusing through gases and the mobility of such ions could be calculated from their diffusion coefficient by means of the relation (7).

According to the Chapman-Enskog theory, the ion-molecule mutual diffusion coefficient is given to a second order by the expression

$$D = \frac{3\sqrt{\pi}}{16}\left(\frac{2KT}{M_r}\right)^{\frac{7}{2}} \frac{1 + \varepsilon_o}{(N_1 + N_2)P} \tag{14a}$$

where the quantity P is given by

$$P = \int_o^\infty v_o^5 \, q(v_o) \exp\left(\frac{-M_r v_o^2}{2kT}\right) dv_o \tag{14b}$$

and $q(v_o)$, the diffusion cross section, is given by

$$q(v_o) = 2\pi \int_o^\infty (1 - \cos\theta)\, bdb \quad . \tag{14c}$$

In the above expressions M_r is the reduced mass of the ion-molecule system, N_1 and N_2 are the ion and molecule number densities, respectively, and ε_o is a second order correction which is usually less than experimental errors. The parameter P is the diffusion cross section averaged over all molecular velocities v_o where these velocities have a Maxwellian distribution. The diffusion cross section depends on the detailed nature of the ion-molecule interaction through the impact parameter b and the

angle θ which is the scattering angle in center of mass coordinates for an ion-molecule collision. The evaluation of this expression is dealt with in several existing texts[7,8] on gaseous physics.

Kihara[9], Mason and Schamp[10] have extended the Chapman-Enskog theory to obtain second and third order approximations.

In 1931 Hasśe and Cook[11] published a theory of ionic mobility utilizing an inverse ninth power repulsive force in addition to Langevin's polarization attraction. Their formula, however, gave values of the mobility that are in no better agreement with experiment than those given by Langevin's expression.

In recent years mobilities have been calculated from quantum mechanical considerations. In most cases the results of these calculations are in no better agreement with experiment than those of Langevin. In several cases, however, these calculations lead to drastically different results, for instance, in the case where resonance proton or electron exchange is possible. The most important of these cases is the one of an ionized gas molecule or noble gas atom in its parent gas. Dalgarno, McDowell, and Williams[12] have worked out a theory for the mobility of ions in an unlike gas. Dalgarno[13] has presented a theory for ions in their parent gas.

In these theories $q(v_o)$ is computed from quantum mechanical rather than from classical considerations. The quantum mechanical expression for this quantity is substantially the same as the classical expression if energies are high enough so that the sum over states may be replaced by the integral over b and if no particle exchange is involved.

The assumption is implicit in Langevin's mobility theory and in several others mentioned so far that the energy which the ion acquires

from the electric field between collisions is negligible compared to its thermal energy. The results of this theory are valid only for low values of E/p where this is true. In 1951 Wannier[14] extended the theory of mobility into the range of higher E/p where this is not so. According to his theory the drift velocity should be proportional to E/p at low E/p and proportional to $\sqrt{E/p}$ at high E/p. The value of E/p at which the transition between these two regions occurs depends on the properties of the ions involved.

Previous Mobility Measurements

Many inconsistancies appeared in early mobility measurements. Some ions appeared to have mobilities in very good agreement with those predicted by theory, while others did not. Mobilities of some ions measured by several different methods seemed to have different values. Gradually as evidence accumulated, a tendency for ions to "age" was recognized. By "aging" it is meant that these ions would have one mobility immediately after formation but a different mobility after having been exposed for a few hundreths of a second to the gas through which they were to drift. Tyndall and Powell[15] made a series of mobility measurements in which the presence of several different kinds of ions was strongly suggested by the results. Their conclusion was that the so-called "aging" process was actually the result of ion-molecule reactions, including charge transfer, between the ions of interest and traces of various impurities in the gas. These reactions changed the identity of the ions being studied from those supposed to be in the apparatus to some other kind having an inherently different mobility.

This effect was especially pronounced in helium whose ions apparently participate in an irreversible charge transfer with almost any other kind of molecule they encounter. In the present experiment several exploratory studies of helium were made, and it was concluded that not enough helium ions could be gotten through the apparatus to justify further effort. These results did suggest, however, the possible usefulness of helium as a neutral gaseous diluent to be used to study ion-molecule reactions having extremely large rate constants such as the formation of H_3^+ from H_2^+. The function of the helium in such an experiment would be to slow up the reaction by allowing the investigator to cut down the concentration of hydrogen molecules in the drift tube while maintaining a pressure at which diffusion and mobility theory may be applied to interpret the results.

Tyndall and Powell performed several more experiments[16] with improved apparatus in which considerable effort was made to eliminate impurities. Some fairly unambiguous results were finally obtained for alkali ions in the rare gases. According to Langevin's theoretical formula for the mobility we should have

$$K \sim \sqrt{1 + \frac{M}{m}} \tag{15}$$

for highly polarizable gases. The above experiments showed that this proportionality held very well for alkali ions in argon. Small deviations from it appeared for the same ions in neon and considerable deviations appeared for the ions in helium. In these cases the deviations were all in the expected direction.

In 1934 Mitchell and Ridler[17] performed a similar series of experiments in which the mobilities of various ions in nitrogen were measured. The mobilities of all of these agreed with the proportionality (15) very well except for ions of nitrogen itself for which a mobility was obtained that was lower than was predicted for N_2^+ at mass 28. Because the measured mobility corresponded roughly to that predicted for an ion of mass 40, the possibility was considered that the observed ion was N_3^+. Their conclusion was that the ion was N_2^+, and that the singular anomalous mobility at low E/p was due to resonance charge exchange. It will later be shown that the situation was not this simple. At higher values of E/p these investigators also noticed the departure from proportionality with E/p of the ion drift velocities as predicted by Wannier's theory.

In recent years several investigators[18,19] have reinvestigated the mobility of nitrogen ions in nitrogen. The result of these investigations showed that the drift velocity of whatever ions were in nitrogen varied as $\sqrt{E/p}$ as expected at values of E/p above about 100-volts/cm-torr. According to the theory, from this value down there would be a gradual transition to the situation in which the drift velocity would vary directly as E/p. As can be seen from Figure 1, this did not happen. As E/p decreased the drift velocity curve formed a minimum, then a maximum, and then started back down along a curve that would suggest an ion with a larger mobility than might be suspected by examining the shape of the portion of the curve above 100-volts/cm-torr. Mitchell and Ridler's data when plotted on the same graph appeared to join onto and extend that portion of the curve corresponding to a higher mobility. This behavior of the drift velocity curve suggested that the drift velocity of ions of one species was being measured at high E/p while that of a different ion was

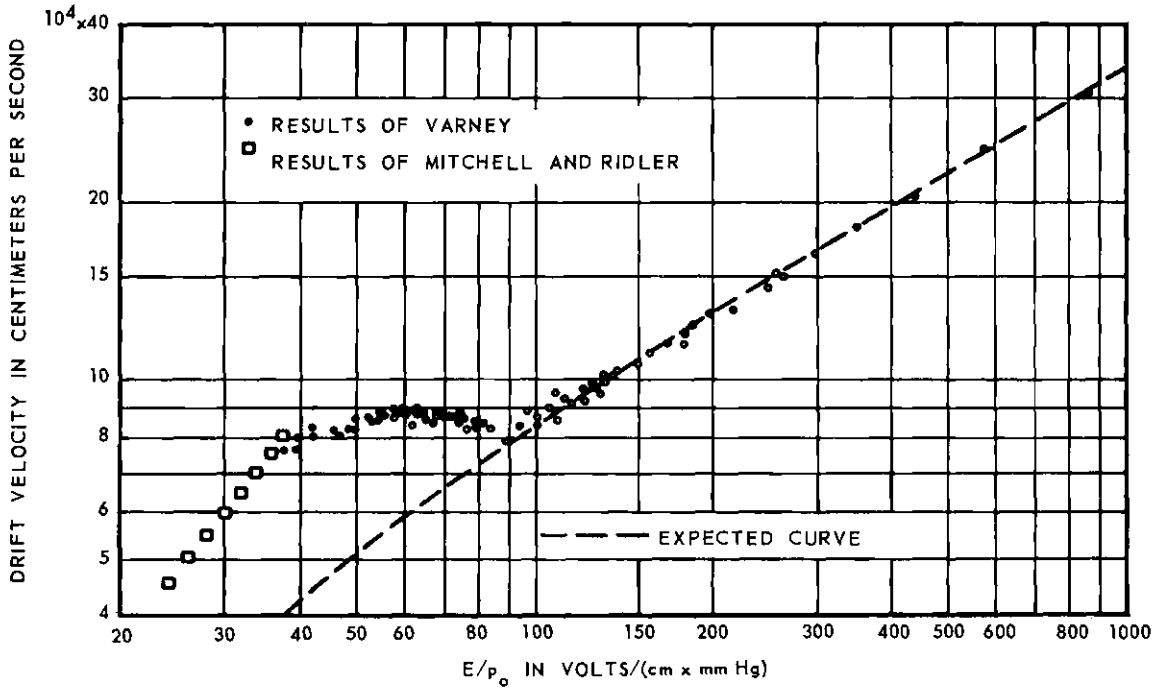

Figure 1. Previous Measurements of the Drift Velocity of Nitrogen Ions in Nitrogen at 0°C.

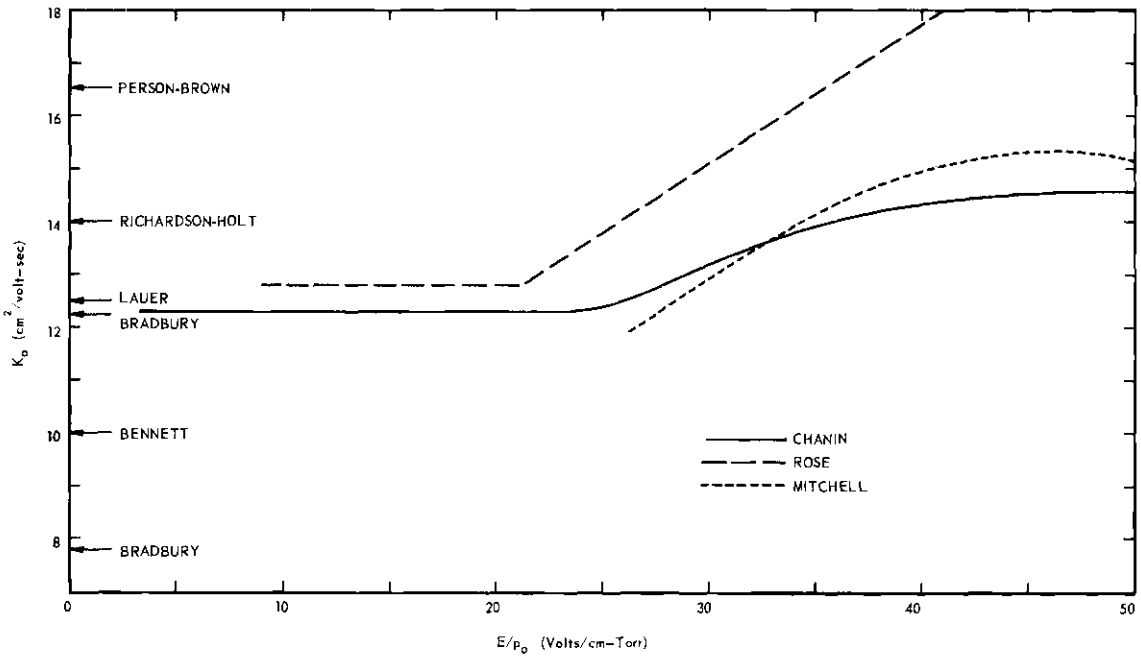

Figure 2. Previous Measurements of the Normalized Mobility K_o of Hydrogen Ions in Hydrogen at 300°K.

being measured at low E/p. It was proposed by Varney that the high E/p ion was N_2^+, and the low E/p ion was N_4^+. In the middle region he proposed that there was a mixture of N_2^+ and N_4^+ in equilibrium with one another. In these experiments no direct measurement of the mass of the ion was made.

The nature of the equilibrium assumed by these investigators was the following. N_4^+ is formed by a reaction of the form

$$N_2^+ + N_2 \rightarrow N_4^+$$

for which the reaction rate was expected to increase with pressure due to an increase in the collision rate. The reverse reaction is of the form

$$N_4^+ + N_2 \rightarrow N_2^+ + 2N_2$$

Varney did not make any hypotheses concerning the details of either of the above reactions, but he did indicate that the first of the above equations was not meant to be taken literally but only showed the chemical transformation that was taking place.

It is thought that the second reaction is endothermic, and the N_4^+ ion must absorb energy during a collision with a nitrogen molecule for this reaction to go. The reaction rate for this reaction increases with E/p due to the increase in collision energies. Varney predicted on the basis of thermodynamic considerations[20] that the transistion point to the equilibrium condition mentioned above was both temperature and pressure dependent. Data given in reference 19 confirms the temperature dependence. This data shows that the transition point moves toward lower E/p as the temperature increases. He further predicted[21] that this transition point will move into the extremely low E/p range at low pressures

such as we used in this experiment. If this happened the portion of the drift velocity curve characteristic of N_2^+ ions would be extended into the low E/p range.

In apparent confirmation of Varney's point of view, Saporoshenko[22] found the appearance potentials of N_2^+ and N_4^+ in his pressurized mass spectrometer source to be 15.5 ± 0.2 ev and 15.8 ± 0.3 ev, respectively, which would make them scarcely distinguishable experimentally as far as his experiment was concerned. In contrast to this he found appearance potentials of 22.1 ± 0.5 ev and 24.2 ± 0.4 ev for N_3^+ and N^+, respectively, suggesting that they have nothing to do with either N_2^+ or N_4^+.

Saporoshenko noted that the densities of N^+ and N_2^+ in his ion source vary linearly with pressure marking them as primary ions, whereas the densities of N_3^+ and N_4^+ vary quadratically with pressure indicating that they are secondary ions. One plausible explanation of these facts would be to assume that N_4^+ is the product ion produced by some reaction in which N_2^+ was the primary ion which, of course, corresponds with Varney's proposal. Notwithstanding the closeness of the appearance potentials of N^+ and N_3^+ Saporoshenko rejects the idea that N_3^+ might be formed by the reaction

$$N^+ + N_2 \rightarrow N_3^+ \quad .$$

Instead he postulates a reaction of the form

$$N_2^{+*} + N_2 \rightarrow N_3^+ + N \quad .$$

Here N_2^{+*} is a nitrogen molecular ion raised to some excited state.

The reaction forming N_4^+ in the form suggested by Varney is impossible to justify on the basis of momentum and energy conservation considerations without some modification. Several other investigators have alternative theories for the formation of N_4^+. Munson, Field, and Franklin[23] believe that N_4^+ may be formed by two different processes in their apparatus, which is a mass spectrometer operated at relatively high pressures for the purpose of studying ion molecule reactions. At low pressures they believe that the so-called Hornbeck-Molnar process is responsible, that is,

$$N_2 + e^- \rightarrow N_2^* + e^- \quad ,$$

$$N_2^* + N_2 \rightarrow N_4^+ + e^- \quad .$$

Here N_2^* is a nitrogen molecule raised to some excited state by a collision with an electron. At high pressures they postulate a three body interaction,

$$N_2^+ + 2N_2 \rightarrow N_4^+ + N_2 \quad .$$

At present there seems to be no certainty among investigators as to the mechanism of formation of both N_3^+ and N_4^+. The hypothesized relationship of N_2^+ and N_4^+ in mobility measurements of ions in nitrogen is therefore still open to question.

The measurement of the mobility of ions in hydrogen has had connected with it uncertainties of the same general nature as those of nitrogen. In 1932 Bradbury[24] noticed the existence of two ions in hydrogen with reduced mobilities of 8.2 cm^2/volt-sec and 13.1 cm^2/volt-sec. Although he claimed to have used "pure" hydrogen in making his measurement;

he was apparently not so certain in the case of nitrogen and oxygen since in these cases he used gases from several different sources and compared results. Most measurements prior to Bradbury's had given values of the reduced mobility between 4.96 and 6.70 cm^2/volt-sec and were apparently entirely due to impurities.

A number of subsequent measurements of the mobility of the positive ions in hydrogen produced only widely scattered results. Some of the more extreme results, including Bradbury's lower one, were later tentatively identified as the results of impurities. Figure (2) shows the values obtained by various investigators[25-31] for reduced mobility of the positive ions in hydrogen.

The exact nature of the positive ions in hydrogen was not definitely settled by the recognition and elimination of impurities. The ions H^+, H_2^+, and H_3^+ were all recognized by J. J. Thomson in positive ray experiments as early as 1916. Since that time the formation of these ions, and particularly H_3^+, has been subject to almost continuous investigation.

In a series of papers from 1936 through 1938 Hirschfelder[32-34] and others made a theoretical investigation of the form and stability of triatomic hydrogen ions and molecules. It was their conclusion that H_3^+ was triangular in shape and stable and that a reaction forming it from H_2^+,

$$H_2^+ + H_2 \rightarrow H_3^+ + H \quad ,$$

would be exothermic by 39.7 kcal/mol. In spite of this conclusion most investigators assumed that the ions whose mobility they were measuring

were H_2^+. In 1959 Mason and Vanderslice[35] computed theoretical values for the mobilities in hydrogen of the ions H^+, H_2^+, and H_3^+. From comparison of several of the more dependable experimental values of the mobility with their results they concluded that H_2^+ was the positive ion being measured in hydrogen mobility experiments. However, this conclusion was not convincing. In his paper[30] Rose declined to identify the positive ion whose mobility he had measured.

In 1960 Varney[36] published his opinion that the ion whose mobility was being measured in hydrogen was H_3^+. As evidence he quoted the large rate constant for the reaction forming H_3^+ from H_2^+ as given by Stevenson and Schissler[37] and pointed out that Mason and Vanderslice had not considered the possibility of proton exchange in making their calculation of the mobility of H_3^+. He also noted that Stevenson assigned a much larger binding energy to H_3^+ than to H_2^+. Actually Stevenson and Schissler reported the reaction cross section for the formation of D_3^+ from D_2^+ which was given as a function of collision energy but had a value of the order $5 \times 10^{-15} cm^2$. If the H_2^+ ion has this large a cross section for this reaction it is highly doubtful that any H_2^+ ions would survive long enough to make a mobility measurement at values of pd for which this concept is meaningful. d here is the distance of drift of the ions, p is the pressure, and the quantity pd is a measure of the total number of collisions undergone by the ions in drifting through the gas.

It was quickly verified[38] in the present investigation that the H_2^+ ion did indeed have a reaction cross section of this magnitude. On the basis of the above evidence Chanin[31] reported that the single ion he found in his mobility measurement was H_3^+. Saporoshenko[39] verified that

the cross section for the formation of H_3^+ from H_2^+ was indeed of the same order of magnitude as the cross section for the corresponding deuterium reaction.

The Problem

Since the Hornbeck-Molnar process has been suggested as the main process for the formation of N_4^+ at low pressures as an alternative to Varney's process and since such a process would be associated with the ion source in an apparatus such as ours the following information would be of interest in establishing the correct relationship of N_2^+ and N_4^+:

(1) Does the drift velocity curve for N_2^+ extend into the low range of E/p for low pressures as suggested by Varney?

(2) What is the "apparent" drift velocity of N_4^+ in the low range of E/p for low pressures?

In addition to these two questions concerning the drift velocities of N_2^+ and N_4^+ it would also be of interest to know:

(3) How does the mobility of N^+ compare with the "apparent" mobility of N_3^+?

(4) What are the transport properties of the other ions associated with nitrogen in this range of E/p?

In the case of hydrogen two pieces of information will be of interest:

(1) What is the ion in hydrogen under conditions similar to those in most previous mobility measurements?

(2) What is the mobility of the ion directly identified as H_3^+ in this experiment?

The Present Experiment

In the present experiment mobility measurements are made of ions which are positively identified as to mass. In addition to this unique feature, the length of the drift distances is great enough to permit mobility measurements to be made at lower pressures than usual in mobility measurements. Because of the additional length the ions will still make enough collisions with molecules to achieve normal drift conditions. In the case of secondary ions the results of such a measurement could only be termed the "apparent" mobility since the identity of the ion throughout the drift time is not unique. The exception to this is H_3^+ which is formed so quickly from the primary ions H_2^+ that it may be treated as a primary ion in hydrogen.

Ions are generated at one of three sources located along the axis of a tube containing hydrogen or nitrogen at pressures of from 0.01 to 2.0 torr. The ions are drawn by a weak electric field of from 1 to 4-volts/cm toward one end of the tube where they are swept into a mass spectrometer. The work divides itself naturally into two phases chronologically. In the first phase a detailed but qualitative investigation was made into the ion-molecule reactions occurring in the system over a wide range of pressures. After a preliminary survey of mass spectra at several pressures to determine the ionic species present the variation with pressure of the several ionic species was measured by monitoring their respective count rates with the mass spectrometer. Some attempt was made to make this investigation quantitative so that rate constants for the various reactions could be determined, but for reasons which will be outlined in Chapter IV this did not prove to be possible under present

conditions. In the second phase the mobilities of the various ionic species in nitrogen and hydrogen are measured by a time analysis method in which the ions are generated by the sources in bursts. The output of the mass spectrometer is time analyzed to determine the drift time and the spread of each ion burst. From the average drift time and spread of the ion bursts the mobilities and diffusion coefficients can theoretically be separately determined. An initial spread of the ion bursts caused by the crude nature of the present ion sources renders a realistic measurement of the diffusion coefficient impossible. Except for a lowering of resolution of this experiment the configuration of these bursts is such as to have little effect on the mobility measurement.

CHAPTER II

APPARATUS AND TECHNIQUES

The apparatus used in this experiment consists essentially of a drift tube containing several ion sources, two differential pumping chambers, a mass spectrometer, and various electronic components to count or otherwise analyze the ion current. The ion sources generate ions inside the drift tube. These ions drift under the influence of an electric field through whatever gas is in the drift tube until they arrive at one end of the tube. Here they stream out through a pin-hole into a series of two differential pumping chambers and finally into a mass spectrometer where ions of a given mass are counted. The two differential pumping chambers serve as successive pressure steps from the relatively high pressures of the drift tube to the low pressure required in the mass spectrometer. The electronic components amplify, count, and analyze the pulses taken from the mass spectrometer detector in several different ways depending upon the mode of operation being used. A more complete description of this apparatus may be found elsewhere.[40]

One of the unique features of this apparatus is the size of the drift tube. Ions may be allowed to drift through a gas several different distances, the largest of which is 37 centimeters, before being "analyzed". These distances are larger than the drift distances in any mobility experiments that have come to the author's attention and are an order of magnitude larger than most. The advantage gained by this feature is the ability to measure mobilities at lower pressures without reducing the product

of the pressure and the drift distance (pd) below acceptable limits. A second advantage is that ion-molecule reactions of interest, even those with very small reaction rates, will have an adequate opportunity to appear. The second named advantage turns out to also be a disadvantage in one respect. Minute traces of impurities, whose nature and origin will be discussed later, react with the ions of interest and indeed dominate the situation in the drift tube at higher pressures.

Apparatus

Drift Field and Ion Sources

An approximately uniform drift field is established in the central region of the drift tube by nine uniformly spaced steel rings called drift field electrodes and labelled E_1 - E_9 in Figure 3. Their shape can be seen better in Figure 4. The total voltage of the drift field is distributed uniformly between the drift field electrodes by the series string of resistors R_1 - R_9 each of which is a 100-ohm ceramic, glass encapsulated resistor except for R_1 which is two such resistors in series. Electrical contact to R_9 is made through a Kovar seal in the side of the drift tube; R_1 is grounded internally to the drift tube. The voltage for the drift field is provided by a Universal Electronics Regulated Power Supply, Model 300B. Drift field electrodes E_2, E_4, and E_6 each carry a grid consisting of vertical stainless steel wires spaced 1/5 inch apart to prevent the distortion of the drift field in the "downstream" direction caused by the adjacent ion source.

The drift tube contains four ion sources labelled S_A - S_D in Figure 3. Each source consists of a thoriated iridium filament and an anode. Each filament is bent in the shape of a V and projects downward from a

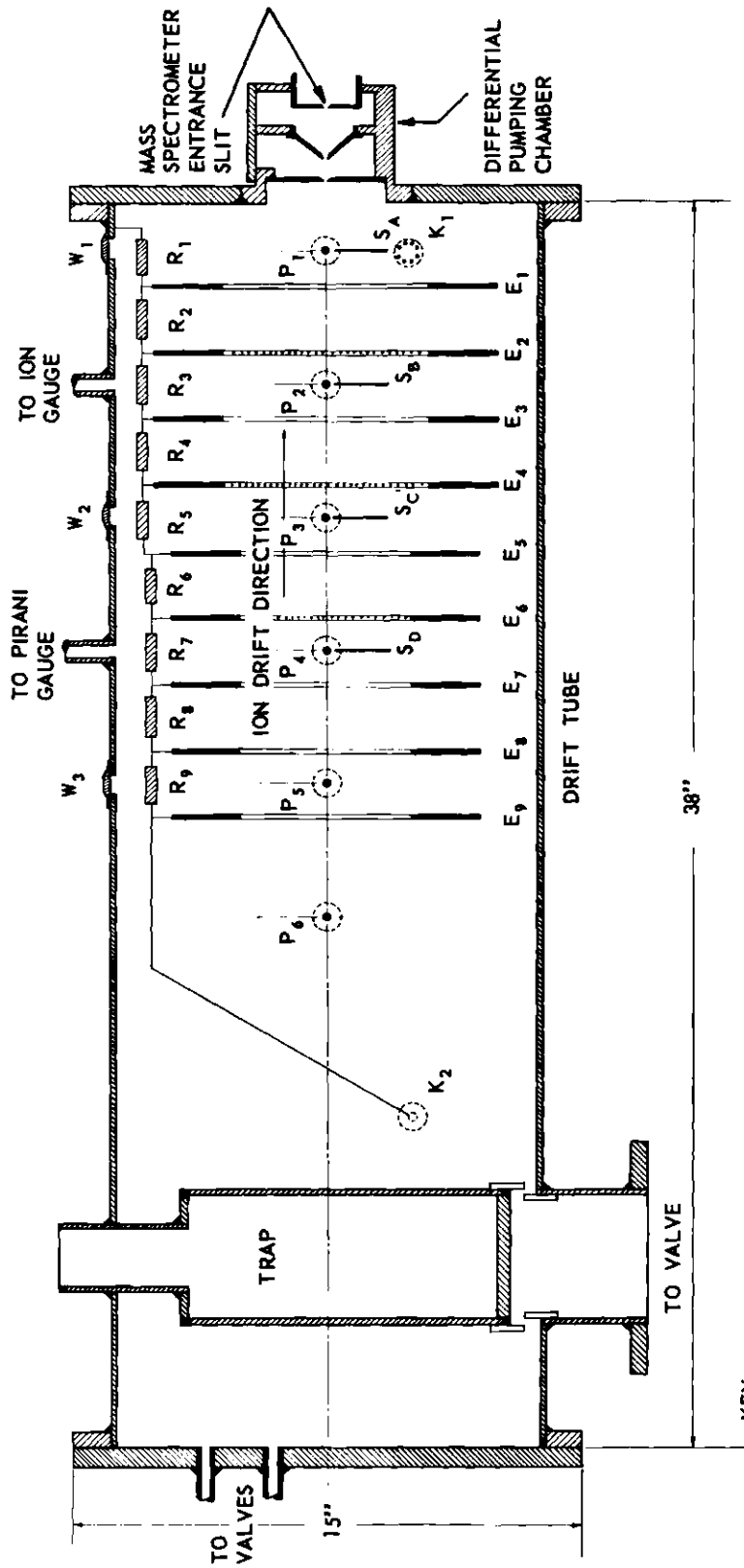

Figure 3. Vertical Section of the Drift Tube and Differential Pumping Chambers.

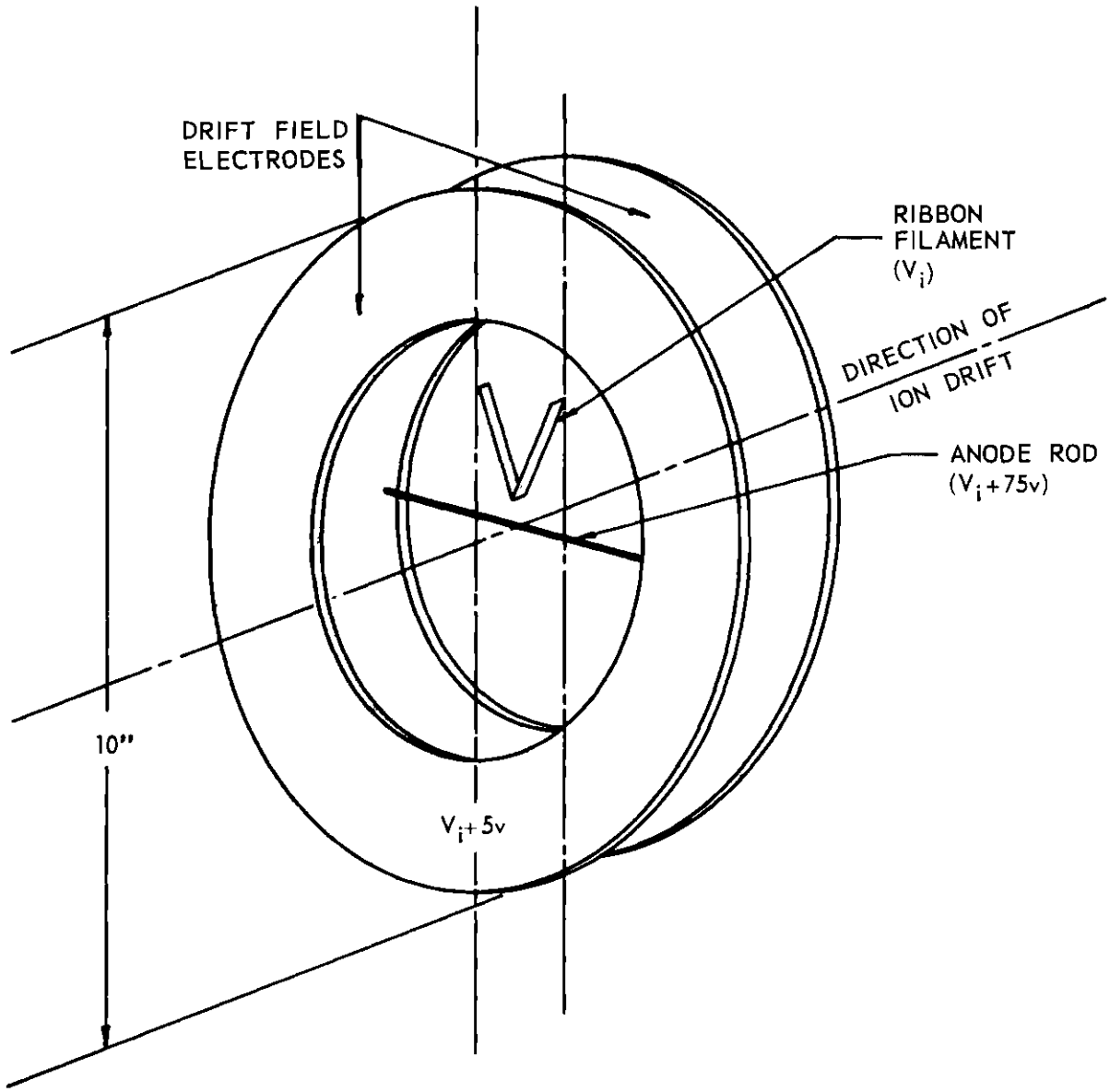

Figure 4. An Ion Source in Position Between Two Drift Field Electrodes.

mount attached to the drift field electrode immediately behind it so that its mean potential is nearly equal to the local potential of the drift field. Each anode consists of a straight cylindrical, gold plated, brass rod 0.040-inches in diameter which projects horizontally inward from a port opposite each source position.

Two basic experimental techniques are used in this experiment, one in which the source produces a relatively constant flow of ions and one in which the source produces ions in bursts. These techniques will be discussed in detail in the second part of this chapter.

In the first mode of operation the source was operated with a DC voltage of from 70 to 130 volts maintained between the anode and the filament by means of two B batteries and a potentiometer. The filament voltage was provided by a Variac and was further controlled by an emission regulator (Figure 5) which uses current collected by the anode as the controlling variable. In DC operation over a wide range of pressures it was attempted to hold the collected current constant at 0.10 ma, the anode voltage constant at some appropriate value, and to let the emission regulator control the filament voltage. It is believed that this technique held the ion production of the source relatively constant for small changes in pressure and made the ion production of the source go through the same history on successive runs over wide variations of pressure.

In the other mode of operation a square positive voltage pulse generated by a Stamford Electronics Company, TS 592A/UPM-15, pulse generator was imposed periodically in conjunction with a 20 volt DC voltage between the anode and the filament. The duration of the voltage pulse used was from 20 to 50 microseconds while its rate of repetition was varied, depending on circumstances, from 49 to 400 cycles per second.

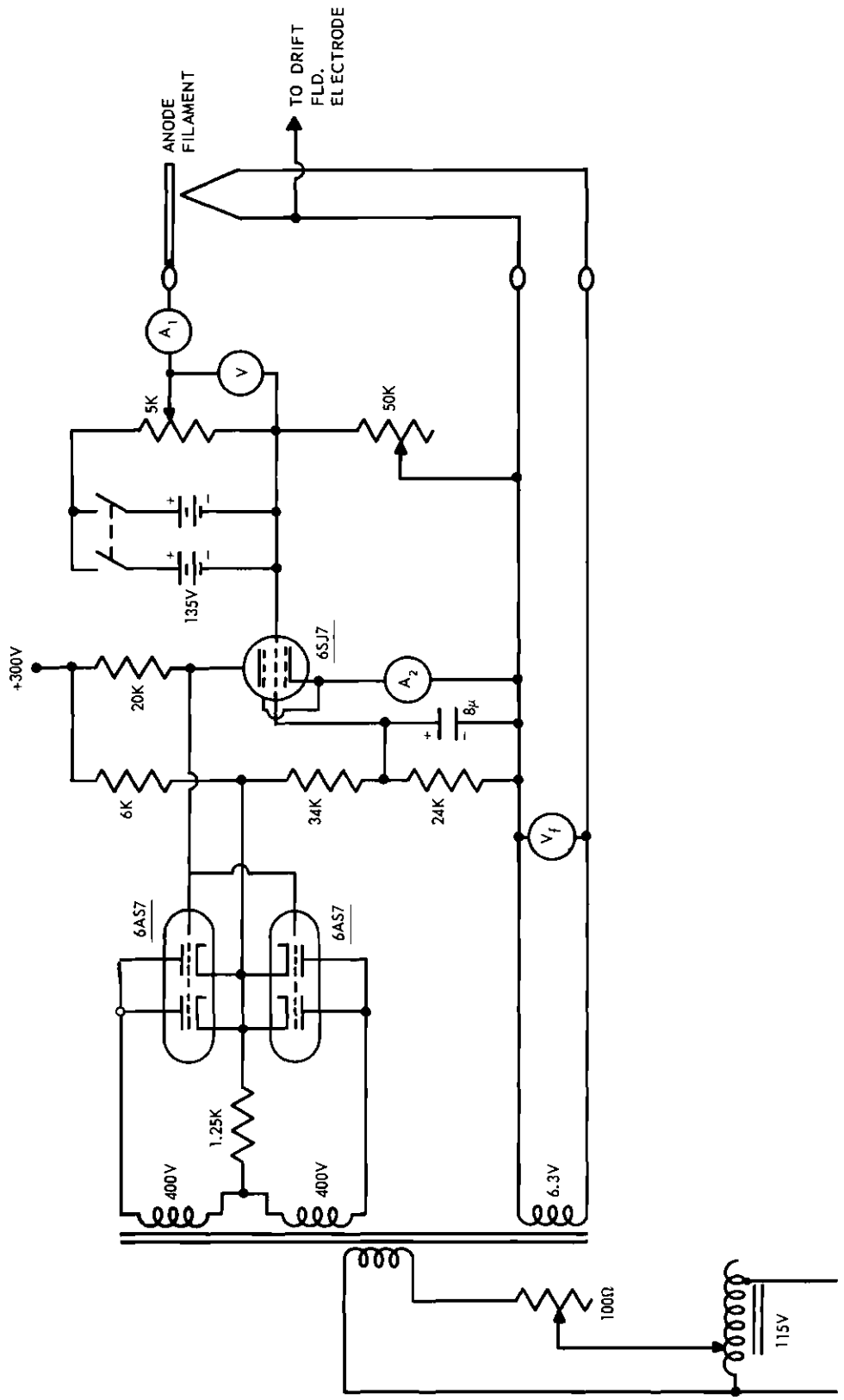

Figure 5. Emission Regulator Circuit for the Ion Source.

The magnitude of the voltage pulse was adjusted to the minimum value giving an adequate supply of ions which usually put it somewhere between 50 to 100 volts. In this mode of operation the filament voltage was adjusted to give the optimum number of ions but was otherwise unregulated. The relative positions of anode and filament can be see in Figure 4.

As a practice the same anode voltage is used wherever possible for a complete series of runs to eliminate this as a variable. Over a period of several weeks of continuous running, however, the minimum anode voltage at which enough ions are generated gradually increases. When anodes that have "aged" in this way are removed from the apparatus considerable discoloration is found, especially on the part nearest the filament. It is known that hydrocarbon vapor polymerizes when subject to electron bombardment and forms semi-conducting or non-conducting layers on metallic surfaces.[41]

It is thought that pump oil or other heavier impurities may, over a period of weeks, form a thin non-conducting layer on the surface of the anode as a result of chemical reactions connected with source activity. This layer might also contain metallic oxide from the metal on the surface of the anode. Before the anodes were gold plated the brass surfaces of the anode were exposed and the "aging" process took place much more quickly. Such a non-conducting layer would accumulate a surface charge and would prevent conduction of the electrons to the anode thus causing a negative space charge to build up in the neighborhood of the anode weakening the anode field in this vicinity. It is thought that as the portion of the anode surface nearest the filament becomes contaminated the ionizing activity of the source must move out the anodes in

either direction towards the sides of the drift tube where losses due to diffusion of ions against the side will be greater. As the centers of ionizing activity move away from the filament and, hence, from the electron cloud a larger anode voltage becomes necessary to draw the same collected current to the anode. It is noted that the apparent ion population at the pin-hole at a given pressure diminishes slowly over a period of weeks even though the collected current is maintained at 0.10 ma.

Gas Control System

Gas is admitted to the drift tube through either of two openings in the rear wall. Copper feed lines (3/8 inch in diameter) lead from these openings first to cut-off valves then to Edwards High Vacuum, Ltd., needle valves. The hydrogen and nitrogen used in these experiments is prepurified gas prepared by the Matheson Company, Inc., and Matheson regulator valves are used on both tanks. The feed line from the regulator valves to the needle valves is 1/4-inch copper tube, and a section of each line is coiled into a spiral of about 8 turns 1/2 inch in diameter which may be inserted into a bath of acetone and dry ice for the purpose of trapping out condensibles.

Gas leaves the drift tube normally through either of two openings, a line entering the bottom of the drift tube near the rear wall and the pin-hole in the forward end of the drift tube leading to the differential pumping chambers.

The drift tube may be quickly evacuated by means of a mechanical pump which is connected to the drift tube through the line entering the bottom of the drift tube. This line consists of a 3/4 inch copper tube containing a Jamesbury ball cut-off valve immediately below the drift tube followed by a U-bend which may be immersed in liquid nitrogen as a

safeguard to prevent condensible impurities from being carried from the mechanical pump into the drift tube by back-streaming. The mechanical pump used to pump the drift tube is a Duo-Seal Vacuum Pump, Model 1402-B, made by the W. M. Welch Manufacturing Company. The other two mechanical pumps used with this apparatus are of the same type.

During operation gas from the drift tube streams through a 1/32-inch pin-hole in the forward end of the drift tube into the first differential pumping chamber. The jet emerging from the pin-hole fans out and changes rapidly from viscous flow to essentially molecular flow as the density of the gas decreases. A second pin-hole of the same diameter leading into the second differential pumping chamber is located on the axis of the jet and 1.5 cm from the first pin-hole. It is estimated that only 0.1 per cent of the ions and molecules issuing from the first pin-hole passes through the second. The stream of ions and molecules is further collimated by passing through a slit (1/16 inch by 1/2 inch) leading into the mass spectrometer tube. The mass spectrometer tube and the second differential pumping chamber are each pumped by individual 2-inch Consolidated Electrodynamics Corporation MCF-60 oil diffusion pumps. The first differential pumping chamber is pumped by a similar 4-inch pump, type MCF-300. These diffusion pumps are backed through a common fore line by a mechanical pump of the type described above and each pumps its respective chamber through a baffle and a cold trap which is normally iced with a mixture of dry ice and acetone.

It is desired in this experiment that collisions between ions and molecules in the differential pumping chambers be at substantially the same energies as similar collisions in the drift tube. The purpose of

this was to keep ions, stable at collision energies in the drift tube, from being decomposed by more energetic collisions in the differential pumping chambers. To achieve this result it was deemed necessary to use no electrostatic or electromagnetic focusing in the differential pumping chambers even though this resulted in a low efficiency of transmission of ions from the drift tube to the mass spectrometer. At this point in the system stray electrostatic fields or variations in the small component of the magnetic field of the mass spectrometer which manages to penetrate the differential pumping chambers can cause the ion count rate at the mass spectrometer detector to vary by hundreds of per cent. All important surfaces inside the differential pumping chambers are gold plated to render the chambers as free as possible from electrostatic fields and are carefully shielded from the magnetic field of the mass spectrometer by foils of high permeability alloy.

The pressures in the drift tube line and in the common fore line for the three diffusion pumps are monitored by individual Veeco thermocouple gauges. The pressure in the mass spectrometer tube is measured by means of a Veeco ionization gauge, type RG-75. The two thermocouple gauges and the ionization gauge are read on the panel of a Veeco Vacuum Gauge, type RG-31A. The drift tube pressure may be monitored continuously over a range of from 1 micron to 2000 microns by means of a Consolidated Electrodynamics Corporation Pirani vacuum gauge, type 2201-03, which is calibrated or spot checked with a Consolidated Electrodynamics McLeod Vacuum Gauge, type GM-100A. The sensing element of the Pirani gauge enters the drift tube through an opening in the top above source C. The McLeod gauge has access to the drift tube through a cold trap, a cut-off valve, and the port P_6.

The drift tube contains an internal trap in the form of a stainless steel bottle which projects down into the rear end of the drift tube and may be filled with liquid nitrogen. The purpose of this trap is to reduce the level of condensible impurities in the drift tube to a very low level. A brass cup and sleeve baffle covering the opening leading to the drift tube pump is mounted on the bottom of the bottle to assure efficient trapping of impurities backstreaming from the mechanical pump.

The McLeod gauge was used to investigate the amount and kind of impurities present in the drift tube. Since condensible impurities might have an effect on the accuracy of the McLeod gauge great care was exercised in its use at all times to prevent such condensible impurities from getting into its central column. From time to time it became necessary to remove the McLeod gauge from the apparatus. At these times when the McLeod gauge was open to the atmosphere it was most convenient to have all the mercury down in the flask at the bottom of the gauge thus exposing the interior of the central column to the atmosphere. Upon reinstallation and after evacuation, the McLeod gauge cold trap was iced with liquid nitrogen while it was attempted to drive condensibles out of the central column by heating it several times gently with an acetelyne torch. Upon completion of this operation the mercury was allowed to rise sealing off the central column and was never lowered unless the trap was iced.

During the investigation involving hydrogen, nitrogen played an important role as an impurity. Although nitrogen had been used in the drift tube from time to time it is believed that this nitrogen came mostly through leaks to the atmosphere and not primarily from outgassing of the metal parts on the inside of the drift tube. The drift tube was pumped

continuously for several days and heated to moderate temperatures several times between the times it contained nitrogen and the times that any serious investigation of hydrogen was attempted. Pressure measurements were taken with the McLeod gauge at regular intervals over 8 and 9 hour periods while the system was being pumped continuously through the 1/32-inch pinhole leading into the differential pumping chambers. Under such conditions the McLeod gauge gave pressure readings of less than 10^{-4} torr. If the atmosphere in the drift tube was mostly condensible vapors, putting liquid nitrogen in the internal drift tube trap would cause an abrupt drop in pressure by freezing out most of the condensible vapor. When a test was tried, a drop in pressure of less than 20 per cent resulted. This drop could be accounted for by the mere chilling of the gas residue in the drift tube even if no condensible vapors were present. This residual pressure increased about 40 per cent when the anodes were removed for cleaning and then put back in the drift tube indicating that the seating of the teflon gaskets in one or more of the anode ports was not quite as good as before the removal. For all of the above reasons it was concluded that the residual gas in the drift tube was mostly air.

When one of the source filaments was turned on, the pressure in the drift tube jumped in about an hour to over a micron. When liquid nitrogen was placed in the internal drift tube trap under these conditions the pressure went down below 0.2 microns within a half an hour. In this case it is believed that condensible impurities were evaporated off of the metal surfaces inside the drift tube by the thermal radiation of the filaments. Examination of the mass spectrum before and after placing liquid nitrogen in the drift tube trap during ordinary operation suggests that these condensible impurities are mostly pump oil vapor. A mass

spectrum with any gas in the drift tube and with the internal drift tube trap not filled will display mass peaks at almost all mass numbers from 12 to 60 excluding only a few. This spectrum would be the cracking pattern of pump oil superimposed on the mass spectrum of water and whatever gas was in the drift tube. When liquid nitrogen is placed in the internal drift tube trap most of these peaks disappear leaving only the mass spectrum of water and whatever gas (including impurities) is in the drift tube.

Mass Spectrometer and Counting Apparatus

The mass spectrometer is basically of the Nier 1947 type[42] employing a 60° wedge-shaped field and has a resolution of about 1 per cent. The accelerating voltage is supplied to the ion gun by a Beva Laboratory Model 301 1-5.1-kv power supply modified to permit linear voltage scanning at any of nine predetermined speeds corresponding to periods ranging from 20-sec to 85-min. The resistor network, shown on Figure 6, associated with the ion multiplier power supply, is designed to maintain proper focusing and to supply post acceleration so that all ions enter the ion multiplier tube with roughly the same energy. A Sensitive Research 0-3000-volt electrostatic volt-meter is used to measure the accelerating potential. The magnetic field is variable from 0 to 6000-gauss.

A Dumont 12-stage ion multiplier with silver-magnesium dynodes serves as the detector at the end of the spectrometer tube. An unmodified Beva power supply of the type used for the ion gun supplies power to the network (Figure 6) associated with the ion multiplier.

The exit aperture from the mass spectrometer tube is neither wider than the incident ion beam nor is it extremely narrow compared with the

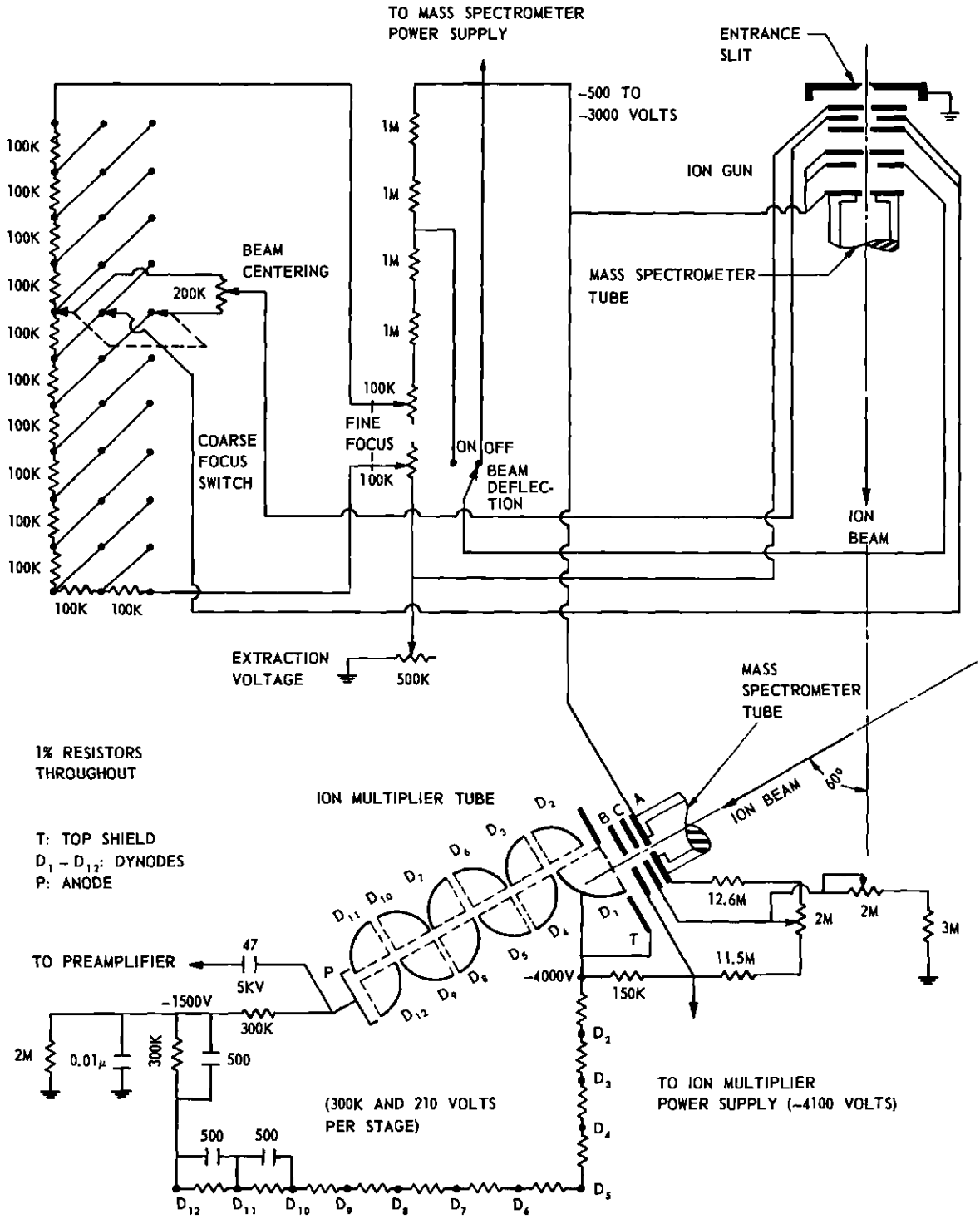

Figure 6. Mass Spectrometer Tube Circuitry.

width of the beam so that the peaks obtained on a typical voltage sweep are neither flat topped nor do they represent the relative ion intensities in different parts of the cross-section of the beam. Thus the peak heights, i.e., the total ion fluxes falling on the exit aperture with each of several ion beams centered in turn on the exit aperture, do not provide a true measure of the relative ion populations in the neighborhood of the drift tube pin-hole without extensive corrections for variable resolution. However, in view of the sensitiveness of the count rate to small electric and magnetic field variations around the slit system it was concluded that true relative ion populations could not really be obtained in any case. Therefore, the relative peak heights of the several ion species in the spectrum have been taken as rough indicators of the relative populations without making any corrections. Attention is centered not so much on the absolute magnitude of the peak heights as on the shifts in the relative peak heights which result from changes in the experimental parameters.

The magnetic field of the mass spectrometer was initially measured with a Harvey-Wells nuclear magnetic resonance gauss meter. As work progressed the magnetic field was calculated from the voltages at which various peaks in the several familiar mass spectra appeared.

Pulses taken from the anode of the multiplier tube are sent through a preamplifier into a linear amplifier, Baird Atomic Models 219A and 218, respectively.

In the steady state mode of operation the output of a pulse height discriminator at the output of the linear amplifier goes to a binary scaling unit, Nuclear Chicago Model 161A, and a tap from the scaling factor selector leads to a count rate meter, Nuclear Chicago Model 1620, and

thence to a Wheelco Model 8000-500 pen recorder, where the spectra or count rate variations are continuously mapped. The count rate that this system can handle has an absolute upper bound of about 136,000-counts/sec., being limited by the response time of the first binary scaling stage of the scaling unit.

In the pulse mode of operation the output of the linear amplifier goes to an Eldorado Electronics, System 1500, twenty channel time analyzer whose timing is triggered by the same pulses that operate the ion source.

The chief sources of noise in this system are electronic noise in the preamplifier unit and static introduced through the wall circuits into the Beva power supplies and the preamplifier unit. The electronic noise from the preamplifier unit is adequately eliminated by the setting of the discriminator of the linear amplifier; the setting used throughout this research reduced the count rate from this source below 500 counts/day. Line static is spasmodic, coming in bursts of from several counts/sec to several hundred counts/sec at unpredictable times throughout the day. Bursts of static are more common during normal working hours than at other times, and integrated counts over periods of 24 hours have ranged from about 1000 to about 5000-counts. Such static bursts are easily distinguishable from peaks obtained while running a DC spectrum because of their narrow shape. All of the electronic units previously mentioned which effect the conditions inside the drift tube, the functioning of the mass spectrometer, or the count rate are supplied with line voltage by a Sorensen Model 2000S AC voltage regulator. This regulator stabilizes the voltage imput of these units against long, slow variations of the line at about 115-volts but is of no use whatever in filtering out abrupt changes or bursts of static.

Experimental Techniques

Steady State Mode of Operation

The steady state mode of operation was used in the first phase of the investigation to determine qualitatively the ion-molecule reactions taking place in the drift tube by mapping the change in the relative densities of the various observed ions with pressure. The steady state mode of operation used in these experiments is basically as follows: The mass spectrometer is set to monitor one of the peaks of interest in the mass spectrum. Gas is admitted to the drift tube until the pressure reaches such a value that no significant number of ions are reaching the ion multiplier from the source being used. No more gas is admitted during the run, and the drift tube is allowed to pump through the pin-hole from this high initial pressure down to a very low pressure, the ball valve in the rear fore line being kept closed during this operation. Graphs of pressure vs time averaged from several runs indicate the pumping speeds at various pressures for nitrogen (Figure 7). The data taken during this pump-down consists of:

a. A continuous relative measurement of the ion density in the neighborhood of the pin-hole in the form of a graph produced by the pen recorder.

b. A set of Pirani readings marked opposite the points of occurrence on the pen recorder graph.

c. A set of McLeod readings corresponding to some of the Pirani readings (1 in 2 or 1 in 3). The variations of the several ion density measurements or combinations of these measurements are then compared to attempt to determine the ion-molecule reactions taking place in the drift tube.

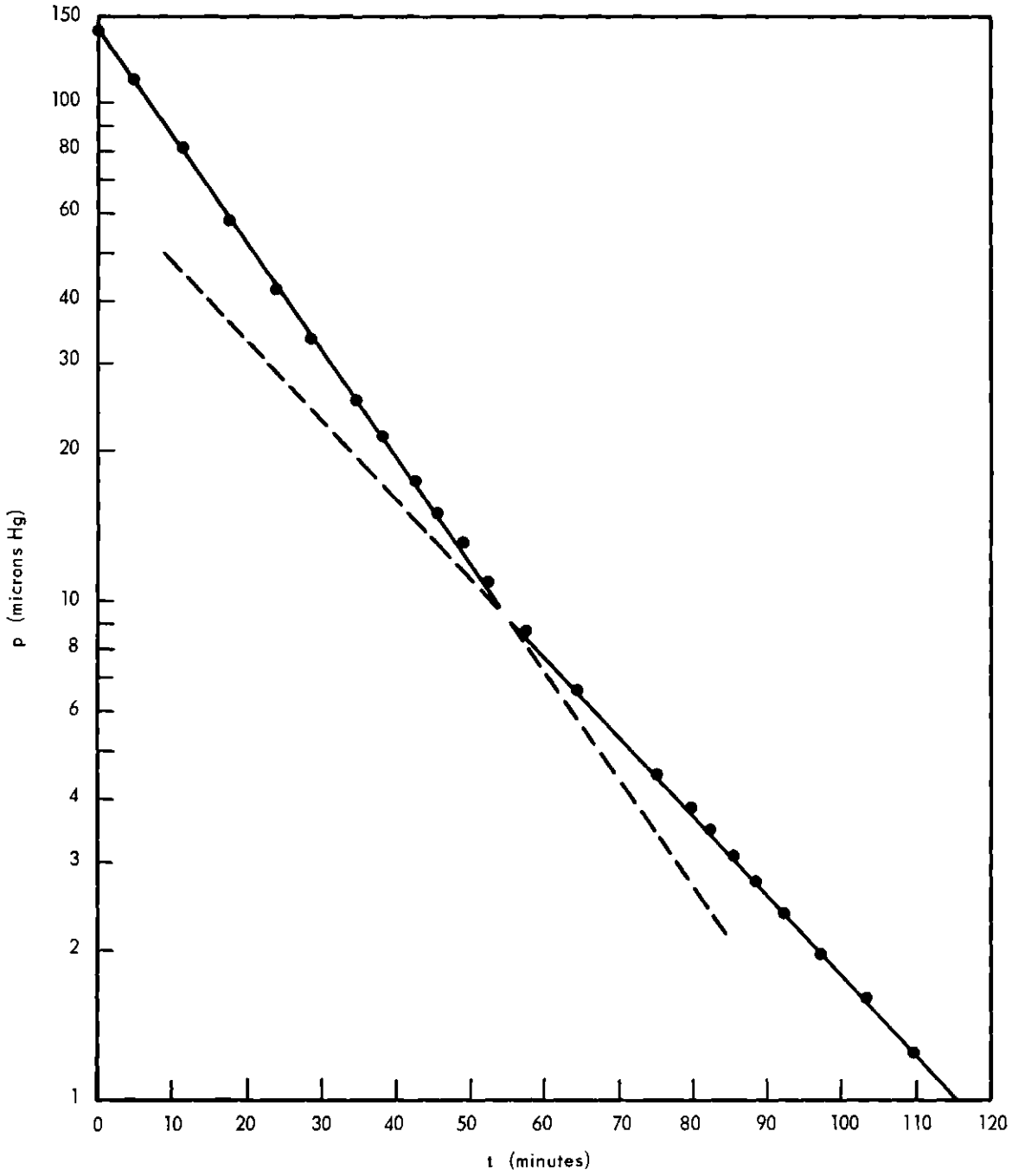

Figure 7. Drift Tube Pressure Vs. Time for a Filling of Nitrogen Leaking Through the Pin Hole.

The Pirani gauge used to measure the pressure in the drift tube has two scales, 0-50 microns and 0-2000-microns. The meter scales have marks on them as follows:

0-50	1,2,3,4,5,6,7,8,9,10,15,20,25,30,35,40,45,50
0-2000	50,75,100,125,150,175,200,250,300,400,500,700,1000,1500,2000

The Pirani gauge is always read when the pressure reading is one of the above marks and a simultaneous McLeod reading is taken if possible. Both readings are recorded opposite the corresponding point on the pen recording. A graph of Pirani vs McLeod readings is prepared each day from which a table of true pressures is prepared to go with the ion density measurements for that day. The several McLeod readings taken on a given day for a given Pirani reading seldom vary more than 2 per cent from one another and never more than 3 per cent except for the 1000, 1500, and 2000-micron readings which may vary 5 per cent or even more in the case of 1500 and 2000 microns. There are several reasons for these variations: First, the Pirani gauge cannot be read any closer than 1 per cent notwithstanding the fact that readings are made only on scale marks. Second, the Pirani gauge usually exhibits a small drift in calibration over the period of a day and, sometimes, a considerable drift over a period of several days.

Because of this drift in the calibration of the Pirani gauge over a period of several days in which both the slope and the shape of the calibration curve may change somewhat, corresponding ion density measurements taken on different days may be taken at slightly different pressures. To resolve these differences graphs of ion density measurements vs corrected pressures are made for each run on each day, and the relative ion densities

corresponding to a predetermined set of pressures are taken from these graphs. For simplicity the predetermined set of pressures used are the scale readings of the Pirani. Ratios and other meaningful mathematical combinations of corresponding relative ion densities may now be formed under the assumption that the pressures at which these relative ion densities occurred did not differ from one another by more than about 2 per cent.

The source is operated in such a way as to keep the apparent current collected at the anode constant at 0.10-ma. Stabilization of the collected current at this value is accomplished by controlling the filament voltage with an emission regulator (Figure 5), and with occasional manual adjustment of the filament supply voltage. The resistance of the filaments themselves is about 0.2-ohm cold and of the order of 1-ohm while in operation. The anode voltage is set at a value that will give a collected current of 0.10-ma with a filament current within the range of the apparatus. Because of the approximately cylindrical symmetry of the anode field in the region in which most of the ions are generated it is impossible to distinguish between the various ions on the basis of appearance potentials.

In this mode of operation attention is focussed on the variation of the relative ion currents with pressure to provide a qualitative indication of the various ion-molecule reactions taking place in the drift tube.

Pulse Mode of Operation

The pulse mode of operation was used to measure the mobility of the various ions in nitrogen during the second phase of the investigation. In

this mode of operation nitrogen is admitted to the drift tube at such a rate that equilibrium between the rate of flow of the nitrogen into and out of the drift tube is achieved at some predetermined pressure. This pressure is selected to correspond to one of the Pirani meter readings and is checked as often as possible with the McLeod gauge, the McLeod gauge readings being treated statistically to determine the actual pressure and the accuracy with which this pressure is known. The square voltage pulse is applied periodically between the anode and the filament. The effect of this pulse is enhanced by a supplementary DC potential of 20 volts. The ion burst generated by this pulse is drawn towards the pin-hole by the drift voltage.

The mass spectrometer sorts the ions as to mass while the time analyzer sorts them according to drift time from the source to the ion multiplier tube. The distribution of ions as a function of drift times is analyzed to determine the mobility and other transport properties of the particular ions being studied.

CHAPTER III

MATHEMATICAL FORM AND EVALUATION OF THE DATA

The evaluation of the data falls into two steps. First, the mathematical expression for the behavior of a burst of ions in a gas under the influence of an electric field is derived. In making this derivation it is assumed that the basic assumptions of diffusion theory may be applied. In the case of this experiment this means that the ions and molecules both have approximately a Maxwellian distribution of velocities and that the electric field and the pressure are within such ranges that the energies acquired by the ions from the electric field between collisions are very small compared to their thermal energies. In the ranges of electric field and pressure where the assumptions of diffusion theory do not apply, the concept of mobility has no meaning. In the second step in the evaluation of the data the mathematical expression derived above is fitted to the data by adjusting several of its parameters, one of which happens to be the mobility, using either one of two statistical methods, R. A. Fisher's method of maximum likelihood and the method of least squares. The advantages and disadvantages of these two methods will be discussed in later sections of this chapter. A table of values of K computed by these two methods is given in Appendix B.

Basic Equations of the System

In formulating and solving the basic equations for the behavior of the ion bursts, the following assumptions are made implicitly or explicitly:

(1) The gas in the drift tube is of one kind with only minute traces of impurities. (The level of impurities is not great enough to affect the ionic mobility itself appreciably but reactions with the impurities might affect the mobility measurements by changing the time spectrum.)

(2) The gas in the tube has approximately the dielectric coefficient of empty space,

(3) The effects of diffusion may be adequately described by the use of a diffusion coefficient. A diffusion tensor is not necessary,

(4) All magnetic fields are small enough to be ignored,

(5) The geometry of the system is approximately cylindrical with the z-axis coinciding with the axis of the drift tube,

(6) The ions whose mobilities are being measured are formed in the vicinity of the ion source, that is, they are primary ions or they are secondaries which have been formed in reactions having very large reaction rates,

(7) Mutual repulsion plays no significant role, and

(8) Ions of the species under consideration may be changed to ions of different species in ion-molecule reactions with neutral molecules of various kinds in the drift tube (but none are being created in ion-molecule reactions).

If the electric field and pressure are within such a range that diffusion theory applies then the equation of motion of the ion population is given by

$$\underline{J} = -D \nabla n + K\underline{E}n \qquad (16)$$

where n is the ion (charge) density of one of the primary ions, $\underline{J}$ is the current density of that ion, D is its diffusion coefficient, and K is its mobility. The first term in equation (16) describes the current density due to diffusion (Fick's law) while the second term gives the expression for the current density due to the migration of ions under the influence of an electric field at low E/p where p is the pressure. Strictly speaking this and all subsequent formulas to be derived from it are valid only at low values of E/p. A population of primary ions is also subject to an equation of continuity of the form

$$\nabla \cdot \underline{J} + \sum_i \alpha_i \sigma_i n + \frac{\partial n}{\partial t} = 0 \qquad (17)$$

where $\sum_i \alpha_i \sigma_i$ is the combined effect of all reactions using up ions of the species under consideration. The α_i are the rate constants for these reactions, and the σ_i are the densities of the molecular species with which the ions are reacting. Let $A = \sum_i \alpha_i \sigma_i$. The combination of these equations gives the partial differential equation of the system,

$$-D \nabla \cdot \nabla n + K \nabla \cdot (\underline{E} n) + An + \frac{\partial n}{\partial t} = 0 \quad . \qquad (18)$$

Solution of the Equation of the System for the Pulse Mode of Operation

In view of the assumption of no mutual repulsion, $\underline{E}$ shall be taken as uniform and parallel to the axis of the drift tube. If cylindrical symmetry is assumed then equation (18) becomes, when expressed in cylindrical coordinates,

$$-D \frac{\partial^2 n}{\partial r^2} - \frac{D}{r} \frac{\partial n}{\partial r} - D \frac{\partial^2 n}{\partial z^2} + KE \frac{\partial n}{\partial z} + An + \frac{\partial n}{\partial t} = 0 \quad . \tag{19}$$

To separate variables we let

$$n(r,z,t) = R(r)\, Z(z,t) \quad . \tag{20}$$

Further decomposition of $Z(z,t)$ is not attempted since the particular initial condition that will be applied will produce a solution which is not completely factorable into functions of z and t. The substitution (20) leads to the equation

$$\frac{D}{R} \frac{\partial^2 R}{\partial r^2} + \frac{D}{rR} \frac{\partial R}{\partial r} = - \frac{D}{Z} \frac{\partial^2 Z}{\partial z^2} + \frac{KE}{Z} \frac{\partial Z}{\partial z} + A + \frac{1}{Z} \frac{\partial Z}{\partial t} = -m^2 \quad , \tag{21}$$

or

$$r^2 \frac{d^2 R}{dr^2} + r \frac{dR}{dr} + s^2 r^2 R = 0 \tag{22}$$

where

$$s = mD^{-1/2} \quad , \tag{23}$$

$$-D \frac{\partial^2 Z}{\partial z^2} + KE \frac{\partial Z}{\partial z} + \frac{\partial Z}{\partial t} + (A + s^2 D)\, Z = 0 \quad . \tag{24}$$

The r-equation above is the zeroth order Bessel's equation whose solution is

$$R(r) = C\, J_o(sr) \quad . \tag{25}$$

To solve the z-equation we let

$$Z(z,t) = \frac{1}{\sqrt{2\pi}} \int_{-\infty}^{\infty} f(k,t) \exp(ikz)dk \quad . \tag{26}$$

Substitution of this in the z-equation gives a partial differential equation

$$\frac{\partial f(k,t)}{\partial t} + M f(k,t) = 0 \tag{27}$$

where $M = Dk^2 + ikKE + A + s^2D$. The solution of this equation is

$$f(k,t) = f_o(k) \exp(-Mt) \quad . \tag{28}$$

In this expression $f_o(k)$ is the Fourier transform of the function $Z(z,0)$ which gives the distribution of the ions along the axis of the drift tube when $t = 0$. Hence

$$Z(z,t) = \frac{\exp[-(A + s^2D)t]}{\sqrt{2\pi}} \int_{-\infty}^{\infty} f_o(k) \exp[-Dk^2t + ik(z-KEt)]dk \quad . \tag{29}$$

If the time duration of the square voltage pulse is kept small the shape of the initial burst of ions may be described, to a first degree of approximation, by a Dirac delta function. If we let $Z(z,0)$ be a Dirac delta function we will have a normal or bell-shaped ion distribution in z immediately (for all values of t greater than zero). Hence let $f_o(k) = \frac{N_o}{\sqrt{2\pi}}$ where N_o is the number of ions in the original burst. Then $Z(z,0) = N_o\delta(z)$, and $Z(z,t)$ may be expressed in the form

$$Z(z,t) = Z_1(z,t) + iZ_2(z,t) \tag{30}$$

where

$$Z_i(z,t) = \frac{N_o}{2\pi} \exp[-(A + s^2D)t] \int_{-\infty}^{\infty} \exp(-Dk^2t) \cos k(z-KEt)dk \tag{31a}$$

and

$$Z_2(z,t) = \frac{N_o}{2\pi} \exp[-(A + s^2D)t] \int_{-\infty}^{\infty} \exp(-Dk^2t) \sin k(z-KEt)dk \quad . \tag{31b}$$

$Z_2(z,t)$ above is zero since $\exp(-Dk^2t)$ is an even function of k and $\sin k(z-KEt)$ is odd. $Z_1(z,t)$ may be evaluated by reference to a table of integrals.[43]

$$Z(z,t) = \frac{N_o}{\sqrt{4\pi Dt}} \exp\left[-(A + s^2D)t - \frac{(z-KEt)^2}{4Dt}\right] \quad . \tag{32}$$

Thus the complete description of the ion density function is given by

$$n(r,z,t) = \frac{N_o}{\sqrt{4\pi Dt}} \sum_i C_i J_o(s_i r) \exp\left[-(A + s_i^2 D)t - \frac{(z-KEt)^2}{4Dt}\right] \quad . \tag{33}$$

To evaluate the s_i it will be assumed that $n(r,z,t)$ is zero at some fixed value of r because of the loss of ions against the electrodes and sides of the drift tube. In the expression (33) above the Bessel function in the first term will have its first zero at this value of r; the Bessel function in the second term will have its second zero at this value of r; etc. The C_i are determined by the initial radial distribution of the ion burst. In This experiment the initial distribution of the ion burst is not precisely

known. Its effect on our results will be discussed later. The reason that the use of formula (41) based on a Dirac delta function model is still considered justified is that any ion cloud initially restricted to a bounded volume of space but otherwise arbitrarily distributed will approach a form represented by the first term of (33) asymptotically with increasing time because of the effect of diffusion. In our case we obtain a false value of D because of the initial distribution of the cloud.

Distributions for other possible initial ion distributions are given as Appendix C.

Normalization of the Distribution in Time

The solution (33) above gives the ion population density throughout the drift tube as a function of r,z, and t. From this density function it is desired to construct a time distribution function for ions passing through the pin-hole. This function, f(z,t), gives the probability that an ion generated at the source at t = 0 and passing through the pin-hole will be counted by our equipment between the times t and t + dt. Here z is the distance from the source to the pin-hole.

The total number of ions from any given ion burst that eventually pass through the pin-hole is proportional to

$$N(z) = \int_0^\infty n(0,z,t)dt \quad , \quad \text{or} \tag{34}$$

$$N(z) = \frac{N_o}{2\pi}\sum_i C_i \int_0^\infty \exp[-(A + s_i^2 D)t] \int_{-\infty}^{\infty} \exp[-Dk^2 t + ik(z-KEt)]dkdt \tag{35}$$

Integration with respect to time gives

$$N(z) = \frac{N_o}{2\pi} \sum_i C_i \int_{-\infty}^{\infty} \frac{\exp(ikz)\, dk}{Dk^2 + ikKE + (A+s_i^2 D)} \quad . \tag{36}$$

After D is factored from the denominator of each term in the above series, the denominator may then be written

$$k^2 + ik\frac{KE}{D} + \frac{A + s_i^2 D}{D} = (k - k_1)(k - k_2)$$

where

$$k_1 = -\frac{iKE}{2D}\left[1 + \sqrt{1 + 4D\left(\frac{A + s_i^2 D}{K^2 E^2}\right)}\right] \tag{37a}$$

and

$$k_2 = -\frac{iKE}{2D}\left[1 - \sqrt{1 + 4D\left(\frac{A + s_i^2 D}{K^2 E^2}\right)}\right]. \tag{37b}$$

Thus the integrand of the above integral has poles on the imaginary axis, one in the upper half-plane and one in the lower. $z > 0$ corresponds to the case where the drift field E is towards the pin-hole. For $z > 0$ a path of integration (Figure 8) may be chosen starting on the real axis at B, going up the real axis to A, and then passing in a semi-circle in the upper half-plane to B. This path passes around the pole at k_2 and the contribution to the integral by the semi-circular part of the path approaches zero as $A \to +\infty$, $B \to -\infty$, and as the radius of this path approaches infinity. The residue at k_2 is

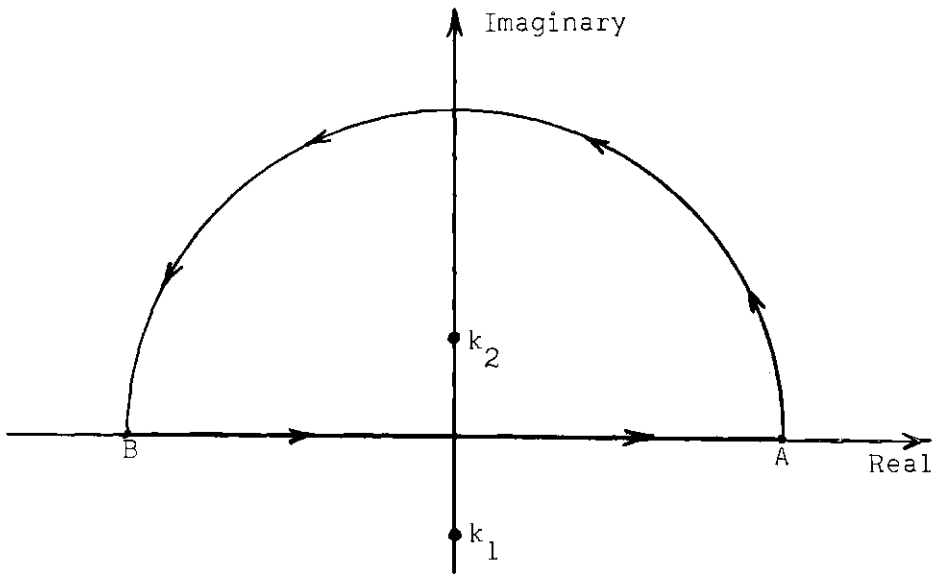

Figure 8. Contour of Integration.

$$R_{i2} = -\frac{\frac{iD}{KE}\exp\left\{\left(1 - \sqrt{1 + 4D\left(\frac{A + s_i^2 D}{K^2E^2}\right)}\right)\left(\frac{zKE}{20}\right)\right\}}{\sqrt{1 + 4D\left(\frac{A + s_i^2 D}{K^2E^2}\right)}} \quad . \tag{38}$$

If we may make the assumption that $K^2E^2 >> 4(A + s_i^2 D)D$ for all s_i's of importance then

$$R_{i2} = \frac{iD}{KE}\exp\left[-\frac{(A + s_i^2 D)z}{KE}\right] \quad . \tag{39}$$

This assumption will be justified by results. The total number of ions arriving at the pin-hole from any given pulse is proportional to

$$N(z) = \frac{N_o}{KE} \sum_i C_i \exp\left[-\frac{(A + s_i^2 D)z}{KE}\right] . \qquad (40)$$

The fraction arriving between t and t + dt is $\frac{n(0,z,t)}{N(z)}\, dt = f(z,t)\, dt$. For any reasonable initial distribution of ions about the source we should have $C_i \ll C_1$ for $i > 1$. Furthermore s_2^2 is approximately four times as large as s_1^2 and the rest of the s_i^2 are even larger so the higher terms decay and vanish much faster than the first. For a first approximation let us take $C_1 = 1$, $C_i = 0$, for all $i > 1$. This is equivalent to representing the initial radial distribution by the Bessel function having its first zero at the cylindrical boundary of the system. This gives

$$f(z,t) = \frac{KE}{\sqrt{4\pi Dt}} \exp\left[\frac{(A + s_1^2 D)(z - KEt)}{KE} - \frac{(z - KEt)^2}{4Dt}\right] . \qquad (41)$$

Statistical Estimators for K, D, and A

The function (41) above has been put in the form of a statistical distribution having a form which we hope from a priori considerations will represent the distribution of ions according to time of drift. A method frequently used to estimate the parameters of such a distribution function from the experimental distribution of data is called the method of maximum likelihood.[44]

To find the maximum likelihood estimators for K, D, and A we maximize the function L where

$$L = \log \prod_{i=1}^{N} f(z,t_i) = \sum_{i=1}^{N} \log f(z,t_i) \qquad (42)$$

by varying parameters. Equating the partial derivatives of L with respect to K, D, and A to zero gives

$$\frac{\partial L}{\partial K} = \frac{N}{K} - \frac{NAz}{K^2E} - \frac{Ns^2Dz}{K^2E} + \frac{NzE}{2D} - \frac{KE^2}{2D}\sum_{i=1}^{N} t_i = 0 \quad , \tag{43}$$

$$\frac{\partial L}{\partial D} = \frac{N}{2D} + \frac{Ns^2z}{KE} - s^2\sum_{i=1}^{N} t_i + \frac{z^2}{4D^2}\sum_{i=1}^{N}\left[\frac{1}{t_i}\right] - \frac{2NzKE}{4D^2} + \frac{K^2E^2}{4D^2}\sum_{i=1}^{N} t_i = 0 \quad , \tag{44}$$

$$\frac{\partial L}{\partial A} = \frac{Nz}{KE} - \sum_{i=1}^{N} t_i = 0 \quad . \tag{45}$$

In these equations we substitute

$$\sum_{j=1}^{20} N_j t_j \text{ for } \sum_{i=1}^{N} t_i \quad \text{and} \quad \sum_{j=1}^{20}\left[\frac{N}{t_j}\right] \text{ for } \sum_{i=1}^{N}\left[\frac{1}{t_i}\right] \quad .$$

Where N_j is the count recorded in the jth channel and t_j is the time period from the center of the source pulse to the center of the channel interval. In the original formulation (42) each ion counted was <u>assigned its own arrival</u> time, t_i; this substitution is made since our data is segregated into 20 classes by the time analyzer according to time of drift. From equation (45) we get

$$K = \frac{z}{E}\frac{N}{\sum_{j=1}^{20} N_j t_j} = \frac{z}{E\bar{t}} \quad . \tag{46}$$

From the combination of all three equations (43), (44), and (45) we get

$$D = \frac{z^2}{2}\left(\frac{1}{N}\sum_{j=1}^{20}\left(\frac{N_j}{t_j}\right) - \frac{N}{\sum_{j=1}^{20} N_j t_j}\right) = \frac{z^2}{2}\left\{\left(\overline{\frac{1}{t}}\right) - \frac{1}{\bar{t}}\right\} \qquad (47)$$

and

$$A = \frac{KE}{z} - s^2 D = \frac{1 + s^2 z^2}{2}\left(\frac{1}{\bar{t}}\right) - \frac{s^2 z^2}{2}\left(\overline{\frac{1}{t}}\right) . \qquad (48)$$

A Least Squares Fit of the Theoretical Curve to the Data

Two computer programs exist to fit a theoretical function of the general form (41) to the experimental data. The distribution (41) is a statistical distribution, and its integral over time from zero to infinity is one. Hence this function must be multiplied by the total number, N, of particles counted in order to be fitted to the data. Hence both programs fit a curve of the form

$$F(z,t) = \frac{NKE}{\sqrt{4\pi Dt}} \exp\left[\frac{(A + S_1^2 D)(z - KEt)^2}{KE} - \frac{(z - KEt)^2}{4Dt}\right] \qquad (49)$$

to the experimental data.

The first of the two computer programs was prepared by Dr. D. S. Harmer at Georgia Tech. This program was written in the computer language, Algol, for use on the Burroughs 220 Electronic Digital Computer. For this Program N was estimated from the total count recorded by the twenty channel analyzer (since this total count was sometimes in error, the estimate was

only a good guess when some of the counts did not fall in any of the twenty channels). The parameter S_1 was estimated from the radius of the drift tube and the first zero of the zeroth order Bessel function. The parameter A was set arbitrarily equal to zero since the shape of the ion burst was not particularly meaningful in this experiment. A least squares fit was then made in which K and D were calculated by a method of successive approximations. The technique used is similar to the one used below for the same parameters.

The second of the two computer programs was prepared by the author at Lawrence Radiation Laboratory, Livermore, California. This program was written in the computer language, Fortran, for use on the IBM 7094 Electronic Digital Computer. The parameter s_1 was estimated as above. In this program a least squares fit was made in which N was calculated directly and K, D, and A, were calculated by a method of successive approximations described in the following paragraphs.

For this program good initial estimates of K, D, and A must be utilized to compute values of F(z,t). These estimates are designated K_o, D_o, and A_o. They may be found by using the statistical estimators of pp. 54-55, or they may simply be good guesses based on experience.

It is first necessary to find the value of the parameter N in equation (49). If the assumptions upon which this equation was derived are correct then

$$N = \sum_j N_j \tag{50}$$

where N_j is the count in the jth time channel. To make a least squares fit of the equation (49) to the data it is necessary to find the values

of K, D, and A, which will make the quantity S a minimum where S is given by

$$S \sum_j [F_j - N_j]^2 Q_j^2 \tag{51}$$

Here F_j is the value of the function (49) evaluated at t_j, the time corresponding to the jth time channel, and the Q_j are weighting factors. Since a population of counts from a given channel will be normally distributed if these counts are all taken under identical circumstances the weighting factors will be taken as

$$Q_j = \frac{1}{\sqrt{N_j + 1}} \tag{52}$$

To find values of K, D, and A that will minimize the function S it is necessary to expand the function F(z,t) as a function of K, D, and A, in a Taylor's series about the point K_o, D_o and A_o:

$$F(K,D,A) = (F)_o + \left(\frac{\partial F}{\partial K}\right)_o \Delta K + \left(\frac{\partial F}{\partial D}\right)_o \Delta D + \left(\frac{\partial F}{\partial A}\right)_o \Delta A + - - - \tag{53}$$

where the subscript zero on the functions in parentheses indicate that they are evaluated at (K_o, D_o, A_o) and where

$$\Delta K = K - K_o \ , \tag{54}$$

$$\Delta D = D - D_o \ , \text{ and}$$

$$\Delta A = A - A_o \ .$$

Utilizing only the terms in this expansion shown above, the values of ΔK, ΔD, and ΔA were found that minimize the function S. To do this we set

$$\frac{\partial S}{\partial(\Delta K)} = 2\sum_j \left(\frac{F_j - N_j}{N_j + 1}\right)\left(\frac{\partial F_j}{\partial K}\right)_o = 0 \quad . \tag{55}$$

$$\frac{\partial S}{\partial(\Delta D)} = 2\sum_j \left(\frac{F_j - N_j}{N_j + 1}\right)\left(\frac{\partial F_j}{\partial D}\right)_o = 0 \quad , \text{ and} \tag{56}$$

$$\frac{\partial S}{\partial(\Delta A)} = 2\sum_j \left(\frac{F_j - N_j}{N_j + 1}\right)\left(\frac{\partial F_j}{\partial A}\right)_o = 0 \quad . \tag{57}$$

To simplify the form of these equations we let

$$u_{11} = \frac{\left(\frac{\partial F_j}{\partial K}\right)_o^2}{N_j + 1} \quad , \quad u_{12} = \frac{\left(\frac{\partial F_j}{\partial K}\right)_o \left(\frac{\partial F_j}{\partial D}\right)_o}{N_j + 1} \quad , \tag{58}$$

$$u_{13} = \frac{\left(\frac{\partial F_j}{\partial K}\right)_o \left(\frac{\partial F_j}{\partial A}\right)_o}{N_j + 1} \quad , \quad u_{22} = \frac{\left(\frac{\partial F_j}{\partial D}\right)_o^2}{N_j + 1} \quad ,$$

$$u_{23} = \sum_j \frac{\left(\frac{\partial F_j}{\partial D}\right)_o \left(\frac{\partial F_j}{\partial A}\right)_o}{N_j + 1} \quad , \quad u_{33} = \sum_j \frac{\left(\frac{\partial F_j}{\partial A}\right)_o^2}{N_j + 1} \quad ,$$

$$v_1 = \sum_j \frac{[N_j - (F_j)_o]\left(\frac{\partial F_j}{\partial K}\right)_o}{(N_j + 1)} \quad ,$$

$$v_2 = \sum_j \frac{[N_j - (F_j)_o]\left(\frac{\partial F_j}{\partial D}\right)_o}{(N_j + 1)} ,$$

and

$$v_3 = \sum_j \frac{[N_j - (F_j)_o]\left(\frac{\partial F_j}{\partial A}\right)_o}{(N_j + 1)} .$$

Equations (55), (56), and (57) then took the form

$$u_{11}\Delta K + u_{12}\Delta D + u_{13}\Delta A = v_1 \qquad (55)$$

$$u_{12}\Delta K + u_{22}\Delta D + u_{23}\Delta A = v_2 \qquad (56)$$

$$u_{13}\Delta K + u_{23}\Delta D + u_{33}\Delta A = v_3 \qquad (57)$$

whose solutions for ΔK, ΔD, and ΔA were found, by utilizing Crámer's rule, as

$$\Delta K = \frac{1}{\Delta}\begin{vmatrix} v_1 & u_{12} & u_{13} \\ v_2 & u_{22} & u_{23} \\ v_3 & u_{23} & u_{33} \end{vmatrix} , \qquad (59)$$

$$\Delta D = \frac{1}{\Delta}\begin{vmatrix} u_{11} & v_1 & u_{13} \\ u_{12} & v_2 & u_{23} \\ u_{13} & v_3 & u_{33} \end{vmatrix} , \text{ and} \qquad (60)$$

$$\Delta A = \frac{1}{\Delta}\begin{vmatrix} u_{11} & u_{12} & v_1 \\ u_{12} & u_{22} & v_2 \\ u_{13} & u_{23} & v_3 \end{vmatrix} , \text{ where} \qquad (61)$$

$$\Delta = \begin{vmatrix} u_{11} & u_{12} & u_{13} \\ u_{12} & u_{22} & u_{23} \\ u_{13} & u_{23} & u_{33} \end{vmatrix} .$$

If all of the ratios $\Delta K/K$, $\Delta D/D$, $\Delta A/A$ were very small (0.001 or smaller) the current values of K_o, D_o, and A_o were taken as the values of K, D, and A that minimize S within acceptable limits. If any of these ratios are too large, the corresponding parameters are corrected towards the computed values. The entire calculation is then done over using the new values of the parameters K, D, or A in place of the previous ones. The program is set to terminate itself if the above criterion for the ratios is not met within a predetermined number of tries. The Fortran version of this program is given in Appendix B.

Since it is believed that the value of K is much more accurately known than that of D and A, the program used initially tries to get better estimates of these parameters by the least squares method before attempting to solve for all three simultaneously.

CHAPTER IV

RESULTS

Ion Molecule Reactions of the System

The data gathered by the steady state mode of operation was so variable from one run to another as to be of only small use for any quantitative determinations. There are several reasons for this. In order of presumed importance some of these are:

(1) The level of H_2O in the drift tube, because it was very small, could vary by several orders of magnitude because of the peculiar conditions in or history of operations in the drift tube on a particular run. As has been pointed out this trace of H_2O produces the reaction in the drift tube which is quantitatively by far the most important.

(2) The transmission characteristics of the differential pumping chambers and mass spectrograph are known to change during operation.

(3) The ion production of the source is subject to a slow change due to "aging" and is also subject to unstable operation under some circumstances.

In addition to these reasons the mathematical expressions for the ion densities are complicated functions of the variables and parameters which would be very difficult to solve for the parameter of interest unless a large amount of accurate data was available for various values of the variables. These mathematical expressions are developed in Appendix F. Nevertheless the data gathered in this mode of operation was of great value

in determining semi-quantitatively the relations between some of the different types of ions found in the drift tube.

On the basis of the study of the variations with pressure of the count rates of the various ionic species it was concluded that the major ion-molecule reactions occurring with nitrogen in the drift tube are:

$$N_2^+ + H_2O \rightarrow N_2H^+ + OH \quad (1)$$

$$N_2H^+ + H_2O \rightarrow H_3O^+ + N_2 \quad (2)$$

The reasons for assuming these reactions are as follows. The reactants and products in the above reactions together with N^+, N_3^+, and N_4^+, constitute over 90 per cent of the ions found in the mass spectra over a wide range of pressures when the drift tube trap contains liquid nitrogen. Figure 9 shows typical mass spectra taken at pressures of 35 microns and 175 microns. The only other ion that shows up in any quantity at all is mass 18 which is thought to be H_2O^+ formed by charge exchange with some of the above ions.

The involvement of hydrocarbon pump oil fragments with the formation of N_2H^+ is thought to be minimal since placing liquid nitrogen in the drift tube trap eliminates practically all of the extensive and complicated spectrum of pump oil and its cracking pattern. Water might enter the system from several sources: atmospheric leaks, oxidation of pump oil, as a contaminant of pump oil, effusion from metallic surfaces inside the drift tube, but by far the most important source is entry with the gas being admitted. The gas coming from the nitrogen cylinder has a dew point of about -28.3° C. The pressure maintained in the feed line between the

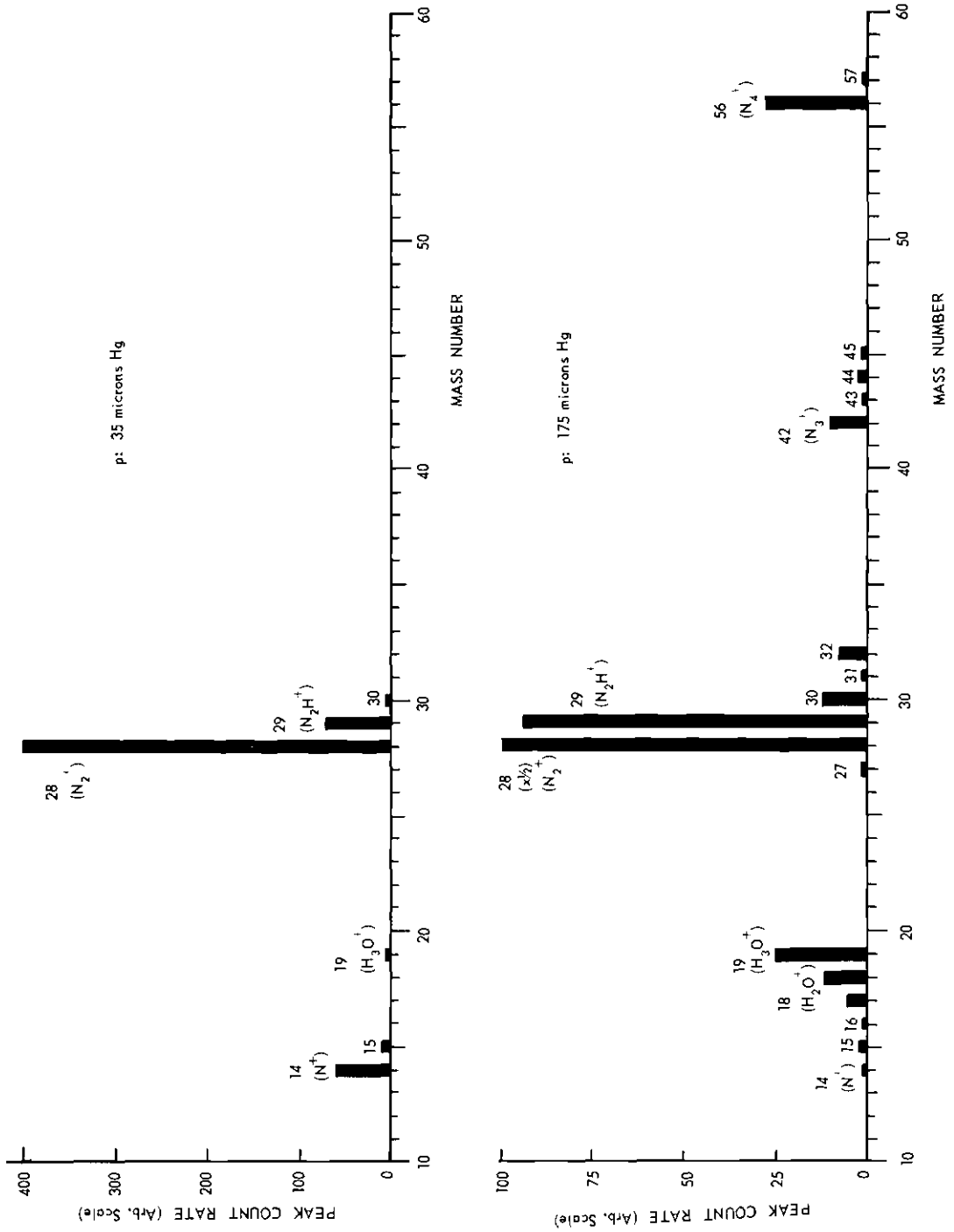

Figure 9. Representative Mass Spectra of Ions in Nitrogen at 35 and 175 Microns.

regulator valve and the needle valve is 1638 ± 25 mm. The acetone and dry ice trap should reduce the vapor pressure in the feed line to about .00048 ± .00005 mm. This means that the partial pressure of H_2O in this gas is $(2.9 \pm .2)\times10^{-5}$ per cent of the total pressure in the feed line. In no single run was the drift tube pressure raised to more than 2000 microns and in most cases less than 1000 microns so that 5.8×10^{-4} microns may be considered as the absolute upper limit on the partial pressure of H_2O admitted on any one filling of the drift tube. However, the outer surface of the drift tube trap, which contains liquid nitrogen, will be at only a slightly higher temperature than -195.8° C, the boiling point of liquid nitrogen. Extrapolation of data from reference 43 and other sources[45] give an equilibrium vapor pressure of H_2O in the presence of this trap of the order of 10^{-20} microns, a scarcely believable figure in view of the results of this experiment. Because of the method of handling the gas in both modes of operation it is highly probable that the equilibrium vapor pressure of H_2O at the temperature of the cold trap is never achieved. Continuous effusion of water from the surfaces inside the drift tube and leaks to the atmosphere would diminish the chances of this equilibrium occurring. For the purposes of this experiment it will be considered that the partial pressure of H_2O in the drift tube remains almost constant at a not exactly known but very low value over almost the whole pressure range.

Figure 10 shows the variation in relative intensities of N_2^+, N_2H^+, and H_3O^+ for a typical run as a function of pressure in this drift tube. Many qualitatively similar graphs serve as the basis for reactions (1) and (2).

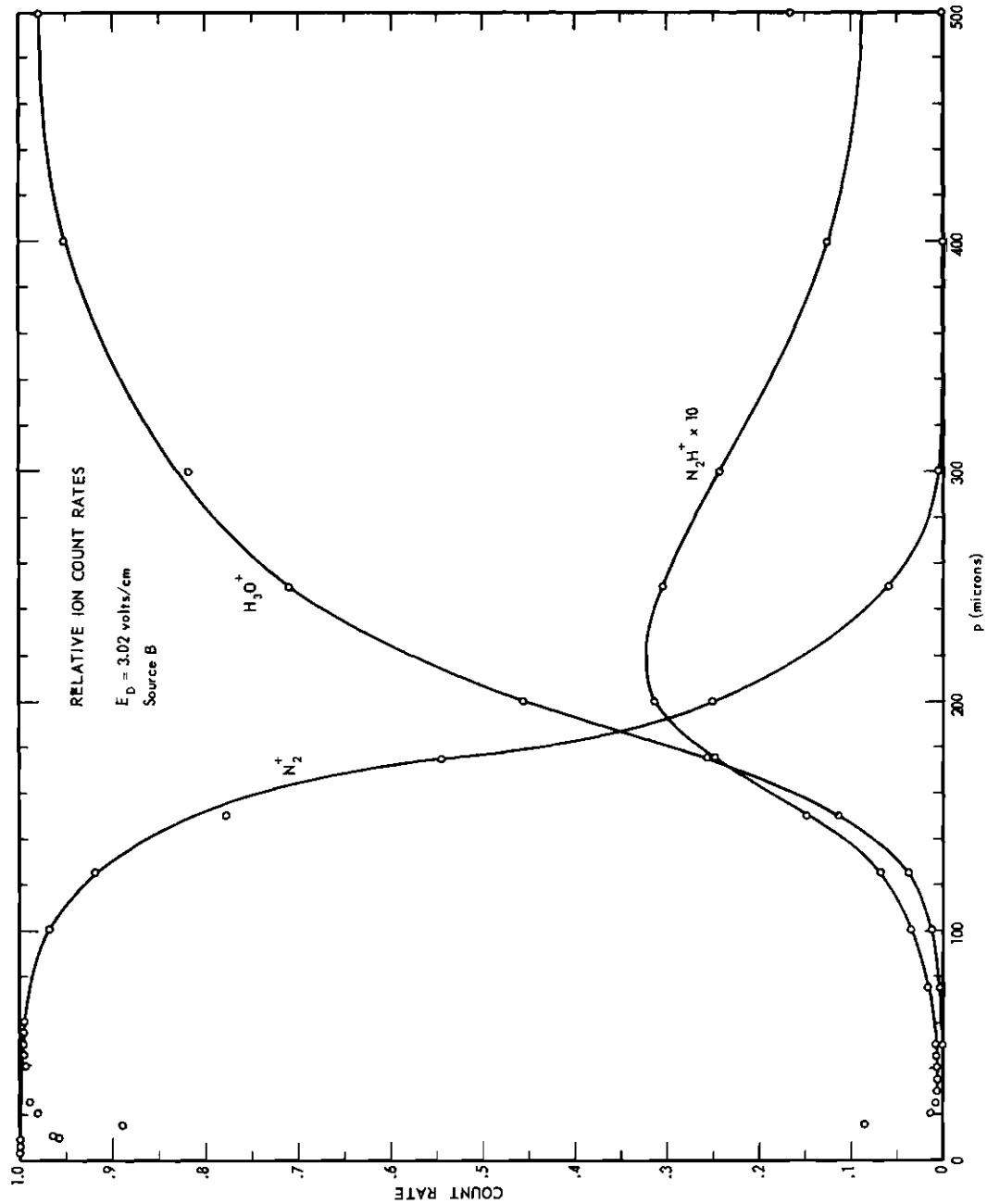

Figure 10. Variations with Pressure of the Fractions of N_2^+, N_2H^+, and H_3O^+ Ions in Nitrogen.

Including N_3^+ and N_4^+ in the calculation of the relative intensities would not qualitatively change the results since they constitute in all runs except one less than 20 per cent of the total ion current.

The variation of the fractions of N_3^+ and N_4^+ are sufficiently diverse qualitatively that no definite conclusions can be reached about the mechanism of formation of these ions from the data gathered here.

On the basis of the study of the variations with pressure of the count rates of the various ionic species it was concluded that the major ion-molecule reactions occurring with hydrogen in the drift tube are:

$$H_2^+ + H_2 \rightarrow H_3^+ + H \qquad (3)$$

$$H_2^+ + N_2 \rightarrow N_2H^+ + H \qquad (4)$$

$$H_3^+ + N_2 \rightarrow N_2H^+ + H_2 \qquad (5)$$

The reactants and products in the above reactions together with H^+ constitute over 95 per cent of the ions found in the mass spectra over a wide range of pressures when the drift tube trap contains liquid nitrogen. The reaction forming H_3O^+ is not as important here as it was in the case of nitrogen because the pressures were seldom carried as high in the hydrogen investigation as they were in the case of nitrogen. Figure 11 shows the variation of the relative intensities of H_2^+, H_3^+, and N_2H^+ for a typical run as a function of pressure in the drift tube. Many qualitatively similar graphs serve as the basis for reactions (3), (4), and (5). As can be seen from the figure the fast decrease with increasing pressure in the number of H_2^+ ions detected by the counter corresponded to a large increase

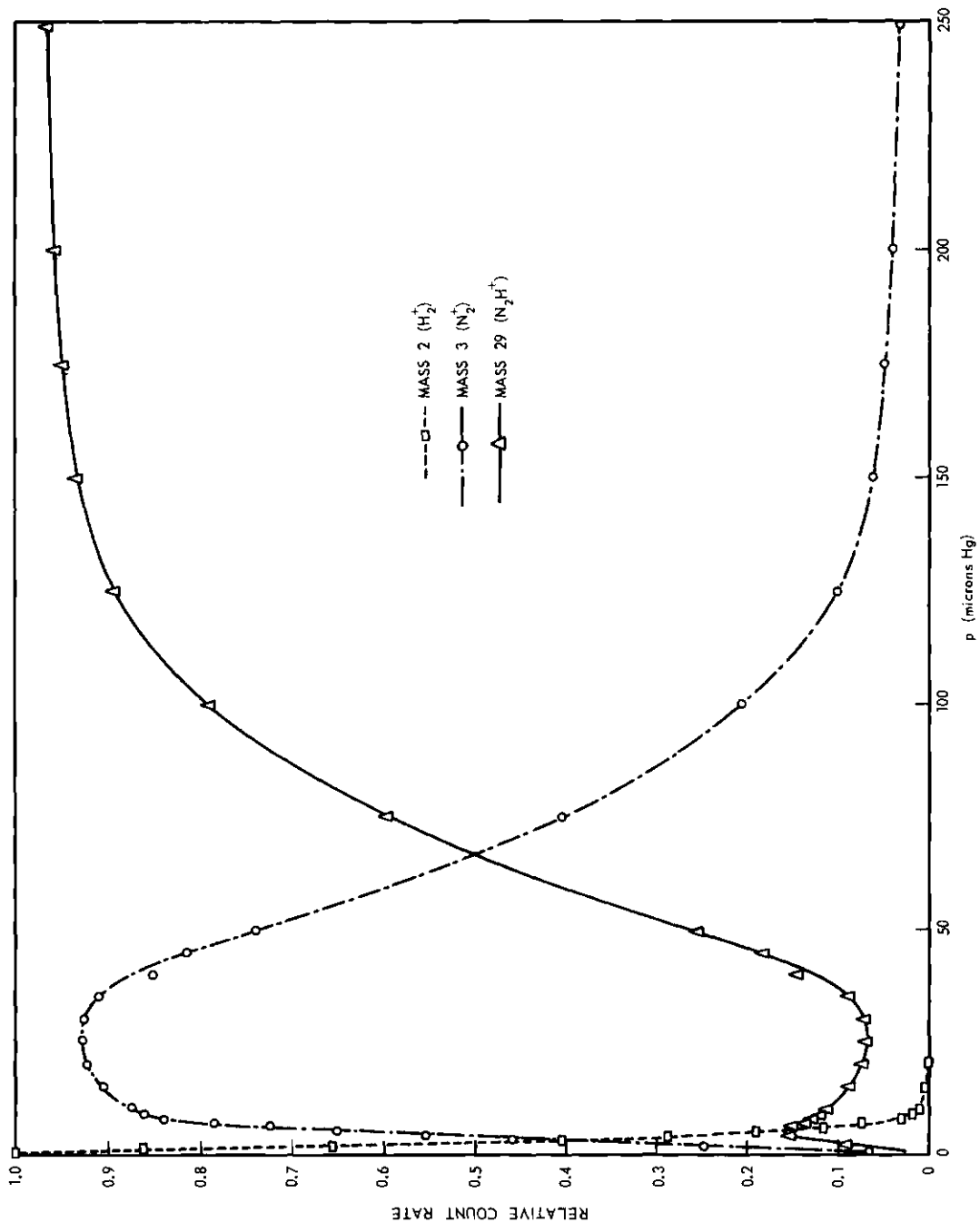

Figure 11. Variations with Pressure of the Fractions of H_2^+, H_3^+, and N_2H^+ Ions in Hydrogen.

in the number of H_3^+ and to a much smaller increase in the number of N_2H^+. The catastrophic decrease in the number of H_2^+ ions with increasing pressure renders it highly unlikely that any previous mobility measurement of ions in hydrogen was affected to any appreciable degree by its presence. In most previous reliable mobility measurements (where N_2H^+ was absent because the apparatus was "clean" compared to ours), the ion whose mobility was measured was certainly, therefore, H_3^+.

Factors Affecting Mobility Measurements

Bursts of ions are generated at one of the several sources in this system by putting a square voltage pulse of from 50 to 100 volts on the anode of the source. In all runs for which data was taken this square pulse was supplemented by a DC voltage of 20 volts. The duration τ of the voltage pulse varied for different series of runs, but the same value of τ was used for all runs in the same series. For most of the early runs τ had a value of 50 microseconds, for most of the later runs it had a value of 30 microseconds, and for a few runs a value of 20 microseconds was used. It did not prove practicable with the present apparatus to reduce τ below 20 microseconds since below this value the shape of the pulse was severly altered by the relatively low input impedance of the system, and the number of ions generated was reduced sharply. The increase of the pulse width above 50 microseconds would secure no obvious advantage and would lower the resolution of the system.

Pulses of the kind described produce ion distributions which are 5 to 25 times wider than might be expected by comparison of K and D by means of the relation (7). Nevertheless these ion bursts have the general shape

predicted by the theory, though not exactly in all cases. For comparison, Figure 12 is a histogram of a typical run superimposed on the graph of the theoretical distribution whose parameters, K and D, have values calculated from the data by the least squares computer program. In addition to this, on a number of occasions the shape of the ion burst arriving at the detector suggested the superposition of two overlapping bursts. In a few instances two peaks were evident. Characteristically there appeared to be a narrow, sharp burst arriving first followed by a broad relatively low tail. Two distributions, one showing this feature and one not showing it can be seen in Figure 13.

These anomalies in the shape of the ion burst are apparently traceable to the crude nature of the ion source used in this experiment. The distribution of the electric field around the anode during the time interval of the voltage pulse is extremely distorted by the presence of drift field electrodes, grids, and the filament. There is evidence that ionization resulting from this field takes place throughout a considerable volume of space in the neighborhood of this anode. The shape of the distribution of ions received by the analyzer may be explained if the initial distribution of ions is affected by the following factors:

(1) From Figure 3, it can be seen that there are grids in front of and behind sources B and C. In each case the one in front is closer. There will therefore be a more intense field in front of the anode and a less intense field behind it although the field should be by far the strongest at the surface of the anode. Source D on the other hand has a grid only in front of it so that mostof the ions will be generated there leading to a value of the mobility for this source just a little larger than the average. This conclusion is borne out by some of the data.

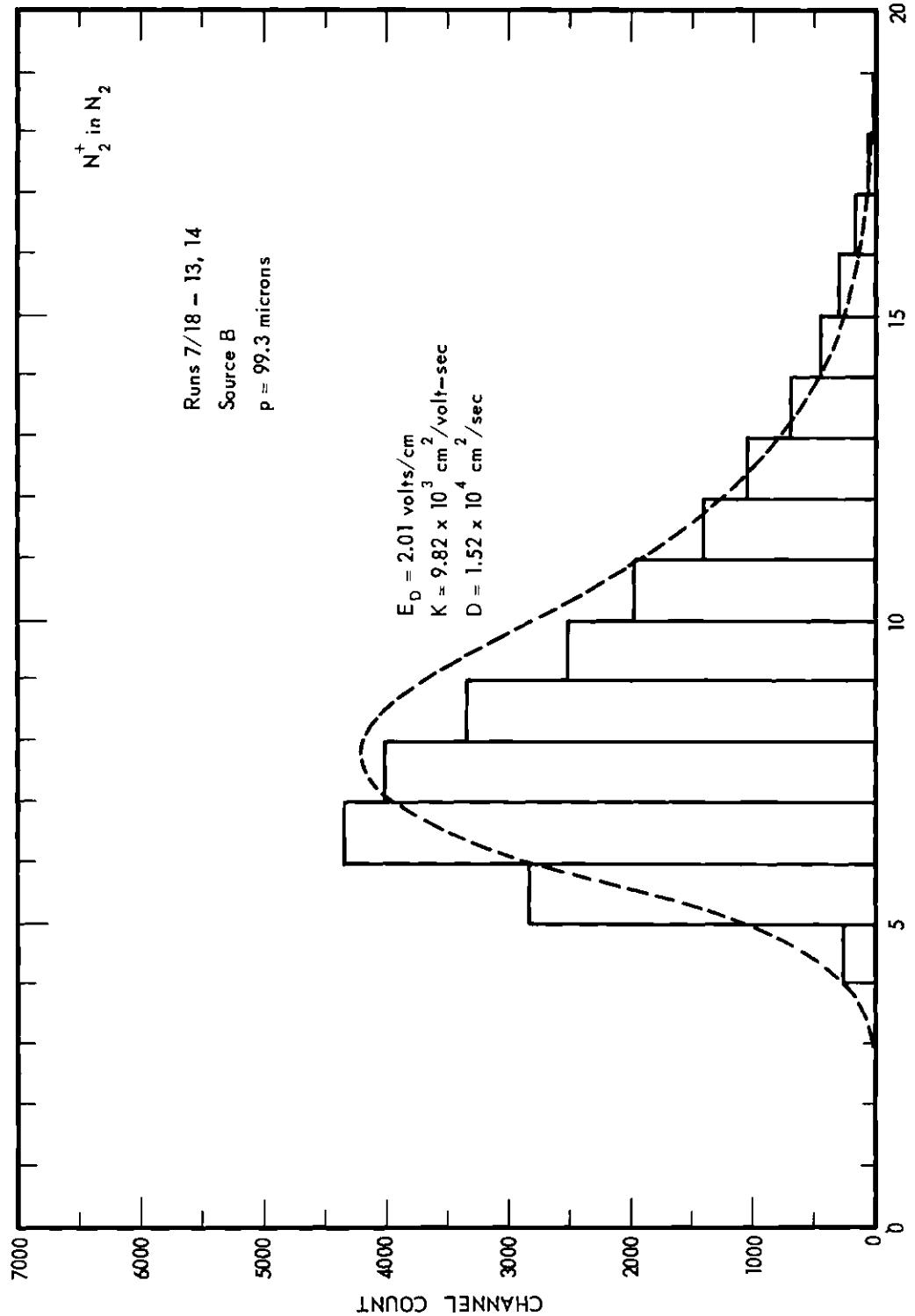

Figure 12. Histogram of an Experimental Time Distribution of N_2^+ Ions in Nitrogen and the Fitted Theoretical Distribution Function.

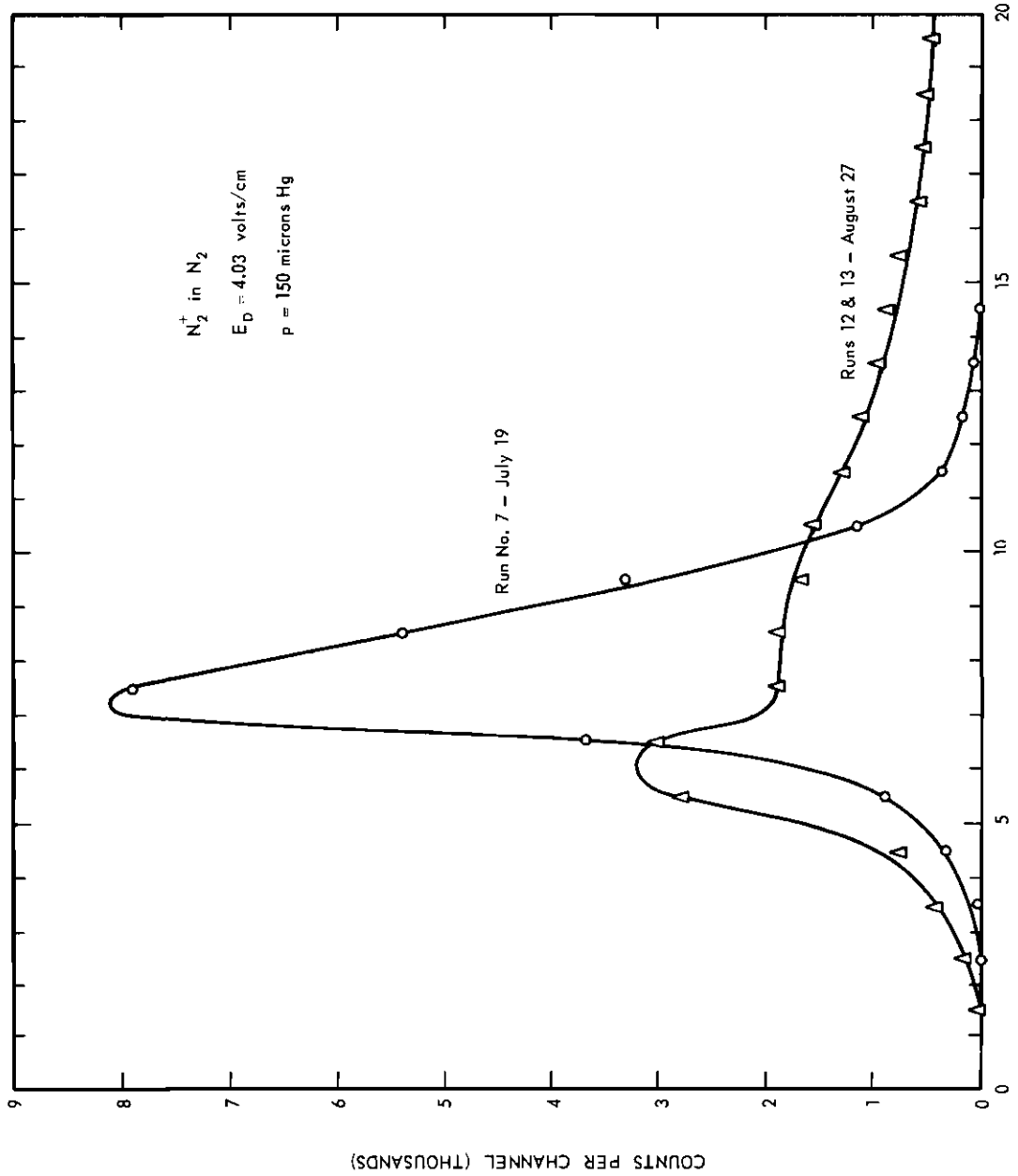

Figure 13. Two Time Distributions of N_2^+ Ions in Nitrogen Showing Variations in the Shape.

(2) The electric field around the source has a second effect which tends to reinforce and magnify the effect of non-uniform ionization described in (1) above. While the positive voltage pulse is on the anode there is a strong electric field which causes the ions to migrate rapidly away from it. This would have the effect of splitting the ion burst seen by the pin-hole into two parts and undoubtedly accounts for the occasional double peaks. As the time of travel of the ion burst increases these two parts become blended together by diffusion and the pin-hole in this case would see only a single peak.

(3) The "aging" process of the anodes described in Chapter II, page 29, undoubtedly contributed to the spreading of the ion bursts. As the centers of the ionizing activity move out away from the center of the drift tube, ions will not only have to drift the distance to the pin-hole but they will have to diffuse toward the center of the tube. This will have the effect of lengthening the tail on the distribution and increasing the estimate of D. A gradual trend downward in the value of K/D over a period of months has been detected.

(4) Each anode passes between and fairly close to the two drift field electrodes adjacent to its position. In fact, the closest grid is mounted on one of these electrodes. A significant amount of ionizing activity must take place between these electrodes especially as the "aging" process described in (3) above proceeds.

(5) The distribution of the electron cloud is affected by many factors such as the thermal gradients in the drift tube, the configuration of the electric field around the source, the presence of conducting surfaces, the rate of emission of the filament, the gas pressure, the possible

presence of molecular species that could attach electrons and become negative ions, and recombination processes with positive ions. The distribution of the electron cloud determines the effectiveness of the anode field in producing ions as described above. It also affects the ion population by causing a loss of positive ions due to recombination.

From all of these factors it might be concluded that during the duration of the voltage pulse there is a narrow region of relatively intense ionization in front of the anode producing the sharp leading edge in the ion distribution. A wider region of less intense ionization behind the anode and the region of ionization between the drift electrodes contributes the tail of the distribution. As the anodes "age" this region between the electrodes becomes more important causing the tail to become more pronounced. This initial ion distribution, whatever its configuration, is violently driven away fron the anode during the time of duration of the voltage pulse.

There are two other factors that might affect the shape of ion burst of one of the supposed primary ions. The first is the possibility that not all of these ions are primary ions but part of them may be secondary ions being created by an ion-molecule reaction from some other ion species having a different mobility than the ion under consideration. The second is the possibility that temporary clustering of the ion of interest with some highly polarizable neutral molecule might reduce its effective mobility. Since this effect would uniformly affect all ions of a given species it could hardly be an explanation for the double peaks sometimes observed. The effect of these factors, in any case, would be negligible compared with the source effects.

It is estimated that the transmission efficiency from the ion source to the multiplier tube is only of the order of 10^{-10}. The original reason for putting a source of this nature in the apparatus was to get enough ions to make useful measurements of count rates, etc.

Results for the Primary Ions

In nitrogen the primary ions are considered to be N^+ and N_2^+; in hydrogen the primary ions are believed to be H^+ and H_2^+. In the case of H_2^+, however, the cross section for the reaction (3), which converts H_2^+ into H_3^+, is so large that it is doubtful that the concept of mobility has any meaning for H_2^+. For the same reason H_3^+ may be considered to be a primary ion in hydrogen as far as the treatment of the experimental results is concerned.

The major variables, aside from the effects produced by the peculiarities of the course, which affected the shape and position of the ion distribution on our time scale were the drift distance, the drift field, and the gas pressure. Figure 14 shows the differences in the shape and position of the ion bursts arriving from sources B, C, and D located at different distances from the pin-hole with the same pressure and drift field in each of the three cases. Figure 15 shows the effect of varying the drift field on the distribution of ions coming from a single source while the pressure is held constant. Figure 16 shows the effect of varying the pressure on the distribution of ions coming from a single source while the drift field is held constant.

The major sources of systematic error were studied to determine their effect on the data. By far the largest source of systematic error

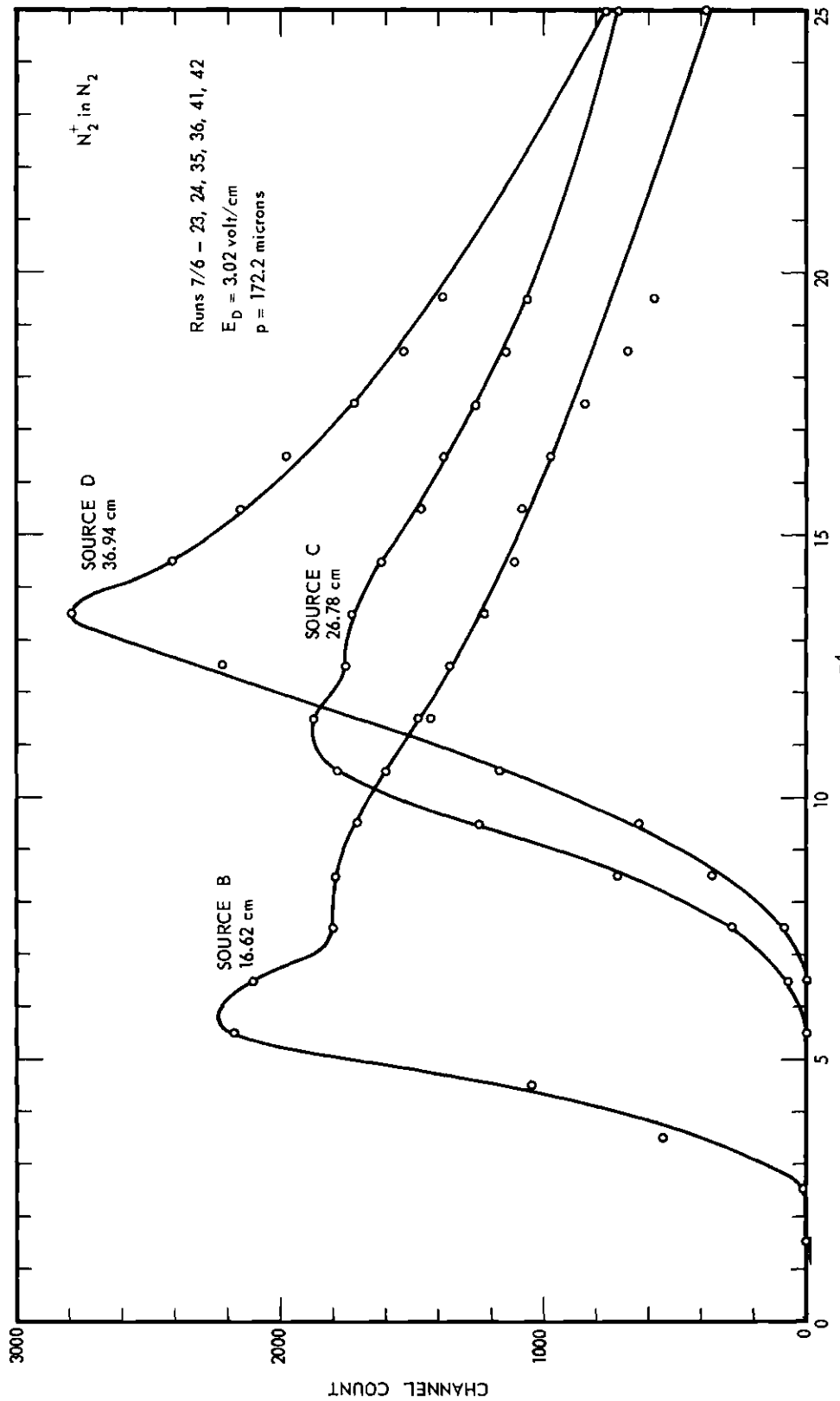

Figure 14. Time Distributions of N_2^+ Ions in Nitrogen for Three Different Drift Distances.

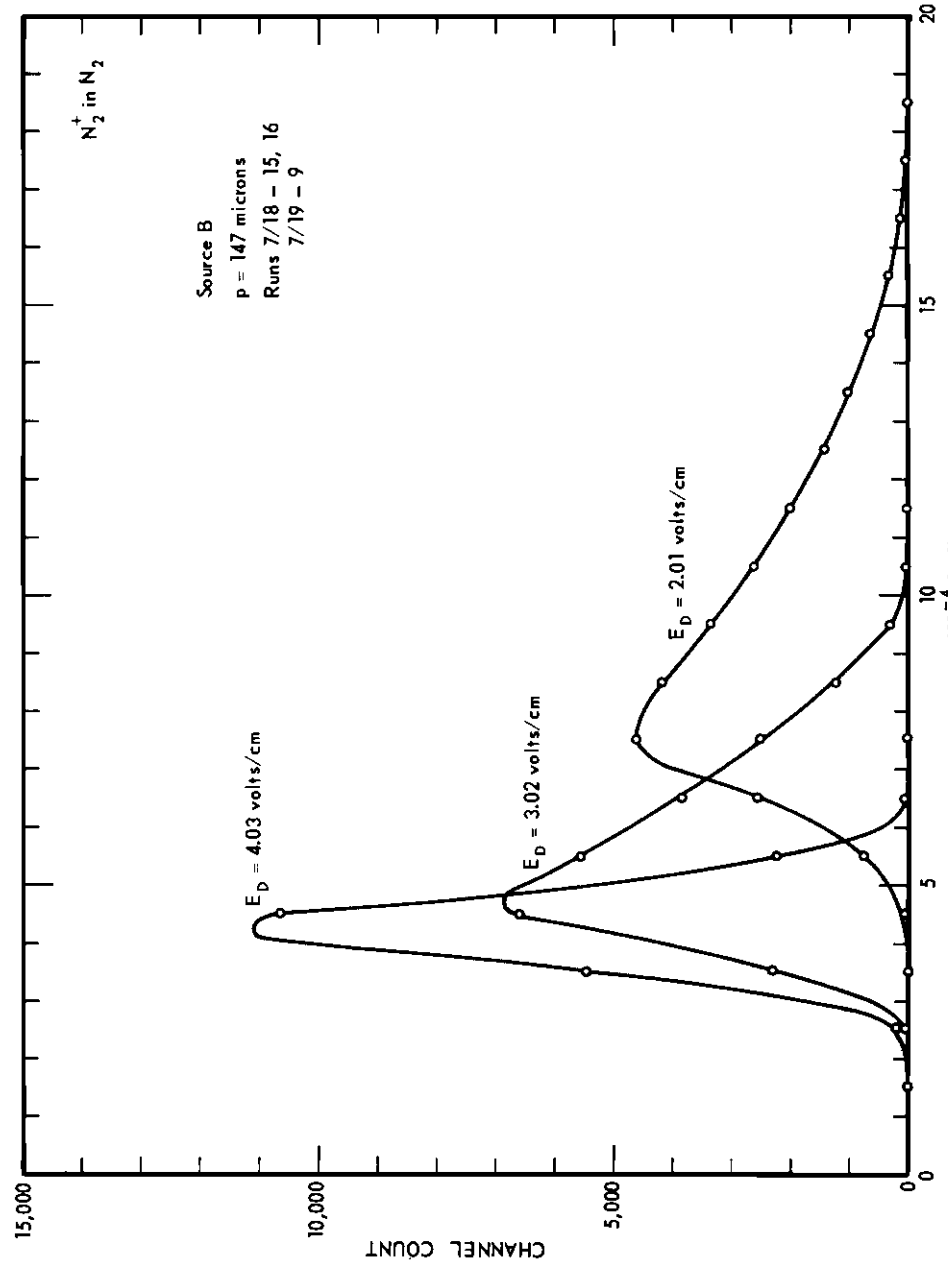

Figure 15. Time Distributions of N_2^+ Ions in Nitrogen for Three Different Values of the Drift Field.

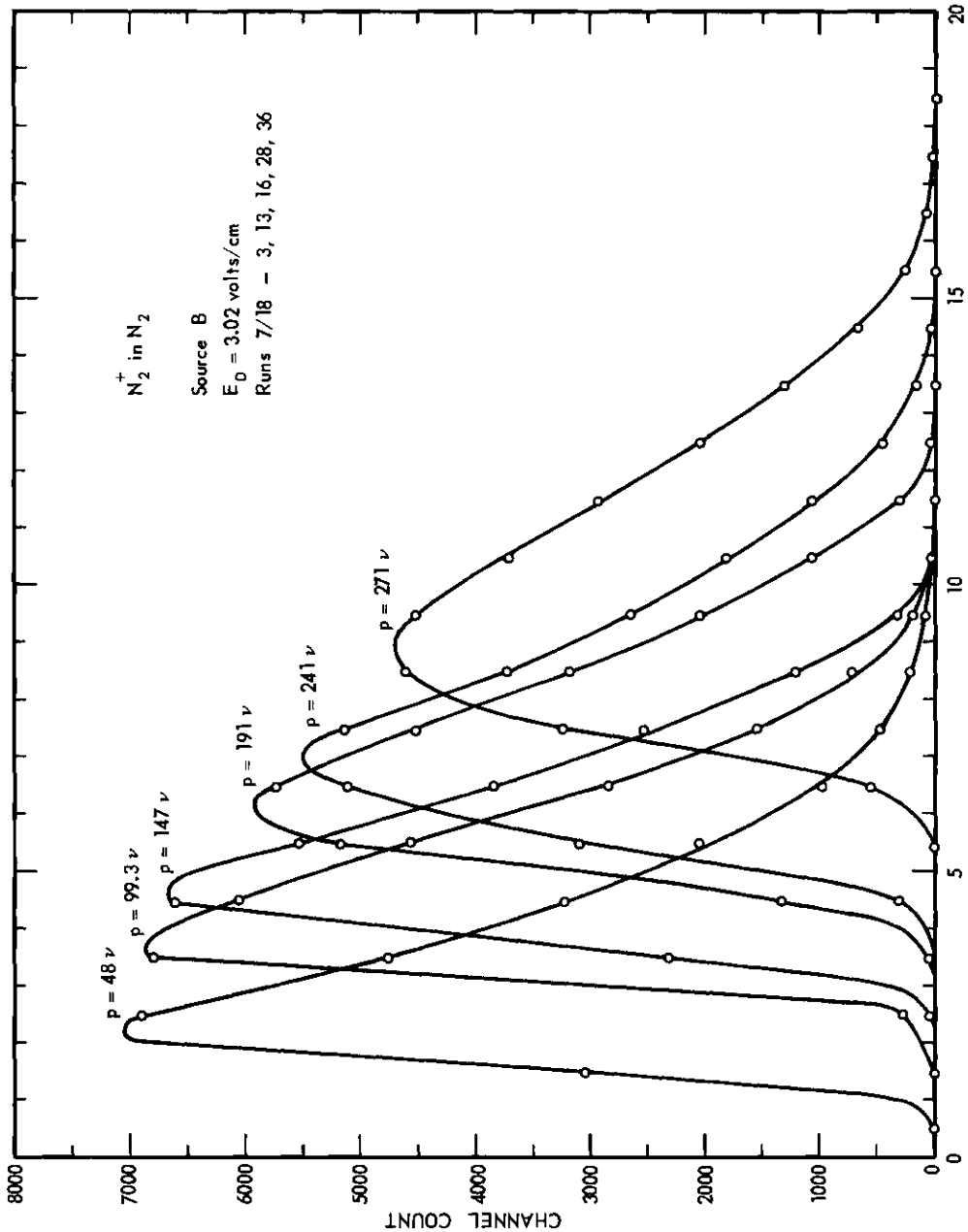

Figure 16. Time Distributions of N_2^+ Ions in Nitrogen for Several Values of the Pressure.

turned out to be the peculiarities of the source. Other sources of systematic error considered were: (a) uncertainty in the measurement of the effective distance from the pin-hole to the source, (b) the time of transit of the ions through the differential pumping chambers and mass spectrometer, (c) possible lack of simultaneity between the triggering of the 20-channel time analyzer and the pulse on the anode of the source, and (d) inaccuracy in the frequency of the crystal controlled oscillator controlling the 20-channel time analyzer. The errors introduced by these other sources of error proved to be negligible compared to the primary source of error.

N_2^+ in N_2

Figure 17 shows the values of the drift velocity v_D of N_2^+ plotted against E/p_o, each on a logarithmic scale. Superimposed on this is a curve representing the best fit Varney made to his data taken at a temperature of 300° K. The value p_o on this graph is the actual value of the pressure adjusted to the value it would have at 273° K with no change in density. In our experiment there is no means provided for measuring the temperature inside the drift tube and there would be some question as to how and where this temperature should be measured considering the temperature gradients due to the filaments and the cold trap. It seems most reasonable to take 300° as the temperature inside the drift tube since this temperature is only a few degrees above the average room temperature of the laboratory. The most important heat sink (or source) in the drift tube is the uninsulated outside wall.

Varney concluded that the upper portion of his curve was due to the N_2^+ ion in the high E/p region. Since, from his data, the exact location of the transition region is not clear it would be difficult to extrapolate

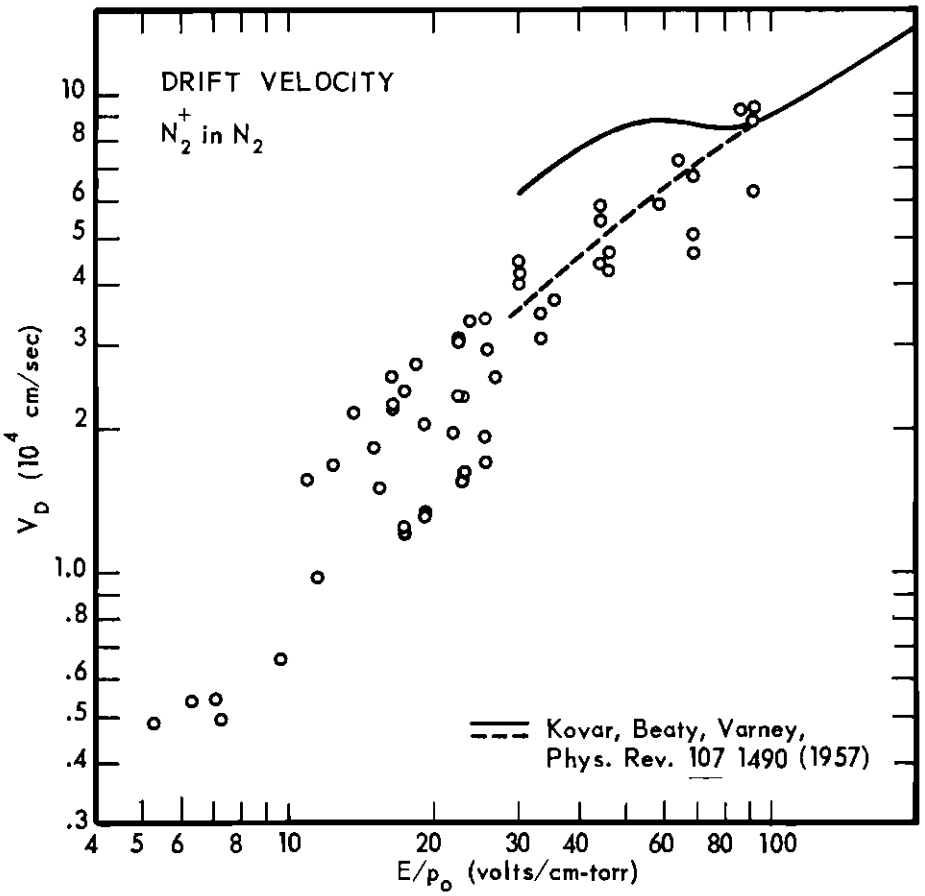

Figure 17. Experimental Results for the Normalized Drift Velocity of N_2^+ Ions in Nitrogen.

this curve into the low E/p region. The present data evidently does this. He concluded that the lower portion of his curve was due to the equilibrium condition between N_2^+ and N_4^+. If this were extended it would give a value of K_o of about $2.5/cm^2/volt/sec$.

To decide whether most of the points on the graph lay in the low E/p region or in the transition region between low and high E/p the data points were first tested to see how closely they came to fitting a straight line. This test consisted of fitting them by the least squares method to the curve

$$\log v_D = \log C(E/p)^a \tag{62}$$

This fit gave a value of 0.93 for a. Since this value is close to 1.0 it follows that these points can be reasonably well represented by an expression of the form

$$v_D = (K_o p_A)(E/p) \tag{63}$$

corresponding to the low E/p behavior of v_D, where p_A is atmospheric pressure and K_o is the reduced mobility. Examination of the data revealed that the data points are approximately uniformly distributed about a straight line when plotted on logarithmic graph paper. This suggested that a direct least squares fit to an expression of the form

$$\log v_D = \log (K_o p_A) + \log (E/p) \tag{64}$$

would weight the points in a manner justified by their relative scatter at different values of E/p. The values of K_o obtained by this technique

are for source B, 1.6 cm^2/volt-sec, for source C, 1.2 cm^2/volt-sec, and for source D, 1.4 cm^2/volt-sec. The fact that these values show no definite trend with z indicates that any correction for end effects would in fact be much less than other errors. The value of K_o obtained by using all points is 1.4 ± 0.1 cm^2/volt-sec. The limits given represent the 68 per cent confidence interval for the means of a population of samples of the size taken here by the methods used here.

As can be seen from Figure 17 all our points seem to lie just below the transition point from low to high E/p and join smoothly into Varney's data for high E/p which he believed to represent the drift velocity of N_2^+. Since some of the points are apparently in the transition region the value of K_o obtained here may be somewhat low.

N^+ in N_2

Figure 18 shows the values of the drift velocity v_D of N^+ plotted against E/p_o, each on a logarithmic scale. In this case a least squares fit to a curve of the form (62) yields a value for a of 0.85 indicating that most of the points are in the low E/p region. It therefore appears justifiable to fit the data by the least squares method to an equation of the form (63). The value of K_o given by this technique is 2.4 ± 0.1 cm^2/volt-sec where the limits have the same significance as above. Since some of the points in this sample also are apparently in the transition region, the value of K_o obtained here may be somewhat low.

Primary Ions in H_2

The mobility of all ions in hydrogen proved to be about an order of magnitude larger than the mobility of the ions in nitrogen, and their time

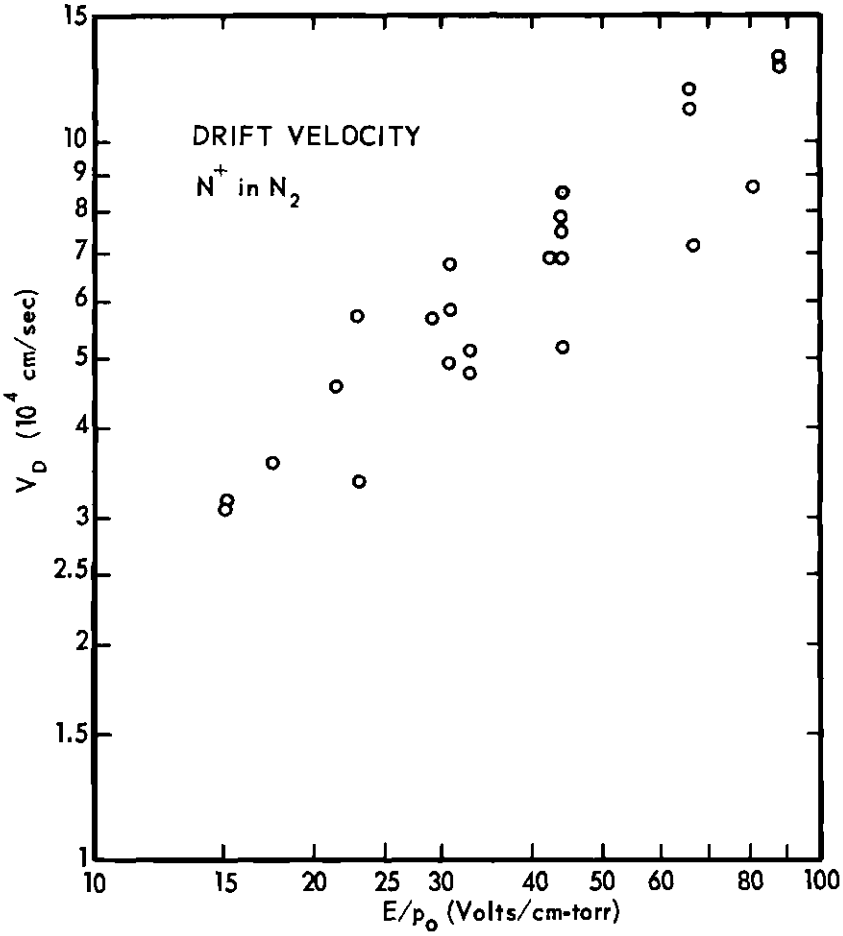

Figure 18. Experimental Results for the Normalized Drift Velocity of N^+ Ions in Nitrogen.

of travel through the drift tube was therefore about an order of magnitude smaller. Hence the dispersion of the ion burst was larger, and the inaccuracy in measurement of the time of travel of the ion burst was correspondingly larger. Under the present circumstances the scatter in the mobility measurements of the ions in hydrogen renders any estimate of K_o from these measurements unreliable. However, the values of K obtained were not inconsistent with earlier measurements.

Results for Product Ions

A set of measurements was made in which the time spectrum of the primary and each of the product ions was taken in immediate succession with all experimental variables being held as nearly constant as possible for all. The purpose of this was to hold uncontrolled variations of the amount of impurities in the drift tube and variations in the operating conditions of the source to a minimum. Ratios of the "mobilities" of these ions measured under identical conditions as calculated by equation (46) were formed. It was felt that these ratios might be more meaningful than the absolute values of the mobilities themselves. The statistical scatter in the data is such that the mobilities of some pairs of these ionic species might be indistinguishable if a comparison of mobilities taken under slightly different conditions was attempted.

A qualitative discussion will be presented to show what use might be made of data on secondary ions under idealized conditions. Consider two hypothetical situations:

(1) Let A and B be two hypothetical ions having identical mobilities and diffusion coefficients. If these ionic species are generated

by the same source and neither is affected by reactions or other factors, their time distributions should be identical under the same conditions. Suppose instead that B is not formed by the source but is formed from A by an ion-molecule reaction. Suppose further that exactly half of the ions of species A react to form an equal number of species B. The ion distributions should not be identical for the following reason. Since the probability that an ion of species A will react is proportional to the time it spends drifting through the gas, the counts in the later time channels will be diminished more than the counts in the earlier time channels when making a mobility measurement of A. This will have the effect of attenuating the tail of the time distribution and increasing the apparent mobility of A if no account is taken of this in the calculations. For the same reason when making a mobility measurement of B the counts in the later time channels will be bigger in proportion to the earlier ones than was the case when A and B had nothing to do with one another. This will have the effect of increasing the tail of the time distribution and decreasing the apparent mobility of B if no account is taken of this in the calculations. In our hypothetical case diffusion to the sides should not have a preferential effect on either ion since they have the same mobilities and, hence, the same diffusion coefficient. Equation (41) takes account of reactions using up ions whose mobility is being measured but no account of reactions forming them. It will therefore give a mobility value that is too small in the case of product ions.

(2) Let A and B be two ions formed by the source having very different mobilities. If mobility measurements are made at sufficiently high pressures and electric fields the ion distribution under idealized

conditions due to these species will be narrow and widely separated on the time base. Suppose now that B is not formed by the source but is formed from A by an ion-molecule reaction. Since the ion distribution of A is narrow its shape will not be changed much by the reaction as described in situation (1) above. Some of the ions of species B will be formed near the source and will arrive at the pin-hole at times determined by the mobility of species B; some will be formed near the pin-hole and will therefore arrive at times determined by the mobility of species A; and many will be formed between these two points. Hence the ion distribution of species B will extend on the time base from the position of the ion distribution of species A to the position that the ion distribution of species B would have if it were a primary ion. The shape of such a distribution could be used to infer the value of the rate constant for the reaction through which B is formed from A.

Unfortunately the broad ion distribution caused by source conditions causes the distributions of different ions to overlap, and the configuration imposed on the ion distributions by the source renders the shape of the distributions of the various ions intractable to mathematical analysis. A mathematical analysis of the shape of the ion bursts for product ions under idealized source conditions is made in Appendix E.

Comparison of N_2^+, N_2H^+, and H_3O^+

In the case of these ions the actual situation is even more complicated than our hypothetical situations. N_2H^+ is expected to have a mobility larger than N_2^+ since it is close to N_2^+ in mass and since the mobility of N_2^+ is decreased greatly from the Langevin theory value by resonance electron charge exchange. Of course there is always the possibility

that N_2H^+ is affected by some factor such as resonance proton exchange. Since N_2H^+ is being used up in a second reaction not many such ions formed near the source will survive to reach the pin-holes; hence most of the N_2H^+ ions counted will have been formed near the pin-hole. For this reason N_2H^+ should have an apparent mobility close to that of N_2^+.

According to Langvin's theory H_3O^+ should have a considerably larger mobility than either N_2^+ or N_2H^+. No speculation has been presented in this paper about any ion-molecule reaction using up H_3O^+, but such a process cannot be eliminated as a possibility. The experimental ratios of the apparent mobilities, N_2H^+/N_2^+, H_3O^+/N_2^+, and H_3O^+/N_2H^+, start just over 1.10 at source B and decrease to values of about 0.78, 0.65, and 0.84 respectively, at source D at a pressure of 192 microns. The apparent mobility ratio N_2H^+/N_2^+ shows no evident trend with pressure and has an average value of 0.8, but the ratios H_3O^+/N_2^+ and H_3O^+/N_2H^+ seem to have a gradual trend upwards from around 0.6 - 0.7 to somewhere between 1.0 and 2.0 as the pressure is increased from 50 to 500 microns. The scatter in the values of these ratios makes it difficult to draw any conclusions from these trends. Figure 19 is a graph of the ion distributions of N_2^+, N_2H^+, and H_3O^+ taken at a pressure of 514 microns and a drift field of 4.03-volts/cm using source C.

According to the reasoning in situation (1) the smaller values obtained experimentally for these ratios is consistent with the hypothesis that N_2H^+ and H_3O^+ are descendents of N_2^+ and H_3O^+ is a descendent of N_2H^+. The resolution of this experiment does not at present permit any reasonable estimate of the mobilities of any of these ions or of the reaction rates for the reactions forming them.

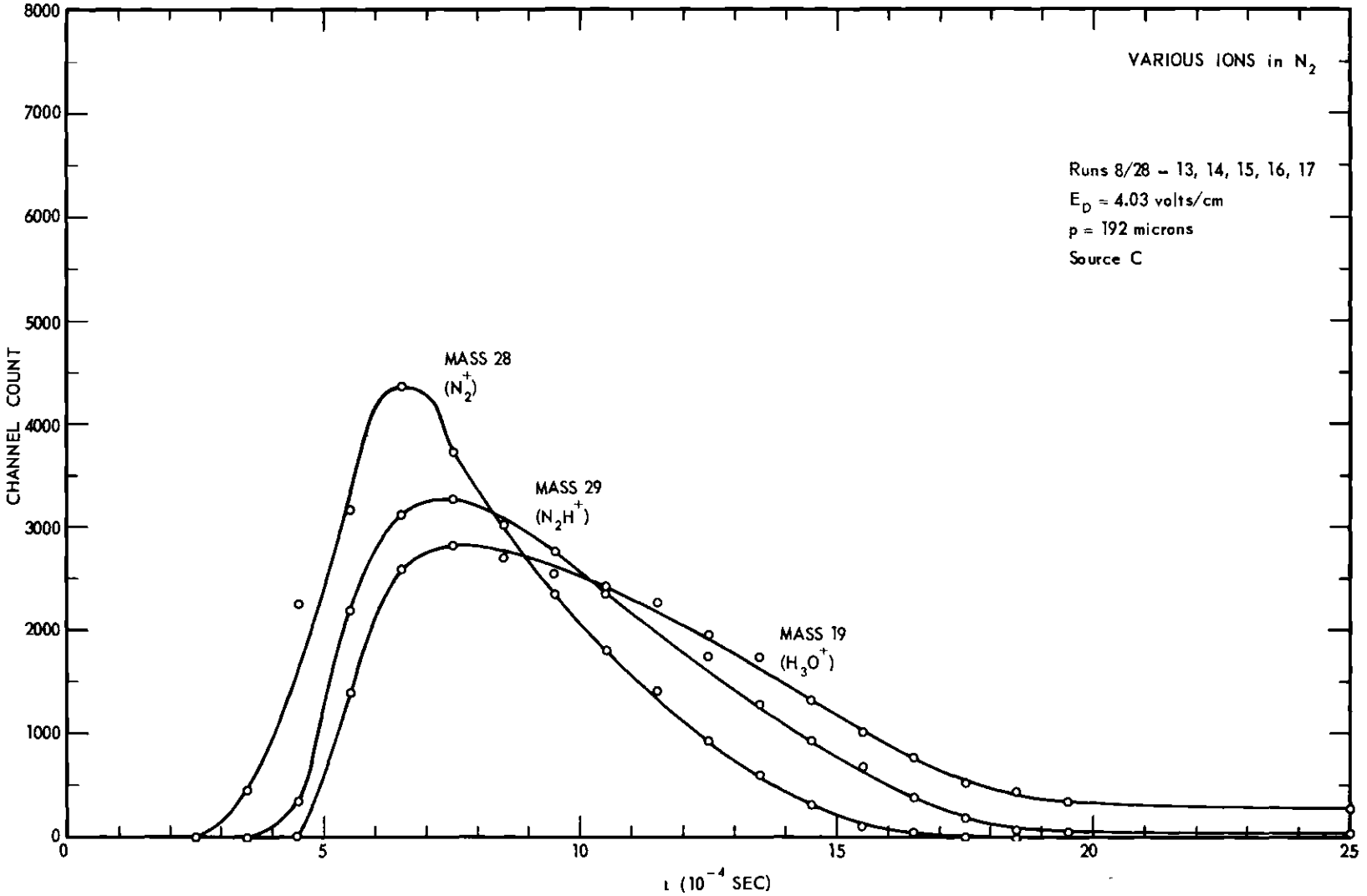

Figure 19. Comparison of the Time Distributions of N_2^+, N_2H^+, and H_3O^+ Ions in Nitrogen Under Identical Conditions.

Comparison of N_2^+, N_3^+ and N_4^+ in N_2

The mobility ratios N_3^+/N_2^+, N_4^+/N_2^+, and N_4^+/N_3^+, showed no recognizable trend. Their average values as determined by this experiment are 0.91, 0.73, and 0.82, respectively. At low values of p such as are used in our experiment Varney predicted[20] that the N_2^+ portion of the curve might very well extend into the low E/p region. To possibly confirm this it might be pointed out that in this experiment we never get large proportions of N_4^+ as have been reported in other experiments where higher pressures were used. Figure 20 is a graph of the ion distributions taken at a pressure of 514 microns and a drift field of 4.03-volts/cm using source C.

Diffusion Coefficients and Rate Constants

The values of the diffusion coefficient calculated from the data in this experiment range from 40 to 400 times larger than the value predicted by equation (7). Even if allowance is made for the fact that the experiment is being performed near the transition region between low and high E/p where the formula might begin to break down, the estimated values of D are too large. It is believed that the wide volume of ionization and the ion dispersion due to the anode field is responsible.

The estimates of the reaction rates show extreme scatter even after being corrected to a standard pressure. In fact many of them turned out to have negative values! In calculating these quantities the shape of the ion distribution was critical. As has been pointed out here the initial shape of the ion bursts were sufficiently distorted and the drift times were sufficiently short so that source conditions had more to do with the shape of the ion distribution than the drift conditions.

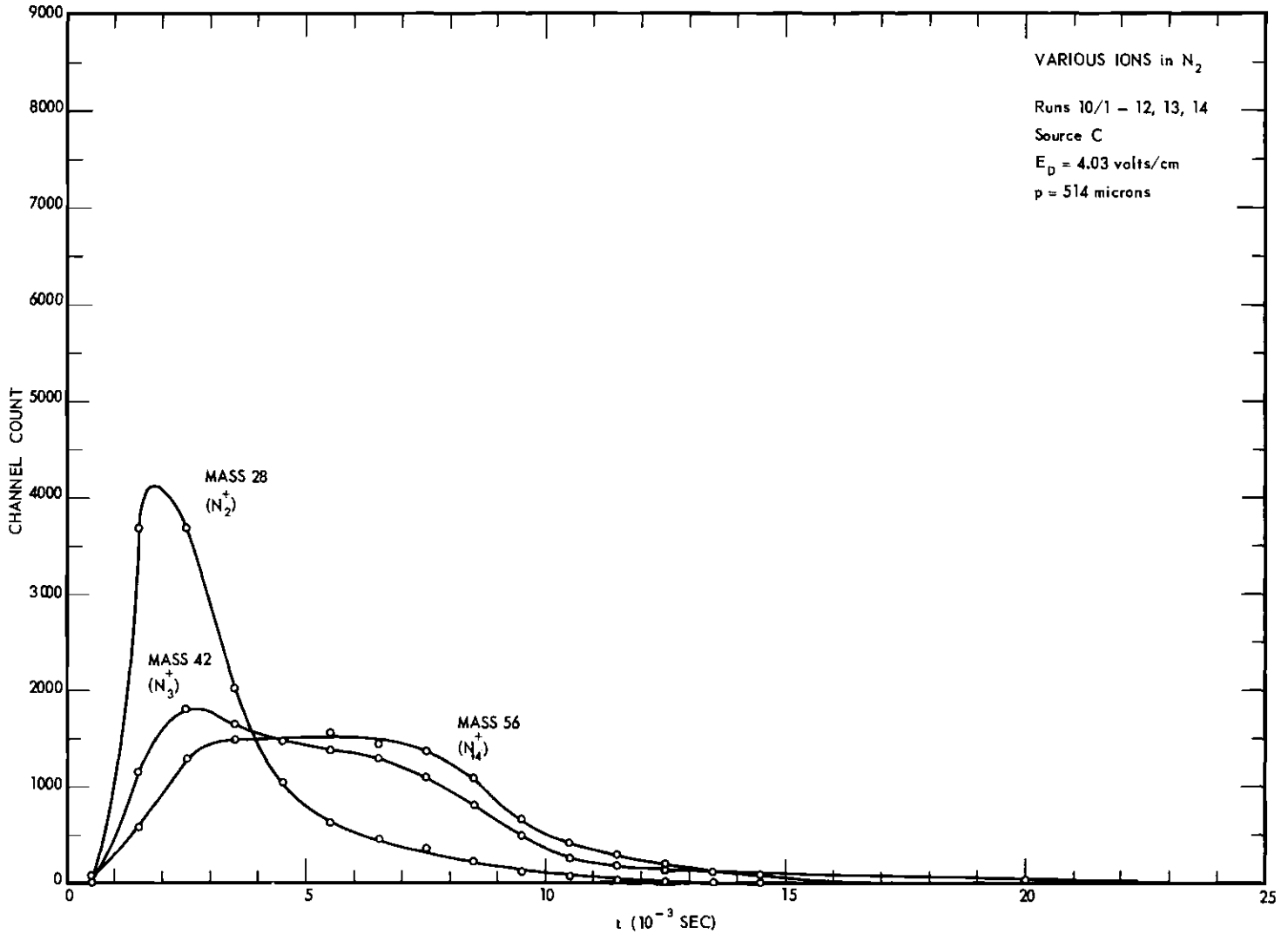

Figure 20. Comparison of the Time Distributions of N_2^+, N_3^+, and N_4^+ Ions in Nitrogen Under Identical Conditions.

CHAPTER V

CONCLUSIONS

a. The data obtained on the mobility of N_2^+ joined smoothly onto that portion of the existing data of Varney for the ions in nitrogen at values of E/p greater than about 90 volt/cm-torr, and extended it into the range of lower E/p. The behavior of the mobility is in general agreement with that expected from the mobility theory of Wannier for a single ionic species not appreciably perturbed by reactions. From this fact it is concluded that Varney's assertion that the ion observed in the higher E/p portion of his data could be presumed to be N_2^+ is correct.

b. It is further concluded that the system of reactions hypothesized by Varney which converts N_2^+ and N_4^+ into each other does not significantly affect the mobility of N_2^+ ions in nitrogen for pressures of 0.7 torr and for values of E/p of more than 4 volts/cm-torr.

c. The range of E/p in which the drift velocity of N_2^+ ions in nitrogen is linear in E/p begins just below 100 volts/cm-torr, and the reduced mobility in this range is 1.4 ± 0.1 cm^2/volt-sec.

d. The range of E/p in which the drift velocity of N^+ ions in nitrogen is linear in E/p lies in a range somewhat below 100 volts/cm-torr. The reduced mobility of N^+ for this range is 2.4 ± 0.1 cm^2/volt-sec.

e. The time spectrum obtained for N_3^+ is not inconsistent with the mobility expected for these ions from a semi-empirical relationship determined by Mitchell and Ridler from their data.

f. The time spectrum obtained for N_4^+ is not inconsistent with the hypothesis that it is in equilibrium with N_2^+.

g. The predominating ion-molecule reactions of the N_2^+ ions in nitrogen at pressures below 0.7 torr are, with the minute trace of water present, as follows:

$$N_2^+ + H_2O \rightarrow N_2H^+ + OH$$

$$N_2H^+ + H_2O \rightarrow H_3O^+ + N_2$$

h. The single ion observed in pure hydrogen under the conditions of most previous mobility measurements must certainly have been H_3^+.

i. The measurement of the mobility of H_3^+ ions attempted in this experiment was inexact due to source effects, but the results were of the same order of magnitude as previous measurements of the mobility of hydrogen ions in hydrogen.

j. The predominating ion-molecule reactions taking place in hydrogen containing a trace of nitrogen at pressures below 0.7 torr are:

$$H_2^+ + H_2 \rightarrow H_3^+ + H$$

$$H_2^+ + N_2 \rightarrow N_2H^+ + H$$

$$H_3^+ + N_2 \rightarrow N_2H^+ + H_2$$

CHAPTER VI

RECOMMENDATIONS

Provision for the Continuous Variation of z

The solutions (109) and (113) of the partial differential equations (19) and (110) respectively in Appendix F are explicit functions of r and z. In these expressions the mobilities, the diffusion coefficients, the reaction rates, the electric field, and the dimensions of the system appear as parameters. These solutions are implicit but not completely understood functions of the pressure through the mobilities, diffusion coefficients, and reaction rates. It is necessary to assume a relationship between these parameters and the pressure before the data gathered by varying the pressure may be interpreted to determine the rate constants for the various reactions. If data were gathered in the steady state mode of operation by varying z continuously while holding the pressure constant, this data could be much more easily interpreted by means of the solutions (109) and (113) above than is the case of data gathered by varying the pressure.

Under the present arrangement only three values of z are available, one for each of three different sources. Each of these sources unavoidably has somewhat different operating characteristics. It is often not clear when comparison is being made between data gathered using different sources whether certain of the differences in the data are due to the different drift distances or are due to the differences between the operating characteristics of the sources. It is therefore recommended that a single

moveable source be provided so that z, the drift distance, may be varied continuously.

In the process of fitting data gathered by varying z to the equations describing the system, various mathematical combinations of the reaction rates and other parameters can be determined from the variation of the different ion populations with z.

Improvement of the Source Geometry

In the present experiment the principle difficulty encountered in making mobility measurements was the broad, non-symmetric initial distribution of the ions. This distribution was produced first by the formation of the ions throughout a considerable volume of space in the neighborhood of the source, then by the further rapid dispersal of the ions by the electric field of the source anode.

A second difficulty encountered was caused by the fact that the positive ions generated by the sources were formed in collisions between the gas molecules and electrons having a very broad spectrum of energies. Because of the spread of electron energies primary ions of all possible kinds, excited and unexcited, are formed uncontrollably while the source is in operation. The primary causes of this difficulty are the non-uniform electric field of the anode and the various points of origin of the electrons.

It is recommended that the present source be replaced by a mass spectrometer type source of a more conventional design. In such a source ions are produced by a thin, directed beam of monoenergetic electrons running perpendicular to the axis of the drift tube. It is further recommended that all external parts of this source, including the exposed parts

of its mount, be held at the local potential of the drift field so that the source will not seriously distort the drift field in its own vicinity.

Short ion bursts produced by such a source would much more closely approximate the Dirac delta function model used for the initial spatial distribution in the theoretical calculations than do the ion bursts produced by the present sources. This improvement would offer the possibility of a much more accurate determination of the mobility. It might also be expected to offer the possibility of a realistic simultaneous determination of the diffusion coefficient.

Such a source would improve the steady state measurement of the reaction rates since the drift distance z would be more unambiguously defined than it is at present.

A close control of the energy of the source electrons would permit certain simplifications in the interpretation of the data. In many cases it would be possible to eliminate several ionic species from the drift tube by holding the accelerating potential of the electron beam below the appearance potential of these ions. Elimination of extraneous ionic species would permit a more unambiguous analysis of the ion-molecule reactions taking place among the remaining species in the drift tube.

Use of a Diluent Gas in the Investigation of Reaction Rate Constants

Several of the ion-molecule reactions encountered in this investigation apparently have rate constants so large that their exact determination by any of the techniques proposed so far would be quite difficult. The most extreme example encountered was the reaction converting H_2^+ to H_3^+.

It is therefore recommended that a non-reacting gas such as helium be used to dilute the reacting gas during the measurement of rate constants

for reactions in which these constants are very large. The purpose of such a diluent would be to allow the drift tube pressure and the concentration of the reacting gas to be varied independently. If this could be done, high enough pressures could be maintained so that mobility and diffusion theory would be applicable in the interpretation of the results while the concentration of the reacting gas could be reduced to a point where the reaction rate would be small enough to be measured with this apparatus.

APPENDIX A

VALUES OF HASSE'S FUNCTION A FOR VARIOUS VALUES OF THE PARAMETER ν

1/ν	A	A/ν	1/ν	A	A/ν
0.0	.5105	.0000	2.1	.3370	.7077
0.1	.5488	.0549	2.2	.3236	.7119
0.2	.5648	.1130	2.3	.3111	.7155
0.3	.5756	.1727	2.4	.2994	.7186
0.4	.5836	.2334	2.5	.2886	.7215
0.5	.5886	.2943	2.6	.2784	.7238
0.6	.5904	.3542	2.7	.2689	.7260
0.7	.5878	.4115	2.8	.2599	.7277
0.8	.5796	.4637	2.9	.2515	.7293
0.9	.5662	.5096	3.0	.2436	.7308
1.0	.5483	.5483	3.1	.2362	.7322
1.1	.5277	.5805	3.2	.2292	.7334
1.2	.5057	.6068	3.3	.2226	.7346
1.3	.4834	.6284	3.4	.2163	.7354
1.4	.4614	.6460	3.5	.2104	.7364
1.5	.4402	.6603	3.6	.2048	.7373
1.6	.4201	.6722	3.7	.1994	.7378
1.7	.4011	.6819	3.8	.1944	.7387
1.8	.3834	.6901	3.9	.1895	.7391
1.9	.3668	.6969	4.0	.1849	.7396
2.0	.3514	.7028			

APPENDIX B

CALCULATION OF THE MOBILITY K

Two basic statistical methods are used to evaluate the parameters K, D, and A in equation (49). In both of these methods the parameter C is taken to be the total of all the channel counts.

The first method, the method of maximum likelihood, is described on pp. 53-55 of Chapter III. The formulas derived by this method were utilized, using desk calculators, to obtain the values of K, D, and A upon which the conclusions of this thesis were based. A computer program (Max. L.) was constructed utilizing the maximum likelihood formulas and this program was used to check the results obtained using the desk calculators.

A computer program (L. Sq. 2) was constructed utilizing the second method, the method of least squares, which is described in pp. 55-60 of Chapter III. In this program the parameters D and A are first adjusted to tend to minimize the functions in equation (51) then the parameter K is adjusted to tend to minimize this function. This process is then repeated until the criterion for a minimum is achieved.

In addition to these two programs a third experimental program (L. Sq. 1) is presented for comparison. This program makes a least squares fit of the data to the equation

$$F(t) = \frac{CKE}{\sqrt{4\pi Dt}} \exp\left[-\frac{(z - KEt)^2}{4Dt}\right]$$

Which is equation (49) with S_1^2 and A set equal to zero. This result would have been obtained if the partial differential equation (18) had been solved in one cartesian coordinate so that diffusion towards the sides plays no part, if no ion-molecule reactions had occurred, and if the resulting expression for the ion density had been used to derive the time distribution. The method used in this program differs further from that used in L. Sq. 2 in that C was not taken to be the total of the channel counts but was determined by initially calculating the value that would minimize S. Then the parameters K and D are adjusted to tend to minimize S. These two operations are repeated until the criterion for a minimum is achieved. This program gave values of S about one to two orders of magnitude smaller than the other least squares program, but it also gave values of C three to four orders of magnitude smaller than its actual value.

Fortran Program Listings

On the following pages is a glossary of symbols used in the Fortran programs followed by listings of the computer programs used. Since the same data decks were used for all programs the maximum likelihood program read instruction is set up to read in initial guesses for K, D, and A although these are not necessary and are never used in this program.

Glossary of Fortran Symbols

	Fortran Symbol	Variable or Parameter	Comment
1	P	K	I, J, K, L, M, N normally used for integers in Fortran.
2	D, A	D, A	
3	PO, DO, AO		Initial guesses of P, D, and A
4	TO		t_j for first channel having a non-zero count
5	DT		Time interval between channels
6	Z, E	Z, E	
7	N		Number of channel counts in sample
8	GU		Signal that channel size has changed.
9	F(I)	N_j	I = j Also see 1 above
10	T(I)	t_j	
11	C	N	
12	FO(I)		F(I) = C·FO(I)
13	R(I)	Z-KEt	I = j
14	H	S_1^2	H is taken to be about .0237 to be consistant with the assumption that the ion population density goes to zero about 15cm from the axis of the drift tube.
15	FU(I)		FI(I) = C·FU(I)
16	FI(I)	f_j	I = j
17	CEW		Factor of the Q(I) to take account of channel size
18	KT		Signal for GO TO command.
19	B	$\Sigma_j(f_jQ_j/C)^2$	

	Fortran Symbol	Variable or Parameter	Comment
20	G	$\Sigma_j f_j N_j Q_j^2/C$	
21	S_1	$\Sigma_j N_j$	
22	S_2	$\Sigma_j N_j t_j$	
23	S_3	$\Sigma_j N_j/t_j$	
24	Q(I)	Q_j	Weighting factors to take acacount of both channel size and statistical scatter in channel counts. I = j
25	U(f), V(I), W(I)		$\left(\frac{\partial f_j}{\partial K}\right)_o$, $\left(\frac{\partial f_j}{\partial D}\right)_o$, $\left(\frac{\partial f_j}{\partial A}\right)_o$, respectively multiplied by the weighting factors Q(I), I = j.
26	AIJ	u_{ij}	I = i, J = j
27	B1	v_i	I = i
28	FLN		Decimal value of integer N
29	S	S	Sum of the squares of the weighted residuals.
30	SU		Stored value of S for future use.
31	KO		Count of initial corrections of D and A.
32	IT		Count of corrections of P.
33	Denom	Δ	
34	DP, DD, DA	$\Delta K, \Delta D, \Delta A$	
35	BE		Fraction of DP, DD, or DA added to P, D, or A respectively. $0 < BE \leq 1$.

```
      MAXIMUM LIKELIHOOD FIT (Max. L.)

      DIMENSION F(40), T(40), FU(40), FI(40), R(40), RES(40)
      DISTF (T,R) = P*E/SQRTF(12.566*D*T)*EXPF (R*((A*H* D)/P/E-.25*R/D/T))
      CALL ERRORS
      H = .02570
   49 READ INPUT TAPE 2, 50, PO, DO, AO, TO, OT, E, Z, N, GU
   50 FORMAT(5E10.2, F8.5, F8.2, 13, F3.0)
      READ INPUT TAPE 2, 51, (F(I), I = 1, N)
   51 FORMAT(6E 12.5)
C     GENERATE T(I) ARRAY. COMPUTE SUMS S1, S2, AND S3.
      S1 = 0.
      S2 = 0.
      S3 = 0.
      T(1) = TO
      KT = 1
      DO 52 I = 1, N
      GO TO (60, 62), KT
   60 TU = T(I) + DT/10.**4
      IF(TU - GU*DT) 62, 61, 61
   61 DT = 10.*DT
      KT = 2
      T(I + 1) = T(I) + .55*DT
      GO TO 63
   62 T(I + 1) = T(I) + DT
   63 S1 = S1 + F(I)
      S2 = S2 + F(I)*T(I)
   52 S3 = S3 + F(I)/T(I)
C     COMPUTE P, D, AND A.
      P = Z/E*S1/S2
      D = .5*Z**2*(S3/S1 - S1/S2)
      A = .5*(S1/S2*(1. + H*Z**2) - S3/S1*H*Z**2)
C     COMPARE FIT WITH DATA
      S = 0.
      DO 53 I = 1, N
      R(I) = Z - P*E*T(I)
      FU(I) = DISTF (T(I) .R(I))
      FI(I) = S1*FU(I)
      RES(I) = (FI(I) - F(I))*Q(I)
   53 S = S + RES(I)**2/S1
C     PRINT OUT RESULTS
      WRITE OUTPUT TAPE 3, 72, P, D, A, S
   72 FORMAT(/10X, 1HP, 14X, 1HD, 14X, 1HA, 14X, 1HS/1X, (4E 1 5.4))
      WRITE OUTPUT TAPE 3, 73, (T(I), F(I), FI(I), R(I), FU(I), I = 1, N)
   73 FORMAT(/8X,4HT(I), 10X, 4HF(I), 10X,5HFI(I),9X,4HR(I), 10X,5HFU(I)/
     1  1X, (5E14.4))
C     PICK UP NEXT SAMPLE
      GO TO 49
      END
```

```
      LEAST SQUARES FIT (L. Sq. 1)

      DIMENSION T(140),F(40),FU(40),U(40),V(40)W(40),R(40),FI(40)
      DIMENSION RES(40), Q(40)
      DISTF (T,R) = P*E/SQRTF (12.556*D*T)*EXPF (-.25R**2/D/T)
      CALL ERRORS
   49 READ INPUT TAPE 2, 50, PO, DO, AO, TO, DT, E, Z, N, GU
   50 FORMAT(5E10.2, F8.5, F8.2, I3, F3.0)
      READ INPUT TAPE 2, 51, (F(I), I = 1, N)
   51 FORMAT(6E12.5)
C     COMPUTE T(I) ARRAY
      T(1) = TO
      CEW = 1.
      KT = 1
      DO 52 I = 1, N
      F(I) = F(I)/CEW
      Q(I) = CEW/SQRTF(F(I) + 1.)
      GO TO (63, 62), KT
   63 TU = T(I) + DT/10.**4
      IF(TU - GU*DT) 62, 61, 61
   61 DT = 10.*DT
      CEW = 10.
      KT = 2
      T(I + 1) = T(I) + .55*DT
      GO TO 52
   62 T(I + 1) = T(I) + DT
   52 CONTINUE
C     COMPUTE C, NUMBER OF IONS COUNTED
      P = PO
      D = DO
      IT = 0.
      DO 70  K = 1, 500
      IT = IT + 1
      G = 0.
      B = 0.
      DO 53 I = 1, N
      R(I) = Z - P*E*T(I)
      FU(I) = DISTF (T(I),R(I))
      G = G + FU(I)*F(I)*Q(I)**2
   53 B = B + FU(I)**2*Q(I)**2
      C = G/B
C     COMPUTE FI(I), DP, DD, DA
      FLN = N
      A11 = 0.
      A12 = 0.
      A22 = 0.
      B1 = 0.
      B2 = 0.
      DO 54 I = 1, N
      RES(I) = (FI(I) - F(I))O*Q(I)
      S = S + RES(I)**2/FLN
      FI(I) = C*FU(I)
```

```
      U(I) = F(I)*(1./P + .5*R(I)*E/D)*Q(I)
      V(I) = F(I)*(-.5/D + .25/T(I)*(R(I)/D)**2)*Q(I)
      A11 = A11 + U(I)**2
      A12 = A12 + U(I)*V(I)
      A22 = A22 + V(I)**2
      B1 = B1 + (F(I) - FI(I))*U(I)*Q(I)
   54 B2 = B2 + (F(I) - FI(I))*V(I)Q(I)
      DENOM = A11*A22 - A12**2
      DP = (B1*A22 - B2*A12)/DENOM
      DD = (B2*A11 - B1*A12)/DENOM
C     TEST FOR MINIMUM S
C     CORRECT P OR D IF NECESSARY
      IF(ABSF(DP) - .001*P) 56, 56, 55
   55 P = P + .25*DP
      IF(ABSF(DD) - .001*D) 70, 70, 57
   56 IF(ABSF(DD) - .001*D) 71, 71, 57
   57 D = D + .25*DD
   70 CONTINUE
C     PRINT OUT RESULTS
   71 WRITE OUTPUT TAPE 3, 72, P, D, C, G, B, S
   72 FORMAT(/10X,1HP,14X,1HD,14X1HC,14X,1HG,14X,1HB,14X,1HS,/1X,(6E15.4))
      WRITE OUTPUT TAPE 3, 73,(T(I), FI(I), R(I), FU(I), U(I), V(I),
     1  I = 1, N)
   73 FORMAT(/8X,4HT(I),10X,4HF(I),10X,5HFI(I),9X,4HR(I),10X,5HFU(I),
     1  9X,4HU(I),10X,4HV(I)/1X,(7E14.4))
      WRITE OUTPUT TAPE 3, 74, A11,A12,A22,B1,B2,DENOM
   74 FORMAT(/9X,3HA11,12X,3HA12,12X,3HA22,12X,2HB1,13X,2HB2,13X,5H
     1  DENOM/1X, (6E15.4))
      WRITE OUTPUT TAPE 3, 75, DP, DD, IT
   75 FORMAT(/8X,2HDP,13X,2HDD,12X,2HIT/1X,2E 15.4,18)
C     PICK UP NEXT SAMPLE
      GO TO 49
      END
```

```
      LEAST SQUARES FIT (L. Sq. 2)

      DIMENSION T(140),F(40),FU(40)FI(40),RES(40),R(40),Q(40),FO(40)
      DIMENSION U(40),V(40),W(40)
      DISTF(T,R) = P*E/SQRTF(12.566*D*T)*EXPF(R*((A + H*D)/P/E-.25*R/D/T))
      CALL ERRORS
      H = .02570
   49 READ INPUT TAPE 2, 50, PO,DO,AO,TO,DT,E,Z,N,GU
   50 FORMAT(5E10.2, F8.5, F8.2, I3, F3.0)
      READ INPUT TAPE 2, 51, (F(I), I = 1, N)
   51 FORMAT(6E12.5)
C     COMPUTE T(I), Q(I), FO(I) ARRAYS, MODIFY F(I). COMPUTE C.
      T(I) = TO
      CEW = 1.
      KT = 1
      C = 0.
      DO 55 I = 1, N
      Q(I) = CEW/SQRTF(F(I) + 1.)
      F(I) = F(I)/CEW
      C = C + F(I)
      GO TO (52,54), KT
   52 TU = T(I) + DT/10.**4
      IF(TU - GU*DT) 54, 53, 53
   53 DT = 10.*DT
      CEW = 10.
      KT = 2
      T(I + 1) = T(I) + .55*DT
      GO TO 55
   54 T(I + 1) = T(I) + DT
   55 CONTINUE
      DO 48 I = 1, N
   48 FO(I) = F(I)/C
C     COMPUTE DO AND DA.
      IT = 0.
      P = PO
      C = DO
      A = AO
   56 KO = 0.
      WRITE OUTPUT TAPE 3, 70
   70 FORMAT(/8X,3HA11,11X,3HA12,11X,3HA22,11X,2HB1,12X,2HB2,12X,1HS,
     1  12X,2HDD,12X,2HDA)
      DO 61 J = 1, 500
      IF(SENSE SWITCH 1) 100, 101
  101 KO = KO + 1
      A22 = 0.
      A23 = 0.
      A33 = 0.
      B2 = 0.
      B3 = 0.
      S = 0.
      FLN = N
      B = 1.
```

```
      DO 57 I = 1, N
      R(I) = Z - P*E*T(I)
      FU(I) = DISTF(T(I),R(I))
      FI(I) = C*FU(I)
      V(I) = FI(I)*(-.5/D + H*R(I)/P/E + .25/T(I)*(R(I)/D)**2)*Q(I)
      W(I) = FI(I)*R(I)/P/E*Q(I)
      S = S + (FO(I) - FU(I))**2/FLN*C**2*Q(I)**2
      A22 = A22 + V(I)**2
   94 A23 = A23 + V(I)*W(I)
      A33 = A33 + W(I)**2
      B2 = B2 + (FO(I) - FU(I))*C*V(I)*Q(I)
   57 B3 = B3 + (FO(I) - FU(I))*C*W(I)*Q(I)
      DENOM = A22*A33 - A23**2
      DD = (B2*A23 - B3*A23)/DENOM
      DA = (B3*A22 - B2*A23)/DENOM
C     TEST FOR MINIMUM S. CORRECT D OR A IF NECESSARY.
      IF(ADSF(DD) - .001*D) 59, 59, 58
   58 D = D + .25*DD
      IF(ABSF(DA) - .001*ABSF(A)) 61, 61, 60
   59 IF(ABSF(DA) - .001*ABSF(A)) 90, 90, 60
   60 A = A + .25*DA
      WRITE OUTPUT TAPE 3, 71, A11, A12, A22, B1, B2, S, DD, DA
   71 FORMAT(1X, 8E14.4)
   61 CONTINUE
   90 WRITE OUTPUT TAPE 3, 72, D, A, B, KO
   72 FORMAT(/1X, 2E14.4, E7.1, I8)
C     MINIMIZE WRT P.
      WRITE OUTPUT TAPE 3, 73
   73 FORMAT(/8X,2HA3,12X,2HB3,12X,2HDP,12X,1HS)
      DO 80 K = 1, 50
      IF(SENSE SWITCH 1) 100, 102
  102 IT = IT + 1
      SU = S
      A3 = 0.
      B3 = 0.
      S = 0.
      DO 62 I = 1, N
      R(I) = Z - P*E*T(I)
      FU(I) = DISTF(T(I),R(I))
      FI(I) = C*FU(I)
      U(I) = FI(I)*(1./P - Z*(A + H*D)/P**2/E + .5*R(I)*E/D)*Q(I)
      S = S + (FO(I) - FU(I))**2/FLN*C**2*Q(I)**2
      A11 = A11 + U(I)**2
   62 B1 = B1 + (FO(I) - FU(I))*C*U(I)*Q(I)
      DP = B1/A11
      WRITE OUTPUT TAPE 3, 74, A3, B3, DP, S
   74 FORMAT(1X, 4E14.4)
      IF(SU - S)210, 210, 211
  210 BE = BE - .5*BE
      GO TO 63
  211 BE = BE + .1*(1. - BE)
```

```
   63 IF(ABSF(DP) - .001*P) 81, 81, 64
   64 P = P + BE*DP
   80 CONTINUE
      IF(IT - 1500) 82, 82, 81
   82 GO TO 56
   81 WRITE OUTPUT TAPE 3, 75, P, D, A, C, S, IT
   75 FORMAT(1OX,1HP,14X,1HD,14X,1HA,14X,1HC,14X,1HS,14X,2HIT/1X,(5E15.4),
     1  I6)
      WRITE OUTPUT TAPE 3, 76, (T(I),F(I),FI(I),R(I),U(I),V(I),W(I), I = 1,
     1  N)
   76 FORMAT(/8X,4HT(I),1OX,4HF(I),1OX,5HFI(I),9X,4HR(I),1OX,4HU(I),1OX,
     1  4HV(I),1OX,4HW(I)/1X,(7E14.4))
C     PICK UP NEXT SAMPLE
      GO TO 49
  100 WRITE OUTPUT TAPE 3, 75, P, D, A, C, S, IT
      WRITE OUTPUT TAPE 3, 76, (T(I),F(I),FI(I),R(I),U(I),V(I),W(I),
     1  I = 1, N)
      CALL EXIT
      END
```

N^+ Mobilities

Run I.D.No.	E (volts/cm)	p (μ)	Z (cm)	$KX10^{-4}(cm^2/volt\text{-}sec)$ Max.L.	L.Sq.1	L.Sq.2
22-1	2.015	50.2	26.78	4.238	6.020	4.24
22-3,4	3.022	50.2	26.78	3.687	4.609	3.69
22-5,6	4.029	50.2	26.78	3.259	4.427	3.28
22-7,8	4.029	50.2	36.94	3.203	4.084	3.17
22-10	3.022	50.2	36.94	2.373	3.218	2.37
22-11	2.015	50.2	16.62	2.491	2.756	2.49
22-13,14	3.022	50.2	16.62	3.860	4.536	3.86
22-15	2.015	144	16.62	1.562	1.621	1.56
22-16	3.022	144	16.62	1.892	2.091	1.89
22-18	4.029	144	16.62	1.687	2.149	1.69
22-20	3.022	144	26.78	1.110	1.170	1.11
22-22	4.029	144	26.78	1.217	1.422	1.22
22-24	4.029	144	36.94	1.448	1.555	1.45
22-25	4.029	100.8	36.94	1.865	2.086	1.87
22-26	3.022	100.8	26.78	1.702	1.849	1.69
22-28	4.029	100.8	26.78	1.700	2.229	1.70
22-29	3.022	100.8	16.62	1.584	1.661	1.58
22-30,31	4.029	100.8	16.62	2.002	2.187	1.95

N_2^+ Mobilities

Run I.D.No.	E (volts/cm)	p (μ)	Z (cm)	$KX10^{-4}(cm^2/volt\text{-}sec)$ Max.L.	L.Sq.1	L.Sq.2
18-1	1.007	48.0	16.62	2.330	2.683	2.33
18-2	2.015	48.0	16.62	2.133	2.537	2.13
18-3	3.022	48.0	16.62	1.669	2.088	1.67
18-6	3.022	48.0	26.78	1.539	2.088	1.54
18-7	3.022	48.0	36.94	2.244	2.725	2.24
18-8	2.015	48.0	36.94	2.314	2.572	2.32
18-13	3.022	99.3	16.62	1.156	1.260	1.16
18-14	2.015	99.3	16.62	.9821	1.071	.982
18-15	2.015	147	16.62	.9044	.9650	.904
18-16	3.022	147	16.62	1.024	1.100	1.01
18-26	3.022	191	16.62	.7976	.8426	.798
18-28	3.022	241	16.62	.7156	.7592	.716
18-36	3.022	271	16.62	.5083	.5273	.559
18-37	4.029	271	16.62	.6384	.6748	.638
18-38	4.029	271	16.62	.6991	.7474	.699
19-1	4.029	48.0	36.94	1.584	1.903	1.58
19-2	4.029	48.0	26.78	2.336	2.433	2.34
19-3	4.029	48.0	16.62	2.233	2.345	2.22
19-4	4.029	99.3	16.62	1.344	1.392	1.34
19-5	4.029	99.3	26.78	1.447	1.464	1.45

N_2^+ Mobilities

Run I.D.No.	E (volts/cm)	p (μ)	Z (cm)	$KX10^{-4}$ (cm^2/volt-sec) Max.L.	L.Sq.1	L.Sq.2
19-6	4.029	99.3	36.94	1.465	1.489	1.47
19-7	4.029	147	36.94	1.049	1.077	1.05
19-8	4.029	147	26.78	1.117	1.137	1.12
19-9	4.029	147	16.62	1.014	1.039	1.01
19-10	4.029	191	16.62	.8341	.8528	.834
4-1	3.022	200	16.62	.7403	.8164	.741
4-2	3.022	200	16.62	.7273	.7975	.727
4-3,4	3.022	305	16.62	.5172	.5135	.518
4-6	3.022	455	16.62	.1646	.2407	.165
4-7	3.022	520	16.62	.1571	.2370	.178
4-9,10	4.029	285	26.78	.3704	.5325	.373
4-11	4.029	455	26.78	.1627	.2371	.166
4-12	4.029	618	26.78	.1348	.1781	.135
4-13	4.029	835	26.78	.1206	.1509	.121
5-1,2	4.029	183	36.94	.8201	.9064	.370
5-4	4.029	310	36.94	.4907	.5551	.491
5-5	4.029	420	36.94	.3938	.4467	.308
5-6	4.029	585	36.94	.3213	.3508	.285
6-1,2	4.029	191.3	36.94	.7533	.8360	.757
6-3,4	4.029	147.2	36.94	.8460	.9976	.851
6-5,6	3.022	147.2	36.94	.7770	.8678	.783
6-7,8	4.029	98.9	36.94	1.097	1.227	1.10
6-9,10	3.022	98.9	36.94	1.012	1.100	1.02
6-11	4.029	51.0	36.94	2.318	2.517	2.32
6-12	3.022	51.0	36.94	2.389	2.490	2.39
6-13,14	3.022	74.9	36.94	1.501	1.590	1.50
6-15,16	4.029	74.9	36.94	1.471	1.604	1.47
6-17,18	4.029	124.0	36.94	.9346	.9802	.936
6-19,20	3.022	124.0	36.94	.8460	.9182	.850
6-21,22	4.029	172.2	36.94	.7353	.7844	.737
6-23,24	3.022	172.2	36.94	.6804	.7416	.684
6-25,26	2.015	191.3	26.78	.4839	.5968	.490
6-27,28	3.022	191.3	26.78	.4086	.5399	.413
6-29,30	4.029	191.3	26.78	.3981	.5282	.402
6-31,32	4.029	191.3	16.62	.3841	.4014	.386
6-33,34	3.022	191.3	16.62	.3943	.4595	.397
6-35,36	3.022	172.2	16.62	.4307	.3954	.434
6-37,38	4.029	172.2	16.62	.4232	.5781	.425
6-39,40	4.029	172.2	26.78	.4712	.4447	.475
6-41,42	3.022	172.2	26.78	.4389	.5230	.444

N_2^+ Mobilities

Run I.D.No.	E (volts/cm)	p (μ)	Z (cm)	KX10^{-4}(cm^2/volt-sec) Max.L.	L.Sq.1	L.Sq.2
7-1,2	4.029	147.2	26.78	.5799	.7464	.583
7-3,4	3.022	147.2	26.78	.5657	.6992	.571
7-6	4.029	147.2	16.62	.6345	1.204	.635
7-7,8	3.022	147.2	16.62	.5865	.7194	.587
7-9,10	3.022	124.0	16.62	.7087	.8361	.709
7-12	4.029	124.0	16.62	.6346	.8318	.635
7-13,14	4.029	124.0	26.78	.6385	.6516	.641
7-15,16	3.022	124.0	26.78	.5534	.6975	.558
7-17,18	4.029	98.9	26.78	.4736	.6600	.478

APPENDIX C

OTHER POSSIBLE INITIAL ION DISTRIBUTIONS

In deriving the spatial distribution of the ion burst at time t in Chapter III it was assumed that when t=0 the distribution of ions along the z-axis may, for practical purposes, be represented by $Z(z,0) = N_o\delta(z)$. This is equivalent to assuming that $f_o(k)$ in equation (29) has the form, $f_o(k) = \frac{N_o}{\sqrt{2\pi}}$. Since the actual distribution is not known and since any bounded distribution will approach the same general bell-shaped distribution asymptotically as time increases, this assumption is as good as any for the present experiment.

Future improvements in the resolution of the apparatus may make the form of the initial ion distributions into an important factor in the interpretation of the results. The ion distributions for $t > 0$ resulting from several other initial ion distributions were investigated in connection with the present research. Attention was focussed principally on the ion distribution in the z-direction rather than on the radial ion distribution. The initial radial ion distribution would determine the C_i in equation (33). Results are presented here for an initial bell-shaped ion distribution and for an initial square-shaped ion distribution along the z-axis.

Bell-Shaped Distribution

Let the initial ion distribution in the z-direction have the form

$$Z(z,0) = \frac{N_o}{\sigma\sqrt{2\pi}} \exp\left[-\frac{z^2}{2\sigma^2}\right] \quad . \tag{65}$$

Then reference to the same integration formula used to produce equation (32) gives

$$Z(z,0) = \frac{N_o}{2\pi} \int_{-\infty}^{\infty} \exp\left[-\frac{\sigma^2 k^2}{2} + ikz\right] dk \tag{66}$$

Thus

$$f_o(k) = \frac{N_o}{\sqrt{2\pi}} \exp\left[-\frac{\sigma^2 k^2}{2}\right] \tag{67}$$

is the Fourier transform of $Z(z,0)$, and from equation (27)

$$f(k,t) = \frac{N_o}{\sqrt{2\pi}} \exp\left[-\frac{\sigma^2 k^2}{2} - Dk^2 t - ikKET - (A + S^2 D)t\right] \tag{68}$$

is the Fourier transform of $Z(z,t)$. Hence

$$Z(z,t) = \frac{N_o \exp\left[-(A + S^2 D)t\right]}{2\pi} \int_{-\infty}^{\infty} \exp\left[-(Dt + \frac{\sigma^2}{2}) k^2 + ik(z - KEt)\right] dk \quad , \tag{69}$$

or, again using the same integration formula used to produce (33),

$$Z(z,t) = \frac{N_o}{\sqrt{4\pi(Dt + \sigma^2/2)}} \exp\left\{-(A + S^2 D)t - \frac{(z - KEt)^2}{4(Dt + \sigma^2/2)}\right\} \tag{70}$$

This distribution is experimentally indistinguishable from a distribution of an ion's which started initially as approximately a Dirac delta function distribution given in equation (32). If such an initial distribution were assumed in this case the estimate of D would be too large due to the term $\sigma^2/2$.

Square-Shaped Distribution

Let the initial ion distribution in the z-direction have the form

$$Z(z,0) = n \ , \quad -a \leq z \leq a \ , \tag{71}$$
$$Z(z,0) = 0 \ , \quad z < -a, \ z > a \ .$$

The special case of equation (26) for t=0 is

$$Z(z,0) = \frac{1}{\sqrt{2\pi}} \int_{-\infty}^{\infty} f_o(k') \exp(ik'z) \, dk' \ ;$$

where Z(z,0) may have the form (71) above. Multiplication of both sides of the above equation by $\frac{1}{\sqrt{2\pi}} \exp(ikz) \, dz$ and integration with respect to z produces

$$\frac{n}{\sqrt{2\pi}} \int_{-a}^{a} \exp(ikz) \, dz = \int_{-\infty}^{\infty} f_o(k') \, \delta(k - k') \, dk' \ . \tag{72}$$

Hence

$$f_o(k) = \frac{n}{\sqrt{2\pi}} \left(\frac{e^{iak} - e^{-iak}}{ik} \right) \ , \tag{73}$$

and

$$Z(z,t) = \frac{n \exp[-(A + S^2D)t]}{2\pi} \int_{-\infty}^{\infty} \exp(-Dk^2t) \left\{\frac{\exp[ik(z+a-KEt)] - \exp[ik(z-a-KEt)]}{ik}\right\} dk \qquad (74)$$

In order to perform the above integration we will first consider the following equation:

$$\operatorname{erf}(u_1) - \operatorname{erf}(u_2) = \frac{1}{\sqrt{2\pi}} \int_{u_2}^{u_1} \exp(-\frac{u^2}{2})\, du \quad . \qquad (75)$$

The right side of this equation may be expressed in its Fourier transform form

$$\operatorname{erf}(u_1) - \operatorname{erf}(u_2) = \frac{1}{2\pi} \int_{-\infty}^{\infty} \int_{u_2}^{u_1} \exp(-\frac{h^2}{2} + ihu)\, dhdu \qquad (76)$$

which upon integration with respect to u becomes

$$\operatorname{erf}(u_1) - \operatorname{erf}(u_2) = \frac{1}{2\pi} \int_{-\infty}^{\infty} \exp(-\frac{h^2}{2}) \left\{\frac{\exp(ihu_1) - \exp(ihu_2)}{ih}\right\} dh \qquad (77)$$

If, in this equation, we let

$$u_1 = \frac{z + a - KEt}{\sqrt{2Dt}} \quad , \qquad (78)$$

$$u_2 = \frac{z - a - KEt}{\sqrt{2Dt}} \quad ,$$

and

$$h = \sqrt{2Dt}\, k \quad ,$$

then the integral on the right of (77) above assumes the same form as the integral on the right of (74). Hence

$$Z(z,t) = n \exp[-(A + S^2D)t] \left\{ \operatorname{erf}\left(\frac{z+a-KEt}{\sqrt{2Dt}}\right) - \operatorname{erf}\left(\frac{z-a-KEt}{\sqrt{2Dt}}\right) \right\} . \quad (79)$$

APPENDIX D

ION BURST FROM A POINT SOURCE IN A UNIFORM ELECTRIC FIELD

In the present apparatus the distances from the sources to the cylindrical sides of the drift tube and to the drift field anodes are smaller than or of the order of the drift distances. Furthermore the sources generate or disperse ions throughout a considerable volume in their own neighborhood in the drift tube. It is therefore believed that the sides of the drift tube and the anodes have a considerable affect on the ion population in the neighborhood of the pin-hole leading to the mass spectrometer. For the above reason the interpretation of the results of this research was most appropriately carried out using cylindrical coordinates.

It was anticipated that in future modifications of the equipment the ion source might be improved in such a way that it might more nearly approximate a point source. There might also be circumstances under which the distance from the source to the pin-hole would be small compared to distances to the sides. Under such circumstances the walls should not have a significant affect upon the ion population in the neighborhood of the pin-hole. In anticipation of such a situation the behavior of an ion burst, initially originating at a point source, diffusing and drifting under the influence of a uniform electric field was investigated. The results of this investigation are presented here.

In working out this result the z-axis shall be taken as parallel to the uniform electric drift field. Equation (18) from Chapter III, expressed in rectangular cartesian coordinates, has the form:

$$-D\left(\frac{\partial^2 n}{\partial x^2}+\frac{\partial^2 n}{\partial y^2}+\frac{\partial^2 n}{\partial z^2}\right)+KE\frac{\partial n}{\partial z}+An+\frac{\partial n}{\partial t}=0 \qquad (80)$$

To separate variables in this equation it is assumed that n may be expressed in the form

$$n(x,y,z,t) = X(x,t)\,Y(y,t)\,Z(z,t) \quad . \qquad (81)$$

Substitution of (81) into (80) above leads to the following three partial differential equations:

$$-D\frac{\partial^2 X}{\partial x^2}+\frac{\partial x}{\partial t}+A_x X = 0 \quad , \qquad (82)$$

$$-D\frac{\partial^2 Y}{\partial y^2}+\frac{\partial Y}{\partial t}+A_y Y = 0 \quad , \qquad (83)$$

and

$$-D\frac{\partial^2 Z}{\partial z^2}+KE\frac{\partial Z}{\partial z}+\frac{\partial Z}{\partial t}+A_z Z = 0 \quad , \qquad (84)$$

where

$$A = A_x + A_y + A_z \quad .$$

To solve (84) let

$$Z(z,t) = \frac{1}{\sqrt{2\pi}} \int_{-\infty}^{\infty} h(k_z,t) \exp(ik_z z)\, dk_z \quad . \tag{85}$$

Substitution of this expression into (84) yields the partial differential equation

$$\frac{\partial h(k_z,t)}{\partial t} + (A_z + Dk_z^2 + ik_z KE)\, h(k_z,t) = 0 \tag{86}$$

whose solution is

$$h(k_z,t) = h_o(k_z) \exp[-(A_z + Dk_z^2 + ik_z KE)t] \quad . \tag{87}$$

Hence

$$Z(z,t) = \frac{\exp(-A_z t)}{\sqrt{2\pi}} \int_{-\infty}^{\infty} h_o(k_z) \exp[-Dk_z^2 t + ik_z(z-KEt)]\, dk_z \quad . \tag{88}$$

The functions $X(x,t)$ and $Y(y,t)$ have a similar form except for the absence of the drift term:

$$X(x,t) = \frac{\exp(-A_x t)}{\sqrt{2\pi}} \int_{-\infty}^{\infty} f_o(k_x) \exp[-Dk_x^2 t + ik_x x]\, dk_x \quad , \tag{89}$$

and

$$Y(y,t) = \frac{\exp(-A_y t)}{\sqrt{2\pi}} \int_{-\infty}^{\infty} g_o(k_y) \exp[-Dk_y^2 t + ik_y y]\, dk_y \quad . \tag{90}$$

In this formulation it is desired to make the initial ion burst proportional to a three dimensional Dirac delta function:

$$N_o\delta(\underline{r}) = \frac{N_o}{(2\pi)^3}\int \exp(i\underline{k}\cdot\underline{r})\, d\underline{k} \tag{91}$$

which when expressed in rectangular cartesian coordinates, is

$$N_o\delta(x,y,z) = \frac{N_o}{(2\pi)^3}\int_{-\infty}^{\infty}\int_{-\infty}^{\infty}\int_{-\infty}^{\infty} \exp[i(k_x x + k_y y + k_z z)]\, dk_x dk_y dk_z$$

Here N_o is the total number of ions in the initial ion burst. If, in equations (89), (90), and (88) above, $f_o(k_x)$, $g_o(k_y)$, and $h_o(k_z)$ are each set equal to $(2\pi)^{-1/2}N_o^{1/3}$, then

$$n(x,y,z,0) = \frac{N_o}{(2\pi)^3}\int \exp(i\underline{k}\cdot\underline{r})\, d\underline{k} = N_o\delta(\underline{r}) \quad . \tag{92}$$

Hence

$$n(x,y,z,t) = \frac{N_o \exp(-At)}{(2\pi)^3}\int_{-\infty}^{\infty}\int_{-\infty}^{\infty}\int_{-\infty}^{\infty} \exp\{-Dt[k_x^2 + k_y^2 + k_z^2] + i[k_x x + k_y y + k_z(z-KEt)]\}\, dk_x dk_y dk_z \tag{93}$$

which, upon integration, is

$$n(x,y,z,t) = \frac{N_o}{(4\pi Dt)^{3/2}} \exp\left\{-At - \frac{[x^2 + y^2 + (z-KEt)^2]}{4Dt}\right\} \quad . \tag{94}$$

The form of this equation gives an ion distribution in the form of a spherically symmetric cloud in which the ions are diffusing outward away from

the geometric center of the cloud. This center is at the same time drifting in the z-direction at a speed of KE. The equation (94) has a single term on the right hand side instead of a series.

APPENDIX E

FORM OF SECONDARY ION BURSTS

Basic Equations for Secondary Ions

A population of secondary ions is subject to an equation of continuity of the form

$$\nabla \cdot \underline{J}_2 + \sum_i \beta_i \sigma_i n_2 + \frac{\partial n_2}{\partial t} = \alpha\sigma n_1 \qquad (95)$$

where n_2 is the ion (charge) density of the secondary ions, $\underline{J}_2$ is the current density of that ion, and n_1 is the ion (charge) density of the primary ion from which this particular secondary ion is formed. In this equation the β_i are the rate constants for reactions using up the secondary ions, the σ_i are the densities of the molecular species with which these ions are reacting, and $\sum_i \beta_i \sigma_i$ is the combined effect of all of these reactions. Let $B = \sum_i \beta_i \sigma_i$. On the right hand side of the equation α and σ are the rate constant and the reagent molecular density respectively for the reaction transforming primary ions into secondaries. Combining the equation (95) with (16) gives the partial differential equation for the density of secondary ions

$$-D_2 \nabla \cdot \nabla n_2 + K_2 \nabla \cdot (\underline{E} n_2) + Bn_2 + \frac{\partial n_2}{\partial t} = \alpha\sigma n_1 \qquad (96)$$

where D_2 and K_2 are the diffusion coefficient and mobility, respectively, of the secondary ions.

Solution of the Partial Differential Equation for Secondary Ions for the Pulse Mode of Operation

If it is assumed that the system is cylindrically symmetric with the electric field $\underline{E}$ uniform and parallel to the z-axis, then (96) may be expressed in cylindrical coordinates as follows:

$$-D_2 \frac{\partial^2 n_2}{\partial r^2} - \frac{D_2}{r} \frac{\partial n_2}{\partial r} - D_2 \frac{\partial^2 n_2}{\partial z^2} + K_2 E \frac{\partial n_2}{\partial z} + B n_2 + \frac{\partial n_2}{\partial t} = \alpha\sigma\, n_1 \qquad (97)$$

Equation (97) is a non-homogeneous partial differential equation. The complementary function, the solution to the corresponding homogeneous equation, will be of the same general form as the solution of equation (19). In this solution the function $Z(r,t)$ has the same general form as (29) except that since there are no secondary ions when $t=0$; $f_o(k)$ in (29) will therefore be identically zero. Hence this complementary function will be identically zero.

To find the particular integral it will be assumed that the solution of (97) will be of the form

$$n_2(r,z,t) = \sum_i J_o(s_i r)\, Z_i(z,t) \qquad (98)$$

where the $J_o(s_i r)$ are introduced explicitly into this assumed solution because the same radial boundary conditions apply to secondary ions as applied to primaries. The expression (33) is substituted for n_1. Hence we have

$$\sum_i \left[D_2 s_i^2 J_o(s_i r) Z_i(z,t) - D_2 J_o(s_i r) \frac{\partial^2 Z_i(z,t)}{\partial z^2} + K_2 E J_o(s_i r) \frac{\partial Z_i(z,t)}{\partial z} \right. \quad (99)$$

$$\left. + B J_o(s_i r) Z_i(z,t) + J_o(s_i r) \frac{\partial Z_i(z,t)}{\partial t} \right]$$

$$= \frac{\alpha\sigma N_o}{\sqrt{4\pi D_1 t}} \sum_i C_i J_o(s_i r) \exp\left[- (A + s_i^2 D_1)t - \frac{(z - K_1 E)^2}{4 D_1 t} \right]$$

where D_1 and K_1 are the diffusion coefficient and mobility of the primary ions respectively. Multiplication of both sides of (99) by $r\, J_o(s_i r)\, dr$ and integration from 0 to 1 reduces each side of the equation to a single term of the summation,

$$-D_2 \frac{\partial^2 Z_i}{\partial z^2} + K_2 E \frac{\partial Z_i}{\partial z} + (B + s_i^2 D_2) Z_i + \frac{\partial Z_i}{\partial t} = \frac{\alpha\sigma C_i N_o}{\sqrt{4\pi D_1 t}} \exp\left[-(A + s_i^2 D_1)t \right. \quad (100)$$

$$\left. - \frac{(z - K_1 E t)^2}{4 D_1 t} \right] .$$

The expression on the right side of this equation may be expressed in the form (29) where $\frac{N_o}{\sqrt{2\pi}}$ is put in place of $f_o(k)$; the expression of the left may be expressed in the form (26). This leads to the partial differential equation

$$\frac{\partial f_i(k,t)}{\partial t} + M_2 f_i(k_1 t) = \frac{C_i \alpha\sigma N_o}{\sqrt{2\pi}} \exp(-M_1 t) \quad (101)$$

where

$$M_1 = D_1 k^2 + ikK_1 E + A + s_i^2 D_1$$

and

$$M_2 = D_2k^2 + ikK_2E + B+s_i^2D_2 \quad .$$

The solution of this equation is

$$f_i(k,t) = \frac{C_i\alpha\sigma N_o}{\sqrt{2\pi}}\left[\frac{\exp(-M_1t) - \exp(-M_2t)}{M_2 - M_1}\right] \tag{102}$$

Here use has been made of the initial condition, $f_i(k,0) = 0$, for all i. Hence in the expression (98) we have

$$Z_i(z,t) = \frac{C_i\alpha\sigma N_o}{2\pi}\left[\exp[-(A+s_i^2D_1)t]\right. \tag{103}$$

$$\int_{-\infty}^{\infty} \frac{\exp[-D_1k^2t-ik(z-K_1Et)]\,dk}{k^2(D_2-D_1)+ik(K_2-K_1)E+(D_2-D_1)s_i^2+B-A} - \exp[-(B+s_iD_2)t]$$

$$\left.\int_{-\infty}^{\infty} \frac{\exp[-D_2k^2t-ik(z-K_2Et)]\,dk}{k^2(D_2-D_1)+ik(K_2-K_1)E+(D_2-D_1)s_i^2+B-A}\right]$$

In Chapter IV, page 83, a situation was discussed in which the primary ion and the secondary ion arising from it have the same mobility. If this situation occurs then, in view of equation (7), their diffusion coefficients will be equal and equation (103) will take the form

$$Z_i(z,t) = \frac{C_i\alpha\sigma N_o}{\sqrt{4\pi Dt}\ (B-A)} \exp\left[-s_i^2Dt - \frac{(z-KEt)^2}{4Dt}\right][\exp(-At) - \exp(-Bt)] \tag{104}$$

where $K_1 = K_2 = K$ and $D_1 = D_2 = D$. Suppose for the sake of argument that $B = 0$, then

$$Z_i(z,t) = \frac{C_i \alpha \sigma N_o}{\sqrt{4\pi Dt}\, A} \exp\left[-s_i^2 Dt - \frac{(z-KEt)}{4Dt}\right] [1 - \exp(-At)] \qquad (105)$$

The last factor in this expression is an increasing function of time. The corresponding factor in the expression for the density of primary ions is the decreasing function of time, exp(-At). Thus the qualitative discussion of situation (1) on page 84 of Chapter IV is confirmed.

APPENDIX F

STEADY STATE MODE OF OPERATION

The steady state mode of operation is described by the partial differential equations (19) and (97) in which $\frac{\partial n}{\partial t}$ has been set equal to zero. The radial boundary conditions are identical to those encountered in the pulse mode of operation.

Primary Ions

Variables may be separated in equation (19) in a manner identical to that in Chapter III, Section 2, except that the function Z, is now only a function of z and does not involve the time t. This separation results in the differential equation (22) whose solution is (25) and in the differential equation

$$-D_1 \frac{d^2Z}{dz^2} + K_1 E \frac{dZ}{dz} + (A + s^2 D_1) Z = 0 \qquad (106)$$

The general solution of this differential equation is

$$Z(z) = C_1 \exp[(P_1 + Q_1) z] + C_2 \exp[(P_1 - Q_1) z] \qquad (107)$$

where

$$P_1 = \frac{K_1 E}{2D_1}$$

and

$$Q_1 = \sqrt{P_1^2 + A/D_1 + s^2}$$

This solution shall be subject to the following boundary conditions:

(1) $Z(z)$ approaches zero as z approaches either (+) infinity or (-) infinity.

(2) The solution, $Z^+(z)$, for the range $z \geq 0$, must equal the solution $Z^-(z)$, for the range $z \leq 0$, at $z = 0$.

Application of these boundary conditions reduces the solution to the following forms:

$$Z^+(z) = \sum_i C_i \exp[(P_1 - Q_{1i})\, z] \quad , \quad z \geq 0 \quad , \qquad (108a)$$

$$Z^-(z) = \sum_i C_i \exp[(P_1 + Q_{1i})\, z] \quad , \quad z \leq 0 \quad , \qquad (108b)$$

where

$$Q_{1i} = \sqrt{P_1^2 + A/D_1 + s_i^2} \quad .$$

In these equations the factors C_i are proportional to the rate of ion production of the source. In addition to being functions of source parameters they are also functions of pressure whose form is not known and, indeed, could be different for different sources. For this reason it did not appear practicable to compare data taken using different sources. It can be shown that in many experimental situations frequently arising, that only the first term in these summations is important. In the analysis of data taken using a single source, ratios and other mathematical combinations of the ion currents were used in which the factor C_1 could be cancelled out.

Hence the general solution of (106) for the boundary conditions given here is

$$n_1(r,z) = \sum_i C_i J_o(s_i r) \exp[(P_1 - Q_{1i})\, z] , \qquad z \geq 0 , \qquad (109a)$$

$$n_1(r,z) = \sum_i C_i J_o(s_i r) \exp[(P_1 + Q_{1i})\, z] , \qquad z \leq 0 . \qquad (109b)$$

Secondary Ions

For simplicity it will be assumed that the secondary ion under consideration arises from an ion-molecule reaction involving only one of the primary ions. If this is not so, the method may be extended very simply to cover more complicated situations.

In the partial differential equation for secondary ions,

$$-D_2 \frac{\partial^2 n_2}{\partial r^2} - \frac{D_2}{r} \frac{\partial n_2}{\partial r} - D_2 \frac{\partial^2 n_2}{\partial z^2} + K_2 E \frac{\partial n_2}{\partial z} + B n_2 = \alpha\sigma\, n_1 , \qquad (110)$$

the term on the right side will be (109a) for $z \geq 0$ and (109b) for $z \leq 0$ or the sum of several such expressions if this particular secondary ion arises from several species of primary ions.

To find the particular integral of this partial differential equation it will be assumed that this integral has the form (98) except that the function Z is a function only of z and does not involve the time t. Multiplication of both sides by $r\, J_o(s_i r)\, dr$ and integration from 0 to 1 permits the corresponding terms in the summations on the left and right sides of the equations to be equated individually:

$$-D_2 \frac{d^2 Z_i}{dz^2} + K_2 E \frac{dZ_i}{dz} + (B+s_i^2 D_2) Z_i = \begin{cases} C_i \alpha\sigma \exp[(P_1 - Q_{1i})z] , & z \geq 0 , \\ C_i \alpha\sigma \exp[(P_1 + Q_{1i})z] , & z \leq 0 . \end{cases} \quad (111)$$

Solution of this differential equation by the method of undetermined coefficients produces the solutions,

$$Z_i^+(z) = \frac{C_i \alpha\sigma \exp[(P_1 - Q_{1i})z]}{D_2[2P_2(P_1 - Q_{1i}) + B/D_2 + s_i^2 - (P_1 - Q_{1i})^2]} , \quad z \geq 0 , \quad (112a)$$

$$Z_i^-(z) = \frac{C_i \alpha\sigma \exp[(P_1 + Q_{1i})z]}{D_2[2P_2(P_1 + Q_{1i}) + B/D_2 + s_i^2 - (P_1 + Q_{1i})^2]} , \quad z \leq 0 , \quad (112b)$$

where

$$P_2 = \frac{K_2 E}{2D_2} .$$

In view of the relationship (7)

$$P_1 \approx P_2 \approx \frac{Ee}{2kt} = P .$$

Hence the particular integral of (110) is

$$n_2^+(r,z,t) = \sum_i \frac{C_i \alpha\sigma J_o(s_i r) \exp[(P - Q_{1i})z]}{B - A(D_2/D_1)} , \quad z \geq 0 , \quad (113a)$$

$$n_2^-(r,z,t) = \sum_i \frac{C_i \alpha\sigma J_o(s_i r) \exp[(P + Q_{1i})z]}{B - A(D_2/D_1)} , \quad z \leq 0 . \quad (113b)$$

Since the homogeneous equation for secondary ions is similar in form to (106), the complementary function for (110) will have a form similiar

to (107). The boundary conditions (1) and (2) of Section 1 apply in this case. Since the sources are not producing secondary ions directly, one additional boundary condition can be applied:

(3) The first derivative of the solution for the range $z \geq 0$ must equal the first derivative of the solution for the range $z \leq 0$ at $z = 0$.

Hence the complete solution of (110) for the assumed boundary conditions is

$$n_2^+(r,z,t) = \sum_i \frac{C_i \alpha\sigma}{B - A(D_2/D_1)} \left\{ \exp[(P-Q_{1i})z] - \frac{Q_{1i}}{Q_{2i}} \exp[(P-Q_{2i})z] \right\} , \quad z \geq 0 , \tag{114a}$$

$$n_2^-(r,z,t) = \sum_i \frac{C_i \alpha\sigma}{B - A(D_2/D_1)} \left\{ \exp[(P+Q_{1i})z] - \frac{Q_{1i}}{Q_{2i}} \exp[(P+Q_{2i})z] \right\} , \quad z \leq 0 , \tag{114b}$$

where

$$Q_{2i} = \sqrt{P^2 + B/D_2 + s_i^2} .$$

More Complicated Situations

In principle the derivation of the expressions for tertiary ions or members of more complicated reaction systems requires nothing new. It is only more tedious.

For example the set of reactions (3), (4), and (5) given in Chapter IV is an example of a more complicated reaction system. The N_2H^+ ions

might be either secondary or tertiary ions. In this case it will be necessary to solve a partial differential equation of the form

$$-D_3 \frac{\partial^2 n_3}{\partial r^2} - \frac{D_3}{r}\frac{\partial n_3}{\partial r} - D_3 \frac{\partial^2 n_3}{\partial z^2} + K_3 E \frac{\partial n_3}{\partial z} + G n_3 = \alpha_1\sigma_1 n_1 + \alpha_2\sigma_2 n_2 \qquad (115)$$

where D_3 and K_3 are the diffusion coefficient and mobility of the N_2H^+, n_3 is the number (charge) density of N_2H^+, and G is the total effect of reactions using up this ion. In this case n_1 is the density of the primary ion H_2^+, n_2 is the density of the secondary ion H_3^+, $\alpha_1\sigma_1$ is the reaction rate for reaction (4), and $\alpha_2\sigma_2$ is the reaction rate for reaction (5).

The solutions of (115) for the boundary conditions (1), (2), and (3) are

$$n_3^+(r,z) = \sum_i C_i J_o(s_i r)\left\{\left(\frac{\alpha_1\sigma_1}{G-A(D_3/D_1)}\right)\left(\exp[(P-Q_{1i})z] - (Q_{1i}/Q_{3i})\exp[(P-Q_{3i})z]\right)\right.$$
$$+\left(\frac{\alpha_2\sigma_2\alpha\sigma}{B-A(D_2/D_1)}\right)\left[\left(\frac{\exp[(P-Q_{1i})z] - (Q_{1i}/Q_{3i})\exp[(P-Q_{3i})z]}{G-A(D_3/D_1)}\right)\right.$$
$$\left.\left.-\frac{Q_{1i}}{Q_{2i}}\left(\frac{\exp[(P-Q_{2i})z] - (Q_{2i}/Q_{3i})\exp[(P-Q_{3i})z]}{G-A(D_3/D_2)}\right)\right]\right\}, \quad z \geq 0, \qquad (116a)$$

$$n_3^-(r,z) = \sum_i C_i J_o(s_i r)\left\{\left(\frac{\alpha_1\sigma_1}{G-A(D_3/D_1)}\right)\left(\exp[(P+Q_{1i})z] - (Q_{1i}/Q_{3i})\exp[(P+Q_{3i})z]\right)\right.$$
$$+\left(\frac{\alpha_2\sigma_2\alpha\sigma}{B-A(D_2/D_1)}\right)\left[\left(\frac{\exp[(P+Q_{1i})z] - (Q_{1i}/Q_{3i})\exp[(P+Q_{3i})z]}{G-A(D_3/D_1)}\right)\right.$$
$$\left.\left.-\frac{Q_{1i}}{Q_{2i}}\left(\frac{\exp[(P+Q_{2i})z] - (Q_{2i}/Q_{3i})\exp[(P+Q_{3i})z]}{G-A(D_3/D_2)}\right)\right]\right\}, \quad z \leq 0. \qquad (116b)$$

These equations are generally applicable to the case of an ion that is both a secondary and a tertiary ion. In the situation assumed here, $\sigma_1 = \sigma_2$ is the molecular number density of H_2O; whereas σ is the molecular number density of hydrogen. These equations may be applied to the case of an ion that is only a tertiary ion by setting α_1 equal to zero.

BIBLIOGRAPHY*

1. A. M. Tyndall, The Mobility of Ions in Gases (Cambridge University Press, New York, 1938).

2. L. B. Loeb, Basic Processes of Gaseous Electronics (University of California Press, Berkeley and Los Angeles, 1955).

3. P. Langevin, Ann. chim. phys., Series 7, 28, 289 (1903).

4. P. Langevin, Ann. chim. phys., Series 8, 5, 245 (1905).

5. S. Chapman, Phil. Trans. Roy. Soc. A216, 279 (1916); A217, 115 (1917).

6. D. Enskog, Dissertation, Uppsala, 1917.

7. J. H. Jeans, The Dynamical Theory of Gases (Cambridge University Press, London, 1916).

8. S. Chapman and T. G. Cowling, The Mathematical Theory of Non-Uniform Gases (Cambridge University Press, London, 1939).

9. T. Kihara, Rev. Mod. Phys. 24, 45 (1952); 25, 844 (1953).

10. E. A. Mason and H. W. Schamp, Annals of Physics 4, 233 (1958).

11. H. R. Hassé and W. R. Cook, Phil. Mag. 12, 554 (1931).

12. A. Dalgarno, M.R.C. McDowell, and A. Williams, Phil. Trans. Roy. Soc. A250, 411 (1958).

13. A. Dalgarno, Phil. Trans. Roy. Soc. A250, 426 (1958).

14. G. H. Wannier, Phys. Rev. 83, 281 (1951).

15. A. M. Tyndall and C. F. Powell, Proc. Roy. Soc., Series A, 129 162 (1929).

16. A. M. Tyndall and C. F. Powell, Proc. Roy. Soc., Series A, 134, 125 (1932); 136, 145 (1932).

17. J. H. Mitchell and K. E. W. Ridler, Proc. Roy. Soc., Series A, 146, 911 (1934).

*Abbreviations follow the form shown in style manual, American Institute of Physics.

18. R. N. Varney, Phys. Rev. 89, 708 (1953).

19. F. R. Kovar, E. C. Beaty and R. N. Varney, Phys. Rev. 107, 1490 (1957).

20. R. N. Varney, J. Chem. Phys. 31, 1314 (1959); 33, 1709 (1960).

21. R. N. Varney, The Formation and Stability of Molecular Ions, Proc. 5th Int. Conf. on Ionization Phenomena in Gases, (North Holland Publishing Co., Amsterdam, Netherlands).

22. M. Saporoshenko, Phys. Rev. 111, 1550 (1958).

23. M.S.B. Munson, F. H. Field, and J. L. Franklin, A High Pressure Mass Spectrometric Study of Reactions of Rare Gases with N_2 and CO., An unpublished report of the Humble Oil and Refining Company, Baytown, Texas.

24. N. E. Bradbury, Phys. Rev. 40, 508 (1932).

25. J. H. Mitchell, quoted in reference (1) of this thesis.

26. W. H. Bennett, Phys. Rev. 58, 992 (1940).

27. J. M. Richardson and R. B. Holt, Phys. Rev. 81, 153 (1951).

28. E. J. Lauer, J. Appl. Phys. 23, 300 (1952).

29. K. B. Persson and S. C. Brown, Phys. Rev. 100, 729 (1955).

30. D. A. Rose, J. Appl. Phys. 31, 643 (1960).

31. L. M. Chanin, Phys. Rev. 123, 526 (1961).

32. J. O. Hirshfelder, H. Eyring, and N. Rosen, J. Chem. Phys. 4, 121 (1936); 4, 130 (1936).

33. D. Stevenson and J. O. Hirshfelder, J. Chem. Phys. 5, 933 (1937).

34. J. O. Hirshfelder, J. Chem. Phys. 6, 795 (1938).

35. E. A. Mason and J. T. Vanderslice, Phys. Rev. 114, 497 (1959).

36. R. N. Varney, Phys. Rev. Ltrs. 5, 529 (1960).

37. D. P. Stevenson and D. O. Schissler, J. Chem. Phys. 29, 282 (1958).

38. W. S. Barnes, D. W. Martin, and E. W. McDaniel, Phys. Rev. Ltrs. 6, 110 (1961).

39. M. Saporoshenko, Formation of H_3^+ Ions, Proc 2nd Int Conf on the Physics of Electronic and Atomic Collisions (W. A. Benjamin, Inc., New York, 1961).

40. E. W. McDaniel, D. W. Martin, and W. S. Barnes, Rev. Sci. Inst. 33, 2 (1962).

41. H. König and G. Helwig, Zeit. für Phys. 129, 491 (1951).

42. A. O. Nier, Rev. Sci. Inst. 18, 398 (1947).

43. Handbook of Chemistry and Physics, 30th Edition (Chemical Rubber Publishing Company, Cleveland, Ohio).

44. A. M. Mood, Introduction to the Theory of Statistics (McGraw-Hill Book Company).

45. G. A. Miller, J. Chem. & Eng. Data. 7, 353 (1962).

VITA

William Spencer Barnes was born in Dayton, Ohio, on March 15, 1923. He attended public schools in Duluth, Minnesota, in Chicago, Illinois, and in Norwalk, Ohio. He first entered Georgia Tech in 1941. He received the degree of Bachelor of Science in Chemistry in 1947, following a period of enlisted service in the U. S. Army from 1943 to 1946. He attended Emory University from 1947 to 1950, and received the degree of Master of Arts in Mathematics in 1951. He reentered the U. S. Army in 1950, where he served as a Nuclear Officer, and rose to the rank of 1st. Lieutenant. He left the service and entered the graduate program in physics at Georgia Tech in 1955. He received the degree of Master of Science in Physics in 1957. Upon completion of the research reported in this thesis in the fall of 1962, he joined the staff of the Lawrence Radiation Laboratory in Livermore, California, where he remains at the present time. He was married in 1953 to Elinor M. Ricketts, and the couple now have four children.